Ministry of Higher Education and Scientific Research

Mohamed Boudiaf University - M'sila

Faculty of Technology

Department of Civil Engineering

THESIS submitted for the academic Master's degree

FIELD OF STUDY: Civil Engineering

SPECIALIZATION: Structures

By: YAGOUBI siham

TOPIC

EVALUATION OF THE SEISMIC PERFORMANCE OF A REINFORCED CONCRETE T-SHAPED CANTILEVER RETAINING WALL WITH COHESIVE BACKFILL C-Φ

Defended before the jury composed of:

Mr. OUZANDJA Djamel	Med Boudiaf University - M'sila	**President**
Mr. HAMITOUCHE Amar	Med Boudiaf University - M'sila	**Examiner**
Mr. MEKKI Lakhdar	Med Boudiaf University - M'sila	**Examiner**
Mr. MENASRI Youcef	Med Boudiaf University - M'sila	**Supervisor**
Mrs. BAKIR Nassima	Med Boudiaf University - M'sila	**Co-Supervisor**

Academic Year: 2024/2025

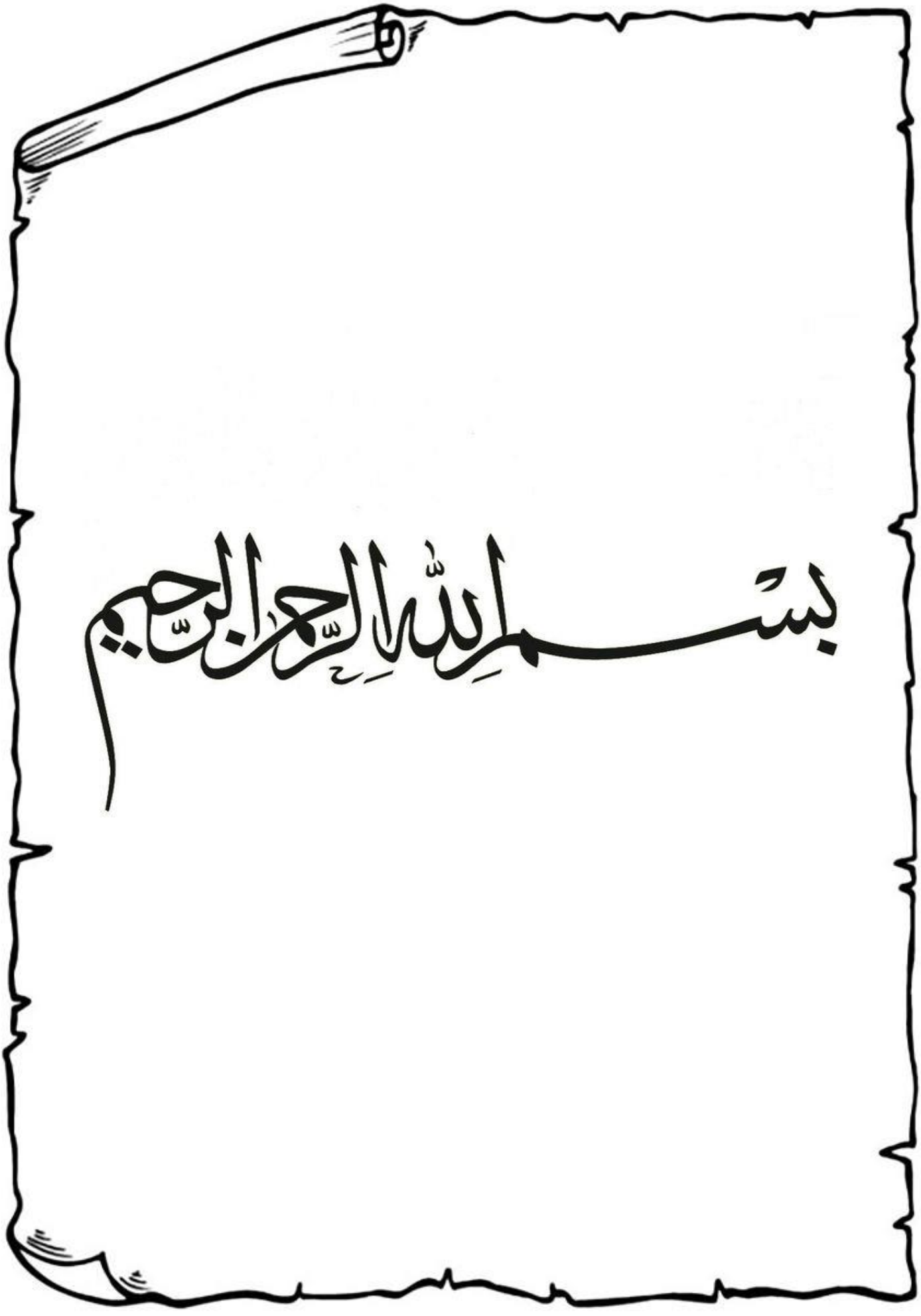
بسم الله الرحمن الرحيم

Dedication

To my beloved parents,

For your endless love, unwavering support, and constant prayers

You are the roots of my strength and the reason behind this achievement.

I dedicate this work to you with all my gratitude and love.

To my family and friends,

For believing in me, encouraging me through every step, and reminding me to never give up

Thank you for being my source of light in times of doubt.

To my dear supervisor, **[Dr. MENASRI youcef]**,

With deep respect and sincere appreciation,

I thank you for your invaluable guidance, patience, and insightful advice.

Your mentorship has left a lasting impact on both my academic and personal growth. And to everyone who walked with me on this journey, even in silence

Acknowledgements

First and foremost, I would like to express my deepest gratitude to Dr. MENASRI Yousef, my supervisor, for his constant availability, rigorous guidance, valuable advice, and unwavering support throughout this work. His professionalism and kindness have been a continuous source of inspiration and motivation.

I also extend my sincere thanks to my co-supervisor, Dr. BAKIR Nassima, for her insightful feedback, patience, and careful attention at every stage of this dissertation. Her support has been invaluable.

I wish to express my heartfelt appreciation to my family, especially my parents, for their unconditional love, sacrifices, and unwavering moral support. You are my strength, and this achievement is the result of your prayers and trust in me.

To my friends and colleagues, thank you for your presence, encouragement, help, and all the moments shared that lightened this academic journey. Your support has meant a great deal.

Finally, I thank everyone who has contributed, directly or indirectly, to the completion of this dissertation.

Abstract

Retaining walls are designed for their resistance and stability by considering the lateral pressures of the soil affecting the wall and any surface loads, if present. Generally, the backfill is executed with non-cohesive soil (such as sandy soil), which is the standard practice in the design codes for retaining walls. They are analyzed using the Rankine or Coulomb method in static conditions or Mononobe-Okabe method in dynamic conditions for non-cohesive soil located in a significant seismic zone. However, it is very costly economically, especially in cases where the length of the retaining wall is considerable and the site soil is cohesive soils (**c-ϕ** Soils). This prompted researchers Saran and Prakash to extend Mononobe-Okabe method to include cohesive soils (c-ϕ soils) In this research, we studied the seismic performance of a cantilever retaining wall made of reinforced concrete with a T-shaped cross-section, constructed in cohesive (c–ϕ) soil. The analysis was carried out using both the analytical method proposed by Saran and Prakash (1968) and numerical modeling with the PLAXIS 2D software. The numerical approach provided a more accurate and realistic representation of the wall's behavior, enabling comprehensive tracking of deformation and precise identification of the failure point. The results were then compared with those obtained using Mononobe-Okabe method, both analytically and through numerical simulations in PLAXIS 2D. The results indicated that the seismic performance of cohesive (c-ϕ Soils), is good, comparable to that of non-cohesive soil. This study enhances the understanding of the behavior of cantilever retaining walls under seismic loads for (c-ϕ Soils), there by contributing to the development of safer, more efficient, and economical design practices.

Keywords: Retaining Walls, Seismic Performance, Cohesive Soils, Plaxis 2d

Résumé

Les murs de soutènement sont conçus pour leur résistance et leur stabilité, en tenant compte des pressions latérales du sol affectant le mur ainsi que de toute charge de surface éventuelle. En général, le remblai est réalisé avec un sol non cohérent (tel que le sable), ce qui constitue la pratique standard dans les codes de conception des murs de soutènement. Ces murs sont analysés à l'aide de la méthode de Rankine ou de Coulomb en conditions statiques, ou de la méthode de Mononobe-Okabe en conditions dynamiques, pour les sols non cohérents situés dans une zone sismique significative. Cependant, cette approche s'avère très coûteuse sur le plan économique, notamment lorsque la longueur du mur de soutènement est importante et que le sol du site est composé de sols cohérents (sols c-ϕ). Cela a conduit les chercheurs Saran et Prakash à étendre la méthode de Mononobe-Okabe afin d'inclure les sols cohérents (c-ϕ soils). Dans cette recherche, nous avons étudié la performance sismique d'un mur de soutènement en béton armé en forme de T, construit sur des sols cohérents (c-ϕ soils), en utilisant la méthode analytique de Saran et Prakash (1968), ainsi que la modélisation numérique avec le programme PLAXIS 2D. Ce logiciel permet une représentation plus précise et réaliste du comportement du mur, offrant un suivi complet des plages de déformation et une détermination exacte du point de rupture. Nous avons ensuite comparé les résultats à ceux obtenus avec la méthode de Mononobe-Okabe, tant de manière analytique que numérique, à l'aide du programme PLAXIS 2D. Les résultats ont montré que la performance sismique des sols cohérents (sols c-ϕ) est satisfaisante, comparable à celle des sols non cohérents. Cette étude améliore la compréhension du comportement des murs de soutènement en porte-à-faux soumis à des charges sismiques dans des sols cohérents (c-ϕ soils), contribuant ainsi au développement de pratiques de conception plus sûres, plus efficaces et plus économiques.

Mots-clés : Murs de soutènement, Performance sismique, Sols cohérents, Plaxis 2D

ملـــــخـص:

إنَّ الجدار الإسنادي يُصمَّم من حيث مقاومته واستقراره، مع أخذ الضغوط الجانبية للتربة المؤثرة عليه بعين الاعتبار، بالإضافة إلى الحمولات السطحية إن وُجدت. وعادةً ما يُنفَّذ الردم الخلفي باستخدام تربة غير متماسكة (مثل الرمل)، وهو ما يُعتمَد عليه في القواعد التصميمية للجدار الإسنادي، حيث يُحلَّل باستخدام طريقة **Mononobe-Okabe** في الحالة الديناميكية للتربة غير المتماسكة الواقعة في منطقة زلزالية معتبرة. إلا أنَّ هذه الطريقة تُعَدُّ مكلفةً اقتصاديًا، ولا سيّما في الحالات التي يكون فيها طول الجدار الإسنادي كبيرًا، وكانت تربة الموقع من نوع التربة المتماسكة ذات التماسك والاحتكاك. وهذا ما دفع الباحثَين **Saran**و **Prakash** إلى توسيع طريقة **Mononobe-Okabe** لتشمل التربة المتماسكة.(c-ϕ soils)

في هذا البحث، قمنا بدراسة الأداء الزلزالي لجدار إسنادي كابولي من الخرسانة المسلحة على شكل حرف **T**، قائم على تربة متماسكة، وذلك باستخدام الطريقة التحليلية لـ **Saran**و **Prakash (1968)**، بالإضافة إلى النمذجة العددية باستخدام برنامج **PLAXIS 2D**، الذي يوفر تمثيلًا أكثر دقة وواقعية لسلوك الجدار، مما يمكّن من تتبع نطاق التشوُّهات بالكامل وتحديد نقطة الانهيار بدقة.ثم قمنا بمقارنة النتائج مع طريقة **Mononobe-Okabe** تحليلًا وعدديًا باستخدام برنامج .**PLAXIS 2D**وقد أظهرت النتائج أن أداء التربة المتماسكة (ذات التماسك والاحتكاك) في الظروف الزلزالية جيد، ويُعادل تقريبًا أداء التربة غير المتماسكة.

تُعزز هذه الدراسة فهم سلوك الجدار الإسنادي الكابولي تحت تأثير الأحمال الزلزالية في التربة المتماسكة، مما يسهم في تطوير ممارسات تصميم أكثر أمانًا وكفاءةً واقتصاديةً.

الكلمات المفتاحية :جدار اسناد، الأداء الزلزالي، التربة المتماسكة، بلاكسيس 2 دي.

Summary

Chapter 01 Overview of Retaining Walls

Chapter 02 Review of seismic analytical methods of retaining walls

Chapter 03 Overview of PLAXIS 2D

Chapter 04 Static and dynamic design of cantilever retaining Wall

Chapter 05 Analytical & Numerical Modeling of a cantilever retaining wall

List of Figures

Chapter 01 Overview of Retaining Walls

Chapter 02 Review of seismic analytical methods of retaining walls

Chapter 03 Overview of PLAXIS 2D

Chapter 04 Static and dynamic design of cantilever retaining Wall

Chapter 05 Analytical & Numerical Modeling of a cantilever retaining wall

List of tables

Chapter 04 Static and dynamic design of cantilever retaining Wall

Chapter 05 Analytical & Numerical Modeling of a cantilever retaining w

LIST OF ABBREVIATIONS AND SYMBOLS

1 – Latin notations:

Pa	Active earth pressure
Ka	Active earth pressure coefficient
α	Batter angle.
δ	Angle of wall friction.
i	Slope of the backfill soil
Kp	The passive earth pressure coefficient
Pp	Passive earth pressure
$(K_A)_{dyn}$	Dynamic active earth pressure coefficient
$(P_A)_{dyn}$	Dynamic Active earth pressure
$(K_p)_{dyn}$	Dynamic passive earth pressure Coefficient
$(P_p)_{dyn}$	Dynamic passive earth pressure
α_h	Horizontal seismic coefficients
α_v	Vertical seismic coefficients
ca	Soil-wall adhesion.
w	Weight of the wedge.
q	Surcharge.
C	Cohesion,
$(Nac)_{dyn}$;$(Naq)_{dyn}$; $(Nay)_{dyn}$	Earth pressure Factor (EPF)
λ	Dynamic earth pressure coefficients
fc	Crack depth factor
$(Nacm)_{stat}$;$(Naqm)_{stat}$;$(Na\gamma m)_{stat}$	Earth pressure cofficients
H1	Total height of retaining wall
ho	Depth of the cracked zone in clayey soils
U	Total displacement
E_{ref}	Effective Young modulus
υ	Poisson's ratio
Ψ	Angle of dilatancy
EA	Normal stiffness
EI	Bending rigidity
γ	Unit Weight of soil
$\bar{\sigma}$	Effective Stress In Soil Mechanics
W_{soil}	Total weight of the soil (backfill)

W_{stem}	Total weight of the stem for the cantilever retaining wall
W_{base}	Total weight of the base for the cantilever retaining wall
σ	Normal stress
N	Normal force
T	Shear force
Fs	Factor of saftey
T_n	Natural period of cantilever retaining wall
ω_n	Natural Angular Frequency
K	Lateral stiffness
fc_{28}	Characteristic compressive strength of concrete at 28 days
fe	Effective stress in steel
σ_s	Stress in steel reinforcement
As	Cross-sectional area of the reinforcing steel (rebar)

2– Abbreviations:

PGA	Pick ground acceleration
RPA 2024	Règles Parasismiques Algériennes 2024
MO	Mononobe-Okabe

General introduction

Civil engineering plays an important role in the development of the modern world**.** It is involved in various areas such as construction, design, and the development of essential infrastructure, including roads, bridges, and transportation networks. The role of civil engineering becomes increasingly significant in addressing global challenges such as natural disasters and in finding effective solutions to mitigate their impact.

Retaining walls are among the most common structures designed by civil engineers, playing a key role in supporting soil and preventing collapse across various types of terrain. They are significant in both urban and rural settings, especially in areas such as roads, basement excavations, and hillside developments.

Cantilever retaining walls are one of the most used types, constructed from reinforced concrete and composed of a vertical stem and a base slab. These walls rely on leverage and the weight of the retained soil above the base to resist lateral earth pressure, making them an effective choice for mid-height walls. Their importance becomes bigger under seismic conditions, where earthquakes generate dynamic forces that can significantly increase lateral pressure on retaining structures. If cantilever retaining walls are not properly designed, they may fail due to sliding, overturning, or even more severe structural damage. Therefore, it is essential to analyze the seismic response of these walls, particularly the interaction between the wall and various soil types. This research investigates the seismic performance of a reinforced concrete cantilever retaining wall with a T-shaped cross-section, situated in cohesive (c–ϕ) soil. The study employs both the analytical method developed by Saran and Prakash (1968) and numerical modeling using the PLAXIS 2D software. The numerical simulations offer a more precise and realistic depiction of the wall's behavior, allowing for detailed monitoring of deformation patterns and accurate determination of the failure point. Subsequently, the results were compared with those derived from the Mononobe-Okabe method, through both analytical calculations and numerical simulations conducted in PLAXIS 2D. This dissertation is divided into 5 chapters as follows:

The first chapter provides a strong foundation by discussing the various types of retaining walls, with a focus on the cantilever type, as well as examining failure modes and the significance of soil types and properties, particularly cohesive and cohesionless backfill. The second chapter reviews static analytical earth pressure theories (Rankine and Coulomb), alongside dynamic analytical methods (Mononobe-Okabe theory and the approach developed by Saran and Prakash). Chapter three offers a detailed overview of the finite element software PLAXIS 2D, while chapter four addresses the static and dynamic design of cantilever retaining walls, including stability verification. Finally, chapter five applies and discusses both analytical and numerical methods to evaluate **the seismic performance of a reinforced concrete T-shaped cantilever retaining wall with cohesive (c–ϕ) backfill.**

CHAPTER 01

Overview of Retaining Walls

1.1 Introduction:

In the year one-million BC, or thereabouts, an anonymous man, or woman, laid a row of stones A top another row to keep soil from sliding into their camp. Thus was constructed an early retaining wall, and we've been keeping soil in place ever since……, with increasingly better methods and understanding [1]. A retaining wall is a structure designed to sustain the earth behind it. It retains a Steep faced slope of an earth mass against rupture of slopes faced slopes in cuts and fills and against sliding down. The retained material exerts a push on structures and this tends to overturn and slide it [2]. These walls are essentially characterized by the concept that the lateral earth pressures due to self-weight of the retained fill and accompanied surcharge loads are carried by the structural wall [3]. The main purpose of a retaining wall is to separate two different levels of soil or ground when there is a need for a change in elevation. Retaining walls plays an important role in protecting the structures from collapsing and natural problems such as soil erosion [4]. A retaining wall is any constructed wall that retains soil or other material at locations having an abrupt change in elevation. The major function of any retaining wall is to act as an earth retaining structure for the whole or part of its height on one face, the other being exposed to the elements [5].

1.2 Definition of a Retaining Wall:

When discussing the concept of a retaining "wall", we may be referring to any vertical or nearly vertical-planed structure whose purpose is to retain a soil mass, and resist lateral earth pressures [6]. A Retaining wall is a structure constructed to withstand the earth behind it. The steep faced slope of an earth mass against rupture of slopes faced in cuts, fills and against sliding down will be retained by it [7]. Retaining wall systems, consisting mainly of a retaining wall and backfill soil, is a prevalent structure used in our built environment including basement wall, bridge abutments, residential elevations, highway walls and so on [8]. Earth retaining structures include cantilever retaining wall, sheet pilings, bulkheads, basement walls, and special types of retaining wall [4].

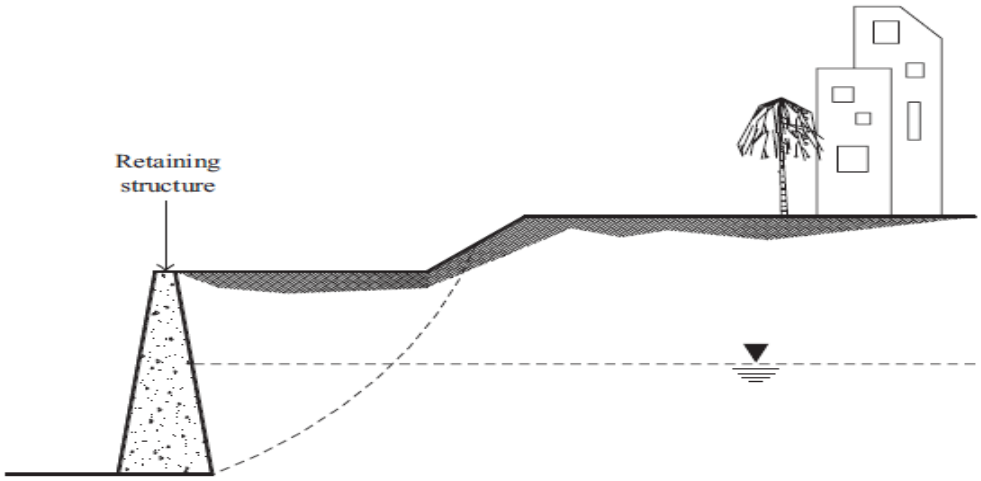

Figure 1.1 Application of retaining walls in civil engineering [9].

1.3 Types of Retaining Wall:

There are several types of retaining walls, some of the popular ones include gravity walls, cantilever walls, counterfort walls, sheet pile walls, anchored walls and reinforced soil retaining walls which are discussed below [3].

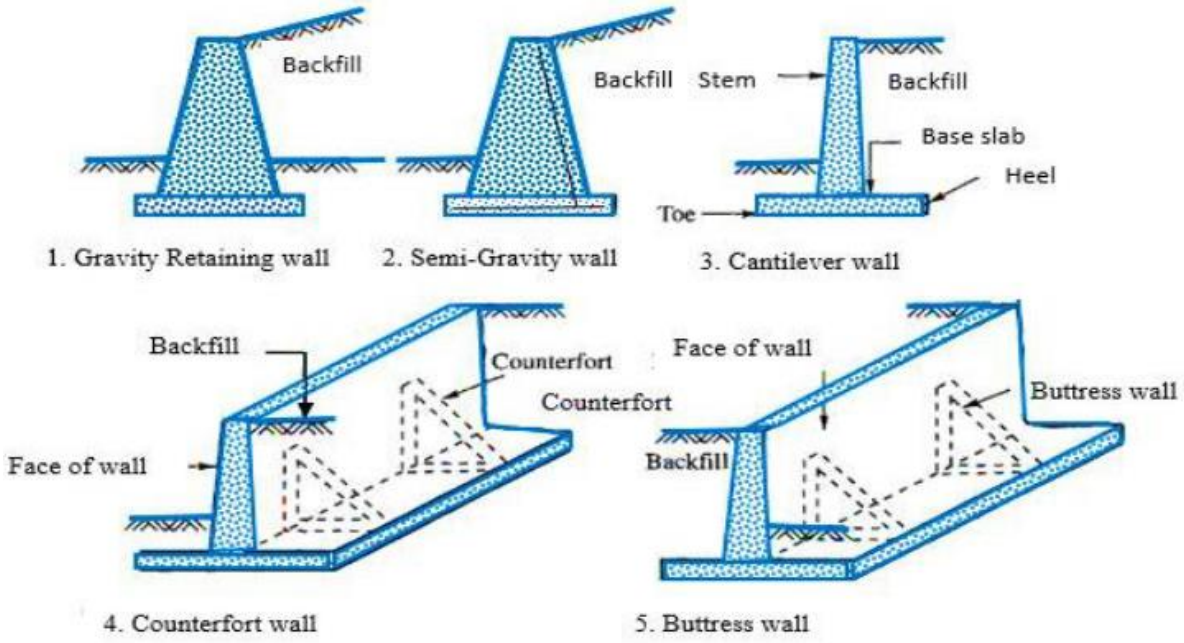

Figure 1.2 Various types of retaining wall [10].

1.3.1 Gravity retaining walls:

These are sometimes called Mass walls and rely upon their own mass together with the friction on the underside of the base to overcome the tendency to slide or overturn [5]. This type of wall depends upon the dead load mass of the wall for stability rather than cantilevering from a foundation [1] Gravity retaining walls are suitable for height up to 2 to 3 m. A key benefit of gravity walls is their rugged construction, but they are not economical for walls higher than 3 m [3]. A gravity wall is usually sufficient in mass to be without steel reinforcing, and can be constructed on site, or brought in as prefabricated sections. The prefabricated sections may require special transportation and hoisting considerations due to their mass [6].

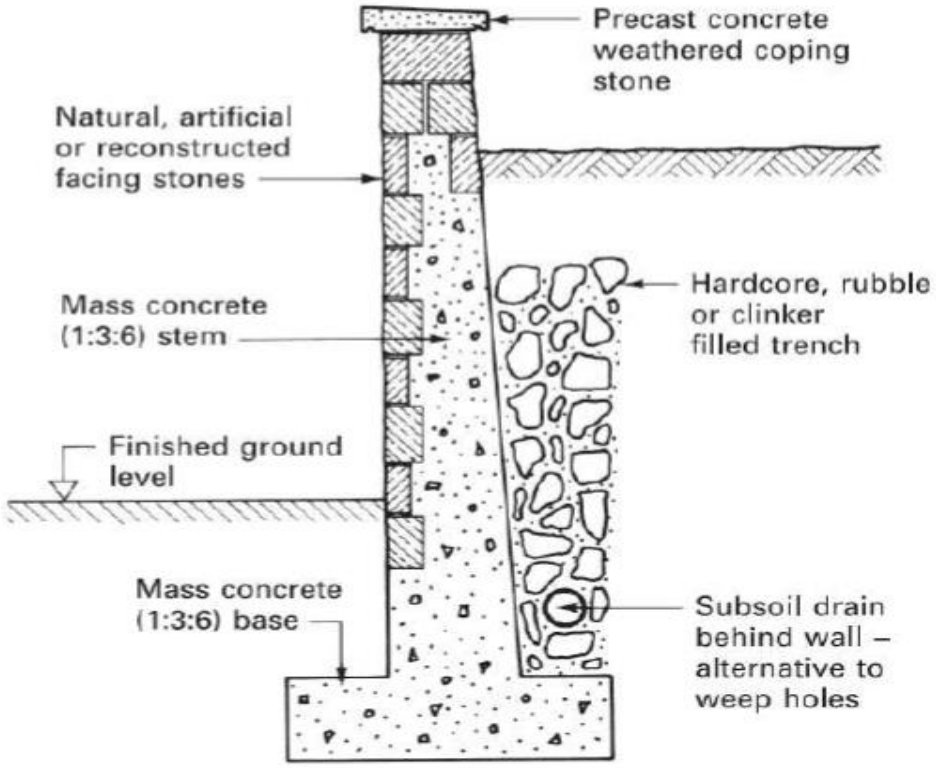

Figure 1.3 Mass Concrete Retaining Wall with Stone facings [5].

1.3.2 Cantilever retaining walls:

They are the most common type of retaining walls. Cantilever walls (Figure 1.3) rest on a slab foundation which allows horizontal pressures from behind the wall to be converted to vertical pressures on the ground below. This slab foundation is also loaded by

back-fill and thus the weight of the back-fill and surcharge also stabilizes the wall against overturning and sliding its stability is a function of strength of its individual parts. The very simple form of L or inverted T are suitable for low walls (less than 6 m) [3], These types of retaining walls can be precast in a factory or formed on site. The benefit of a using a cantilevered wall design, is that they require much less concrete than a monolithic gravity wall, however they require more attention to detail in their design and construction, due to structural, reinforcing, and formwork requirements [6].

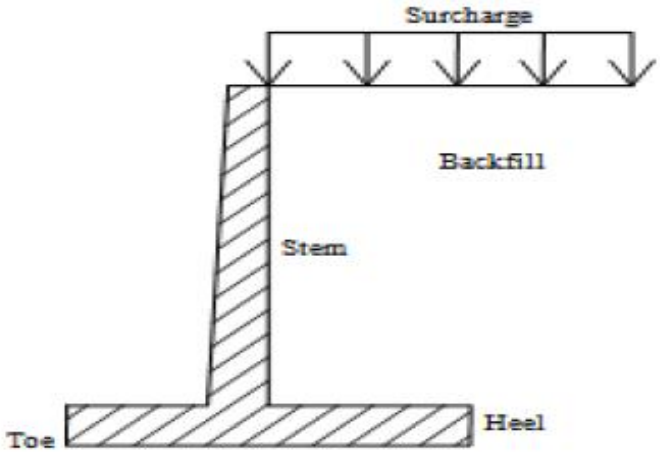

Figure 1.4 Cantilever retaining Wall [11].

1.3.3 Counterfort retaining walls:

These walls are similar to the cantilever walls with the exception that they have thin vertical concrete webs (counterforts) at regular intervals along the backside of the wall (Figure 1.5) [6]. Counterfort cantilevered retaining walls incorporate wing walls projecting upward from the heel of the footing into the stem. The thickness of the stem between counterforts is thinner (than for cantilevered walls) and spans horizontally, as a beam, between the counterfort (wing) walls. The counterforts act as cantilevered elements and are structurally efficient because the counterforts are tapered down to a wider (deeper) base at the heel where moments are higher. The high cost of forming the counterforts and the infill stem walls make such walls usually not practical for walls less than about 16 feet high [1].

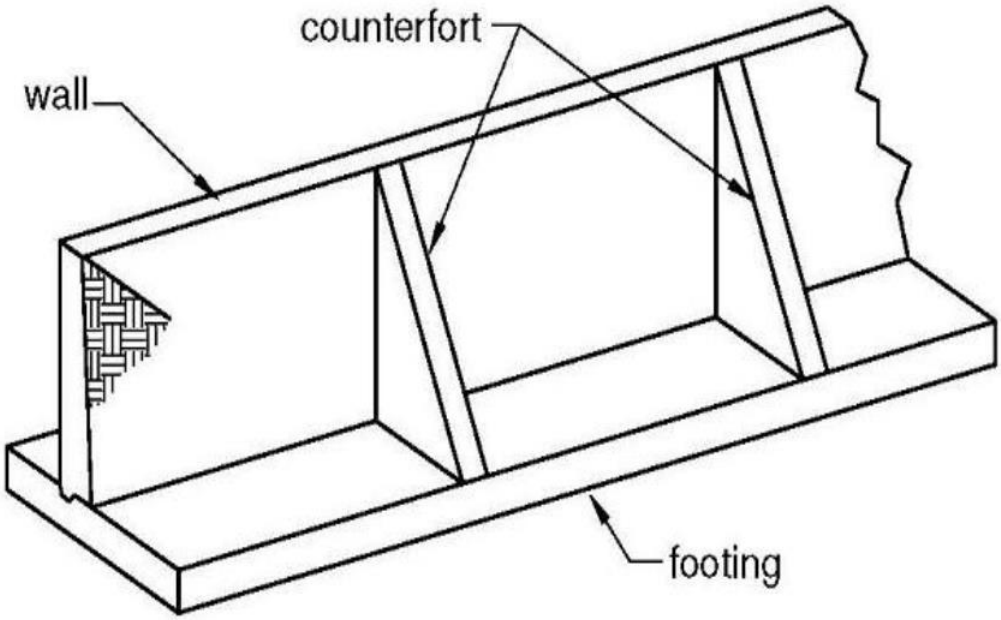

Figure 1.5 Counterfort retaining walls [5].

1.3.4 Buttress Retaining wall:

The buttress retaining wall is as same as counterfort retaining wall. The counterforts are replaced by providing buttresses wall on the opposite side of the backfill pressure [12].

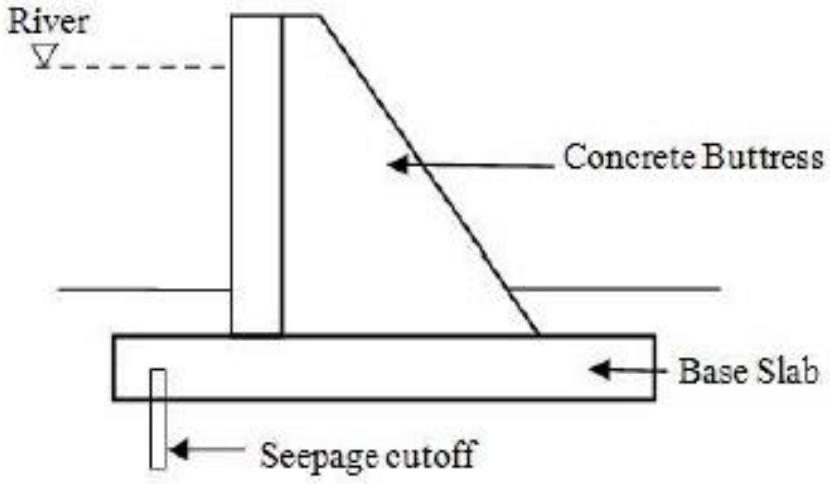

Figure 1.6 Buttress retaining walls [5].

1.3.5 Anchored wall:

They are often used for higher walls where a cantilevered wall may not be economical. Restraint is achieved by drilling holes and grouting inclined steel rods as anchors into the zone of earth behind the wall beyond the theoretical failure plane in the backfill. The anchors can be placed at several tiers for higher walls, and can be post-tensioned rods grouted into drilled holes, or non-tensioned rods grouted into the drilled holes. The latter are also known as soil nails [3].

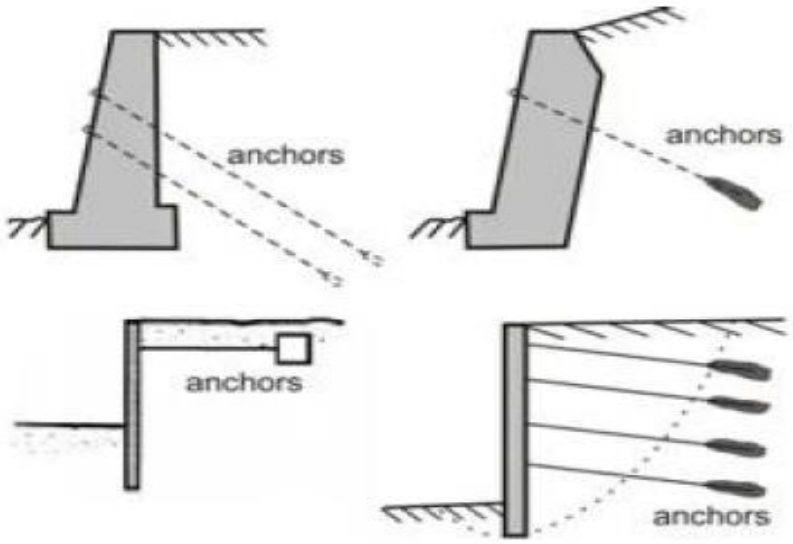

Figure 1.7 Anchored wall [3].

1.3.6 Piling Type Retaining Walls:

A piling type of retaining wall is typically used when there are soft soil conditions or restricted spaces. These may be made of steel, plastics, or timber which is driven into the ground. Generally, pilings might be driven 1/3 above ground, 2/3 into (below) the ground, depending on conditions on site [6].

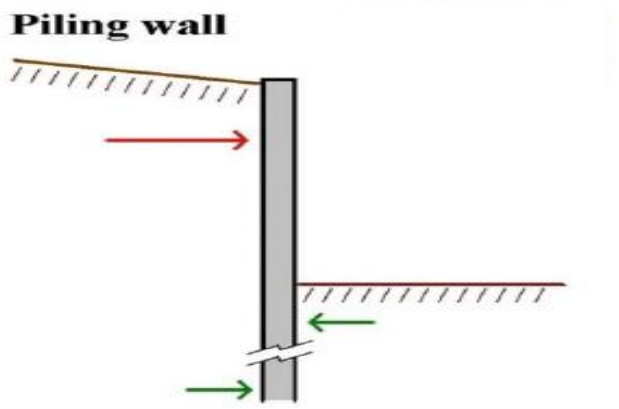

Figure 1.8 Piling Type Retaining Walls [6].

1.3.7 Reinforced earth retaining wall:

Construction of a Reinforced Earth wall is straightforward and simple. Merely place a layer of facing panels, bolt on the reinforcing strips then backfill and compact. Repeat this cycle until the appropriate wall height has been reached. Properly compacted to a uniformly high density, the earth combines with the reinforcement to produce a strong, durable structure with predictable performance characteristics. Figure 1.8 illustrates a typical reinforced earth retaining wall [3].

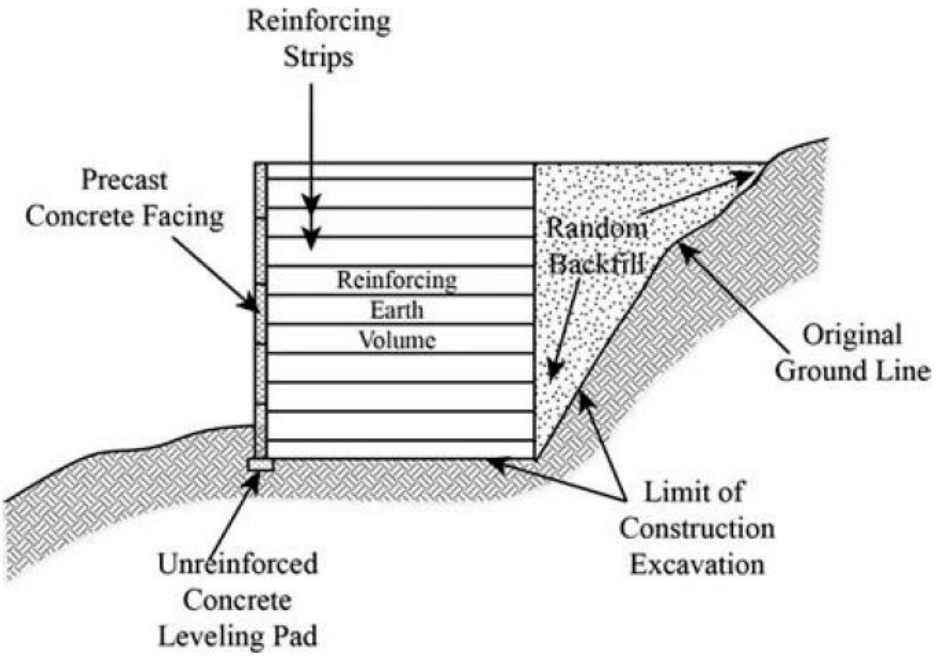

Figure 1.9 Reinforced earth retaining wall [3].

1.4 Cantilever Retaining Wall Terminology:

Cantilevered retaining walls have unique descriptive terminology as illustrated below [1]:

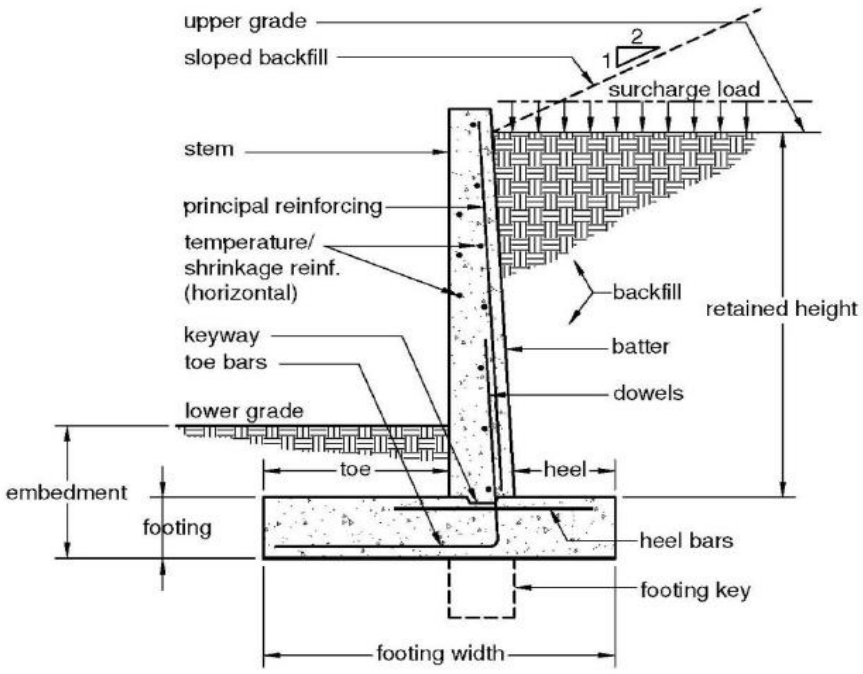

Figure 1.10 Cantilever Retaining Wall terminology [1].

- **Backfill:** The soil placed behind a wall.
- **Backfill slope:** Often the backfill slopes upward from the back face of the wall. The slope is usually expressed as a ratio of horizontal to vertical.
- **Batter:** The slope of the face of the stem from a vertical plane, usually on the inside (earth) face.
- **Dowels:** Reinforcing steel placed in the footing and bent up into the stem a distance at least equal to the required development length.
- **Footing (or foundation):** That part of the structure below the stem that supports and transmits vertical and horizontal forces into the soil below.
- **Footing key:** A deepened portion of the footing to provide greater sliding resistance [5].
- **Heel:** That portion of the footing extending behind the wall (under the retained soil).
- **Keyway:** A horizontal slot located at the base of the stem and cast into the footing for greater Shear resistance.

- **Principal reinforcing:** Reinforcing used to resist bending in the stem.
- **Retained height:** The height of the earth to be retained, generally measured upward from the top of the footing.
- **Stem:** The vertical wall above the foundation.
- Surcharge: Any load placed in or on top of the soil, either in front or behind the wall.
- **Toe:** That portion of footing which extends in front of the front face of the stem (away from the Retained earth) [1].

1.5 Functions of retaining walls:

❖ Whenever there are sudden elevation changes Retaining walls are constructed to protect the soil or any other material from sliding down.

❖ They are usually employed to maintain the difference in level of the ground surface height. Used at places where there is externally exerted loads are high and are used to transfer the forces safely to a below foundation [7].

❖ Preventing soil erosion: A retaining wall can be used to prevent soil from being

❖ washed away, through erosion. The wall prevents rainwater or water from irrigation activities from washing off soil from your property.

❖ Stability: landscaping a sloped garden poses a great challenge. The sloping causes lateral pressure that may lead to the movement of soil downwards. You need to build a retaining wall, which will redistribute and accommodate this pressure, and thus allow you to landscape without the soil sliding downwards [5].

1.6 Failure modes of retaining walls:

A retaining wall must be stable as a whole, and it must have sufficient strength to resist the forces acting on it. There are four basic modes of instability from a geotechnical view relating to the soil/ structure interaction and the overall stability of the wall system. These are limiting eccentricity or overturning, sliding, bearing capacity and global stability. Since these modes of instability assume that the wall is intact, the evaluation of these modes is commonly referred to as the "external stability" analysis [3].

1.6.1 Overturning:

failures occur when moment equilibrium is not satisfied; bearing failures at the base of the wall are often involved. Gravity walls may also be damaged by gross instability of the soils behind and beneath them [5].

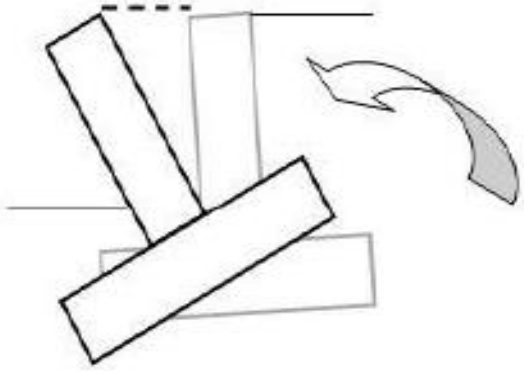

Figure 1.11 Failure occurs due to Overturning [12].

1.6.2 Sliding:

The horizontal force tends to slide the stem and wall away from fill. The tendency to resist this is achieved by the friction at the base. Here, if the wall is found to unsafe against sliding, shear key below the base is provided. Such a key develops passive pressure which resists completely the sliding tendency of wall. A factor of safety of 1.5 is used against sliding [11].

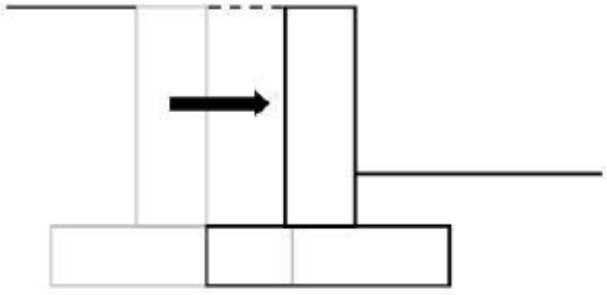

Figure 1.12 Failure occurs due to sliding [12].

1.6.3 Bearing capacity:

The footing should be sized to ensure that the maximum contact pressure does not exceed the bearing capacity of the soil. The width of the base slab must be adequate to distribute the vertical force to the foundation soil [3].

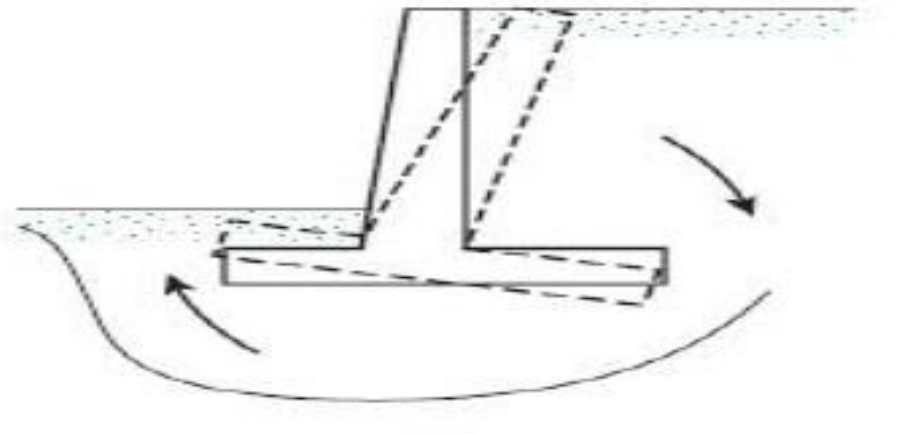

Figure 1.13 bearing capacity failure [7].

1.6.4 Bending Failure:

The stem AB will bend as cantilever so that tensile face will be towards the soil face in case if there is no backfill, where as tensile face will be towards the water face in case there is backfill. The critical section will be at E and B, where crack may occur at if it is not properly reinforced. The soil side slab will have net pressure acting downwards, and will bent as a cantilever having tensile face at top for retaining wall, at the same time the heel slab will be subjected to net upward pressure causing tensile face at bottom [11].

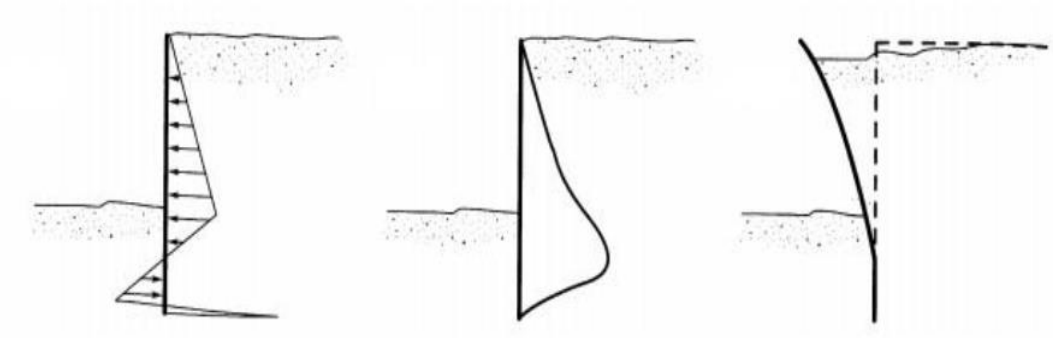

Figure 1.14 bending failure [5].

1.7 Lateral Earth Pressure:

Slopes of earth are generally supported by retaining walls, cantilever sheet-pile walls, and other similar retaining structures. The proper addressing and design of those structures requires an estimation of the lateral earth pressure which is a function of several factors, such as

- ❖ The nature and amount of wall movement,
- ❖ The shear strength parameters of the soil,
- ❖ The specific weight of the soil, and
- ❖ The drainage conditions employed in the backfill [7].

1.7.1 Types of Lateral Earth Pressure:

a) **Active earth pressure (Pa):** Force is applied by the soil on the wall when the wall is free to deflect. The soil is moving towards the wall [13].

b) **At-Rest Condition of Lateral Earth Pressure:** With this category of lateral earth pressure there is no lateral movement of the wall, either away from or toward the backfill soil (image), thus the wall is in a state of static equilibrium [6].

c) **Passive earth pressure:** It is developed as the wall moves towards the backfill or the retained soil. This movement results in an increase in lateral pressure relative to the at-rest condition. The movements required to reach the passive condition are approximately ten times greater than those required to develop active earth pressure [3].

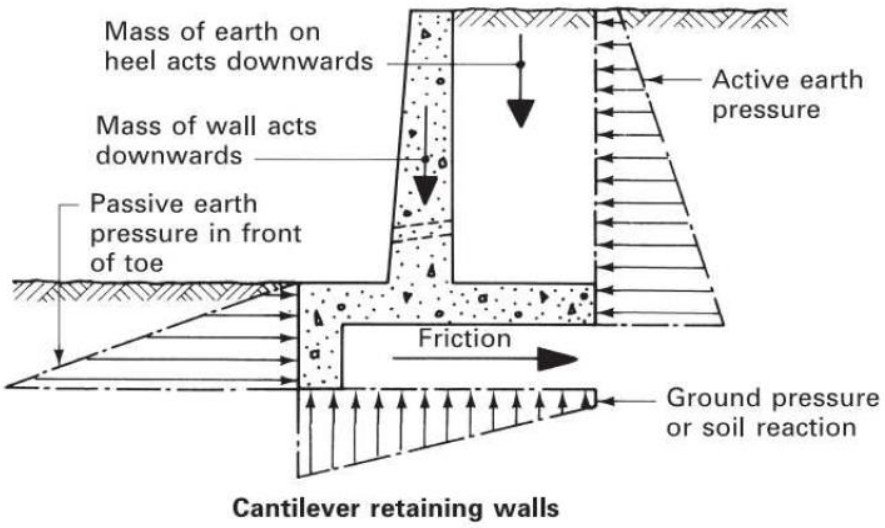

Figure 1.15 Cantilever retaining wall Earth Pressures [5].

1.8 Backfill Soil Conditions:

One of the most important factors to consider, when designing a retaining wall, is the type of soil used in the backfill [6]. The mantle of our earth is composed of water, rock and soil. It is the soil or rock that supports our structures. We need to understand what soil is, how it behaves, and the properties we need for design. Soil is a collective term for any mixture of sand, silt, or clay. Soil is further classified as being cohesive, non-cohesive, or somewhere in between [1].

1.8.1 Non-Cohesive Soils (Sandy Soil):

The preferred soil for backfill behind retaining walls is soil that contains a high percentage of sand and gravel. Such a soil is referred to as a granular soil and has a friction angle of approximately 32° to 36°, depending on the degree of compaction of the soil. The main reason for preferring a granular soil for backfill is that it allows water to pass through it more easily than a non-granular, or clayey soil does. Also, the shear strength of a granular soil does not vary with the moisture content; therefore, its shear strength is more predictable, and thus easier to design for [6]. clean granular material (no silt or clay) is the standard recommendation for backfill material. There are several reasons for this recommendation:

- **Predictable behavior:** Import granular backfill generally has a more predictable behavior in terms of earth pressure exerted on the wall. Also, expansive soil related forces will not be generated by clean granular soil.
- **Drainage system:** To prevent the buildup of hydrostatic water pressure on the retaining wall, a drainage system is often constructed at the heel of the wall. The drainage system will be more effective if highly permeable soil, such as clean granular soil, is used as backfill.
- **Frost action:** In cold climates, frost action has caused many retaining walls to move so much that they have become unusable [14].

1.8.2 Cohesive Soil:

Cohesive soil derives its strength primarily from the cohesive bond between particles. Examples include fine-grained silts and clays. Some clays are highly expansive and change

in volume with changes in water content. Such swelling can cause considerable pressure on retaining structures. It is for this reason that clay backfill should be avoided [1].

1.8.3 Rock as Backfill:

Rock is a desirable choice for use as a backfill for retaining walls, and should be given due consideration whenever available. The rock fill should be consistently graded. A well-graded, densely compacted rock fill should consist of no more than roughly 2% fine grained soils, if it is to remain free draining. Rock fill Is a key component in gabion-style and crib-style walls [6].

1.9 Conclusion:

A retaining wall is one of the most important types of retaining structures. It is extensively used in variety of situations such as highway engineering, railway engineering, bridge engineering and irrigation engineering [2]. Indeed, soil mechanics and the design of retaining structures has advanced dramatically in recent decades giving us new design concepts, a better understanding of soil behavior, and hopefully safer and more economical designs [1].

CHAPTER 02

Review of seismic analytical methods of retaining walls

2.1 Introduction:

Failure of retaining walls in seismic events is a frequently observed problem. Retaining wall damages recorded in large earthquakes are in the form of translational displacements, rotations of the foundation, structural failure due to bending and large settlement of the backfills which effect the stability of the engineered structures located on the backfills. For a long time, the seismic performance of these structures is not considered in the designs because of incomplete understanding of the problem. Because the interactions occurring during and after a seismic excitation are complicated as compared to the static responses [15]. Damage to retaining walls can be great due to an incomplete understanding of the complex soil-structure interaction occurring during an earthquake. The magnitude and distribution of additional seismic lateral earth pressures are particularly in question. Seismic behavior of a retaining wall soil system is a function of a backfill soil properties, relative stiffness of the wall soil system, wall fixity conditions, foundation stability, and characteristics of the applied earthquake motions [16]. During an earthquake, the lateral earth thrust increases and the walls become susceptible to failure which has resulted in frequent damages of the walls [17].

Since the main purpose of building retaining walls is to hold up the slopes, the calculations are important during the design process. Although static loads that affect retaining walls are generally taken into consideration [18], Existing seismic design methodologies are extensions of the static methods and far from accounting for the different parameters affecting the nature of the dynamic response. Since 1930's, the seismic analysis of retaining walls has been based on a simple extension of Coulomb's limit equilibrium analysis, which has become widely known as the Mononobe–Okabe method (1924) [15]. Following the 1923 Great Kantō Earthquake in Tokyo, Japan, the first analytic solution to determine dynamic earth pressure on free-standing retaining walls was developed by Okabe (1924) and Okabe (1926) through an extension of the Coulomb (1776) solution [19].

2.2 Overview on retaining walls earthquakes:

The design of retaining walls in seismic areas poses a complex problem. The traditional design approach usually consists of calculation of a factor of safety against sliding, overturning and bearing capacity failure. This is generally enough for static loads. During seismic loading, the retaining walls tend to get displaced from their original position. The performance of quay walls during the past earthquakes emphasizes this fact. For safe design of retaining walls in seismic areas, the calculation of static and dynamic earth pressure behind the retaining walls is the first requirement. Realistic calculation of displacement of the retaining wall is an equally important aspect [20].

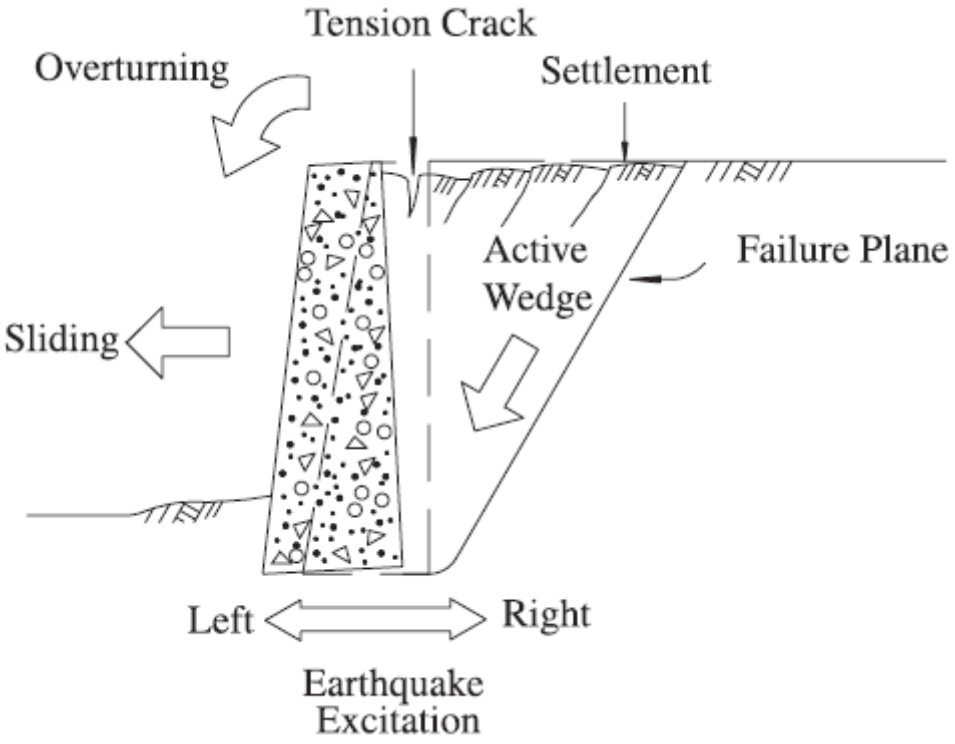

Figure 2.1 Seismic behavior of retaining wall [21].

Figure 2.2 shows the failure of a Retaining wall located at the Taiwan Cinema Culture Town (site 3) near the township of Wu-Fung. The wall was constructed right above the Che-Lung-Pu fault. During the earthquake, the fault rupture caused the wall to slide and overturn. The failure mechanism of the damaged wall is illustrated in **Figure 2.3** The

gravity wall is 4.0 m high and 0.4 m thick at the top. The retaining wall was built on top of the Che-Lung-Pu fault [21].

Figure 2.2 Sliding and overturning of retaining wall at site 3. [21].

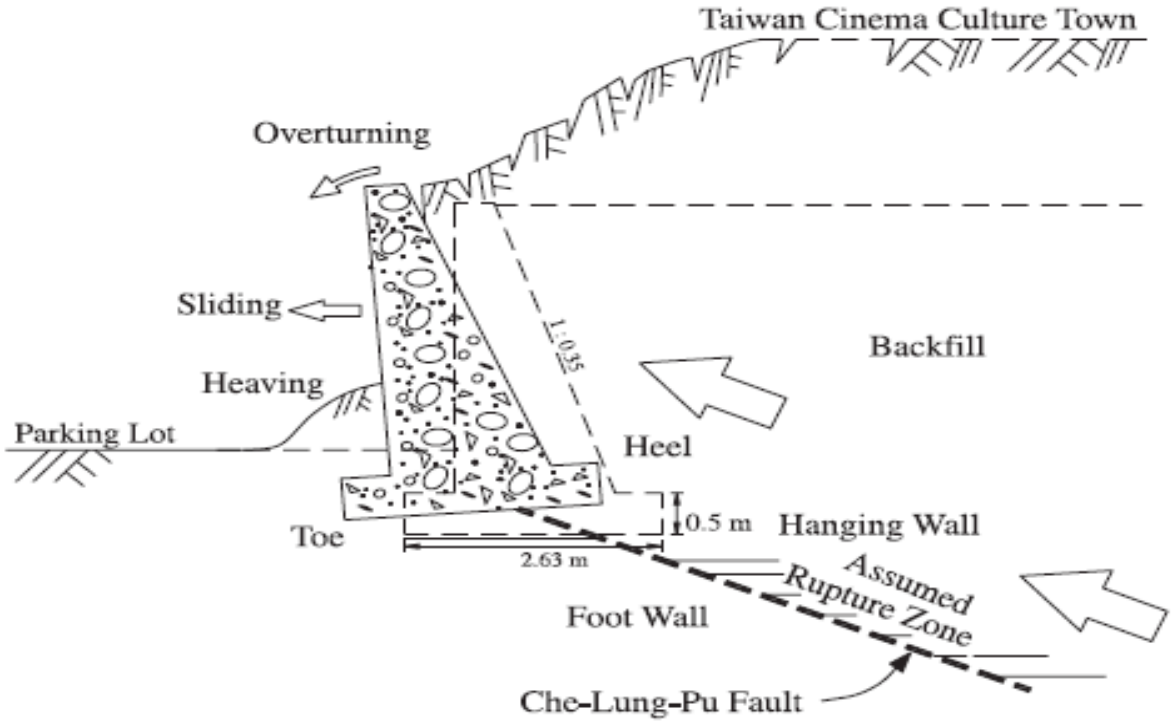

Figure 2.3 Schematic diagram of the wall damaged by fault rupture [21].

2.3 Lateral earth pressure theories:

The purpose of a retaining wall is to retain soil and to resist the lateral pressure of the soil against the wall. Most lateral pressure theories are based upon the sliding soil wedge theory. This, in simple terms, is based upon the assumption that if the wall is suddenly removed, a triangular wedge of soil will slide down along a rupture plane, and it is this wedge of soil that the wall must retain [1].

2.3.1 Coulomb's Earth Pressure Theory:

Coulomb observed that a wedge of soil formed behind the retaining structure when the lateral force became a minimum. He made these observations on walls with a planar back face. These conditions infer that the active state of stress develops behind the wall and the soil within the failure wedge is in a state of plastic equilibrium. The failure wedge is bounded by the back of the wall and a rupture surface through the backfill. To obtain the magnitude of the lateral force, Coulomb assumed: The soil is homogeneous and isotropic; the rupture surface is a plane; the shear resistance is uniformly distributed along the rupture surface; the failure wedge acts as a rigid body; Friction is developed between the wall and the failure wedge and Plane strain applies [3]. When using the Coulomb Theory, procedures are similar to Rankine with these exceptions:

• Friction exists between the wall face and soil.

• Accounts for friction by using a soil-wall friction angle of δ (which ranges from φ/2 to 2φ/3).

• Lateral pressure is not applied only to vertical walls.

• Resultant force not necessarily parallel to the backfill surface because of the soil-wall friction value.

• Coulomb theory considers angle of slope [6].

The active earth pressure Pa acting on a wall is illustrated in **Figure 2.4** and is given by [3]:

$$P_a = \frac{1}{2}\gamma H^2 K_a \tag{2.1}$$

The Coulomb Equation:

The Coulomb Equation where Ka is the coefficient of active pressure, which takes into account backfill slope, friction angle at wall face, angle of rupture plane and angle of internal friction [1]:

c'= 0 for cohesionless soils.

Ka = the active earth pressure coefficient and is given by

α : inclination (with respect to the vertical axis) of the back face of the wall.

δ : friction between the wall and the backfill soil.

i: slope of the backfill soil [3].

$$K_a = \frac{\cos^2(\phi-\alpha)}{\cos^2 \alpha \cos(\alpha+\delta)\left[1+\sqrt{\frac{\sin(\phi+\delta)\sin(\phi-i)}{\cos(\alpha+\delta)\cos(\alpha-i)}}\right]^2} \quad (2.2)$$

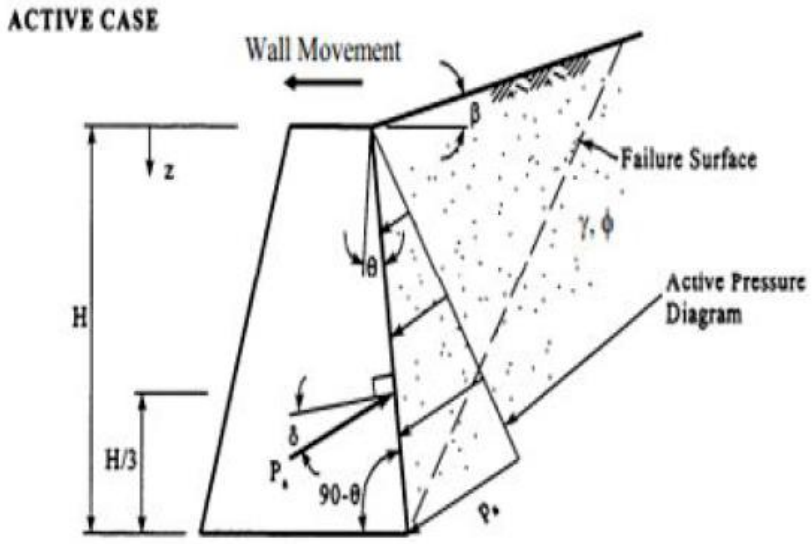

Figure 2.4 Coulomb active pressure (Samtani and Nowatzki, 2012) [3].

The passive pressure acting on a wall with cohesionless backfill is shown in **Figure 2.5** and is given by:

$$P_p = \frac{1}{2}\gamma H^2 K_p \tag{2.3}$$

Kp = the passive earth pressure coefficient, given by:

$$K_p = \frac{\cos^2(\phi+\alpha)}{\cos^2\alpha\cos(\alpha-\delta)\left[1-\sqrt{\frac{\sin(\phi+\delta)\sin(\phi+i)}{\cos(\alpha-\delta)\cos(\alpha-i)}}\right]^2} \tag{2.4}$$

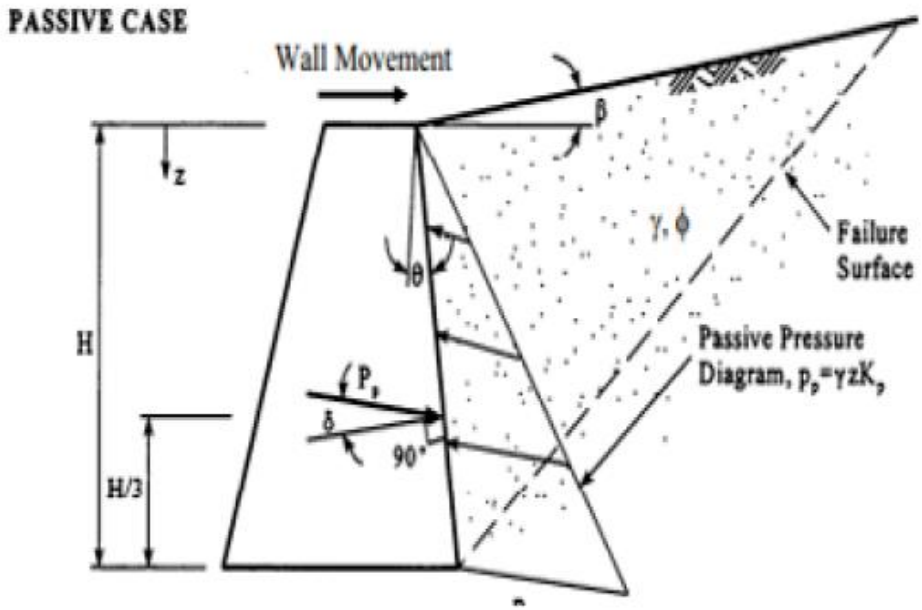

Figure 2.5 Coulomb passive pressure (Samtani and Nowatzki, 2012) [3].

For simple cases involving vertical walls retaining homogeneous soil with a level ground surface, without friction between the soil and the wall face, and without the presence of groundwater, the formulas for computing the earth pressure coefficients can be simplified considerably by substituting, $\delta = \theta = \beta = 0$ in Coulomb's equations. For such simplified cases, Ka and Kp can be expressed by Equations 2.5 and 2.6 respectively:

$$K_a = \frac{1-\sin\phi'}{1+\sin\phi'} \tag{2.5}$$

$$K_p = \frac{1 + sin\phi'}{1 - sin\,\phi'} \tag{2.6}$$

2.3.2 Rankine's Earth Pressure Theory:

The Rankine equation is a simplified version of the Coulomb equation that does not take into account wall batter or friction at the wall-soil interface. As such, it is a conservative approach to the design of retaining walls. An example of its use will be described later for both the Coulomb and Rankine equations. For the case for vertical walls with a level backfill and zero wall friction, the lateral pressure factor Ka will be the same by either approach Rankine's approach was to evaluate the stress at a point in the backfill by using Mohr's circle concepts to obtain the minimum lateral stress at a point in the backfill. The minimum lateral stress corresponds to the "active" case. Integration of that stress with respect to depth leads to a second-order equation (the well-known triangular distribution) for the total lateral force against the wall [1].

When we use the Rankine Theory:

• No adhesion or friction exists between the wall face and soil.

•Rankine method is also applicable to inclined slopes as long as it is not a broken slope.

• Lateral pressure is applied only to vertical walls.

• Failure (in the backfill) occurs as a sliding wedge along an assumed failure plane defined by φ.

• Lateral pressure varies linearly with depth [6].

The active earth pressure is given by:

$$P_a = \frac{1}{2}\gamma H^2 K_a \tag{2.7}$$

Ka is the active earth pressure coefficient, given by:

$$K_a = cos\, i \frac{cos\, i - \sqrt{cos^2 i - cos^2 \phi}}{cos\, i + \sqrt{cos^2 i - cos^2 \phi}} \tag{2.8}$$

The passive earth pressure is given by:

$$P_p = \frac{1}{2}\gamma H^2 K_p \tag{2.9}$$

Kp is the passive earth pressure coefficient, expressed as [3]:

$$K_p = \cos i \frac{\cos i + \sqrt{\cos^2 i - \cos^2 \phi}}{\cos i - \sqrt{\cos^2 i - \cos^2 \phi}} \tag{2.10}$$

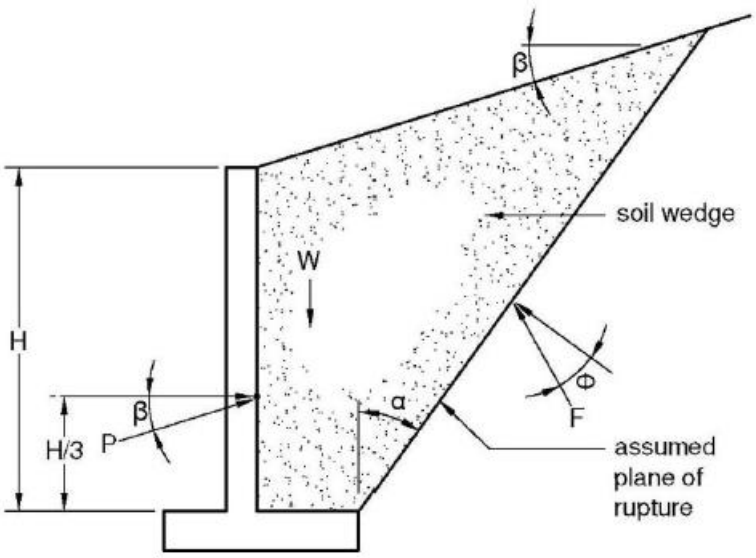

Figure 2.6 Rankine free-body of lateral forces on stem [1].

2.4 Dynamics Analytical Theory (cohesionless soil):

In the seismic zones, the retaining walls are subjected to dynamic earth pressure, the magnitude of which is more than the static earth pressure due to ground motion. Since a dynamic load is repetitive in nature, there is a need to determine the displacement of the wall due to earthquakes and their damage potential. This becomes more essential if the frequency of the dynamic load is likely to be close to the natural frequency of the wall-backfill-foundation-base soil system [22]. Present state of the art for the analysis and design of retaining walls under earthquake loading is based on the method proposed by Mononobe and Matsuo (1929) and Okabe (1926) (M-O analysis) [23].

2.4.1 Dynamic Earth Thrust on Retaining Walls (cohesionless soil):

The earliest studies of dynamic lateral earth pressure on a retaining structure were presented by Okabe (1924) and Mononobe and Matsuo (1929). Their pseudo-static approach became known as the Mononobe-Okabe equation. The method was developed for dry cohesionless material. This method assumes that the wall tilts sufficiently to produce minimum active earth pressure during earthquakes. Under such a condition, a rigid soil wedge behind the wall may move with the wall during earthquakes. This is an extension of the Coulomb Sliding Wedge Theory modified to account for a lateral component of acceleration [24].

2.4.2 Force-Based Approach (The Mononobe-Okabe Pseudo-Static Method):

It is an approximate method which was developed in Japan in the 1920's by Okabe (1924) and Mononobe and Matsuo (1929) for determining the resultant of dynamic lateral earth pressures due to earthquake motions. Still widely used, this approach is called the Mononobe-Okabe (M-O) method [15]. This equation is a modified version of Coulomb's classical solution to account for inertial forces [25].

a. Mononobe-Okabe Method Defects and Limitations:

Some of the limits of M-O method that cause the method not to cover many of the usual engineering problems are as follows.

- ❖ M-O method is applicable for cohesionless soils only c=0
- ❖ Effect of water table behind the wall has not been considered directly in the formula.
- ❖ The conventional problems in civil engineering are not always wall with continues backfill. Sometimes, one has to use equivalent forms of M-O method to model a real problem.
- ❖ M-O method has no answer when $\varphi - \beta - \theta \leq 0$ [9].

b. The most important assumptions of The Mononobe-Okabe method are:

- ❖ The earth-retaining structure has already deformed outwards, thus the generated active pressure is Minimum.

- ❖ A Coulomb wedge, with a planar sliding surface running through the base of the retaining structure, is on the point of failure with a maximum shear strength developed along the length of the surface.
- ❖ The soil behind the retaining structure behaves as a rigid body, so that accelerations can be assumed uniform throughout the backfill at the instant of failure [25].

The extension by Okabe (1924) includes all of the assumptions from Coulomb (1776) theory (excluding the restriction on cohesive soil, from a later study by **Prakash & Saran** [19].

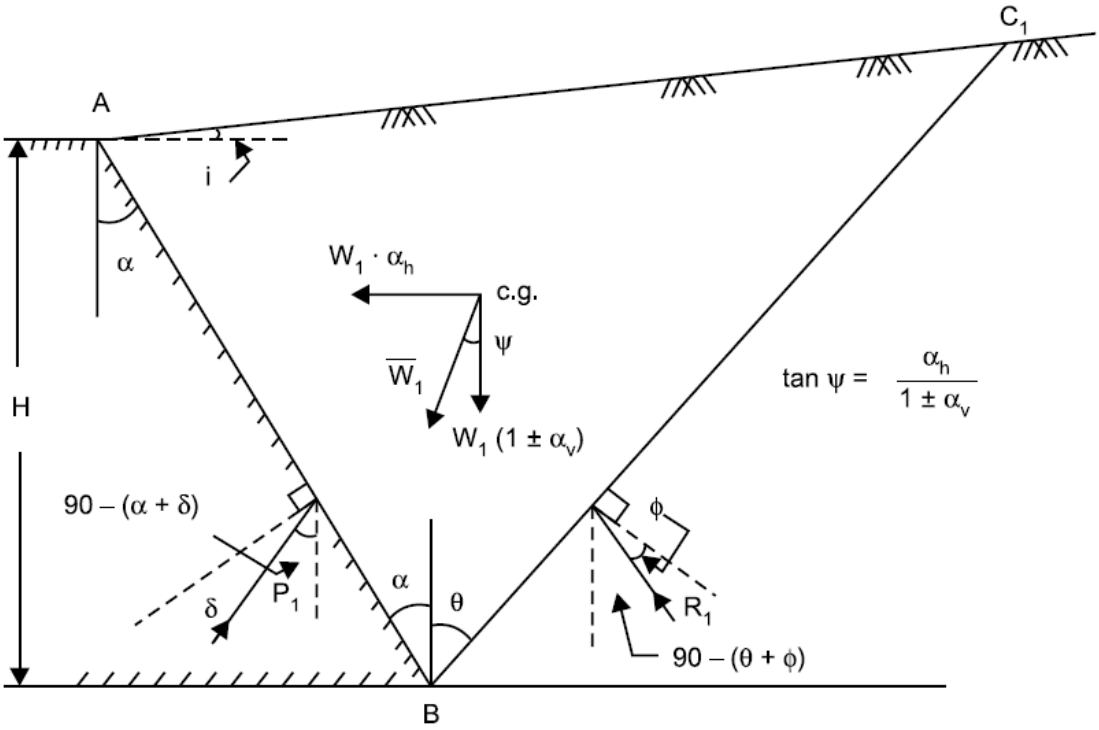

Figure 2.7 Geometry and parameters of M-O method [22].

a. Mononobe-Okabe equations [22]:

- Dynamic active earth pressure coefficient:

$$(K_A)_{dyn} = \frac{\cos^2(\phi-\psi-\alpha)(1\pm\alpha_v)}{\cos\psi\cos^2\alpha\cos(\delta+\alpha+\psi)} \times \frac{1}{\left\{1+\left[\frac{\sin(\phi+\delta)\sin(\phi-i-\psi)}{\cos(\alpha-i)\cos(\delta+\alpha+\psi)}\right]^{1/2}\right\}^2} \quad (2.11)$$

- Dynamic Active earth pressure:

$$(P_A)_{\text{dyn}} = \frac{1}{2}\gamma H^2 (K_A)_{dyn} \tag{2.12}$$

- Dynamic passive earth pressure Coefficient:

$$(K_P)_{dyn} = \frac{(1 \pm \alpha_v)\cos^2(\phi + \alpha - \psi)}{\cos\psi \cos^2\alpha \cos(\delta - \alpha + \psi)} \times \left[\frac{1}{1 + \left\{ \frac{\sin(\phi - \delta)\sin(\phi + i - \psi)}{\cos(\alpha - i)\cos(\delta - \alpha + \psi)} \right\}^{1/2}} \right]^2 \tag{2.13}$$

- Dynamic Passive earth pressure:

$$(P_P)_{dyn} = \frac{1}{2}\gamma H^2 (K_p)_{dyn} \tag{2.14}$$

Therefore, the direction that gives the maximum increase in earth pressure is adopted in practice. If α_h and α_v are respectively the horizontal and vertical seismic coefficients, then [22].

$$\alpha_h = \frac{a_h}{g} \tag{2.15}$$

$$\alpha_v = \frac{a_v}{g} \tag{2.16}$$

The resultant W_1 is inclined with vertical at angle y, such that

$$\psi = \tan^{-1}\left(\frac{\alpha_h}{1 \pm \alpha_v}\right) \tag{2.17}$$

2.5 Dynamic Earth Pressure for c-ϕ Soils:

The solutions So far discussed consider the soil to be cohesionless. A general solution for the determination of total (static plus dynamic) earth pressures for a c-ϕ soil has been

developed by Prakash and Saran (1966) and Saran and Prakash (1968) [22]. here referred to as PSM, expresses the active earth pressure in terms of non-dimensional factors termed here as Earth Pressure Factors (EPFs) similar to Terzaghi's bearing capacity factors. They have considered c-ϕ soil, effect of wall friction, pseudo static inertia force and have separated the contributions of surcharge, cohesion and frictional resistance of soil to the active earth pressure. This leads to simple formulation of total earth pressure [26].

Figure 2.8 shows a failure wedge formed by a planar failure surface in the c-ϕ backfill behind the Retaining Wall having:

- Batter angle α.
- Carrying a surcharge q.
- Weight of the wedge is w.
- Angle of wall friction is δ.
- soil-wall adhesion is ca.
- the depth of tension cracks is Hc.

This depth can be expressed in terms of crack depth factor fc = H c /H. The active earth pressure on the wall is P and makes an angle δ with the normal to the wall-backfill interface.

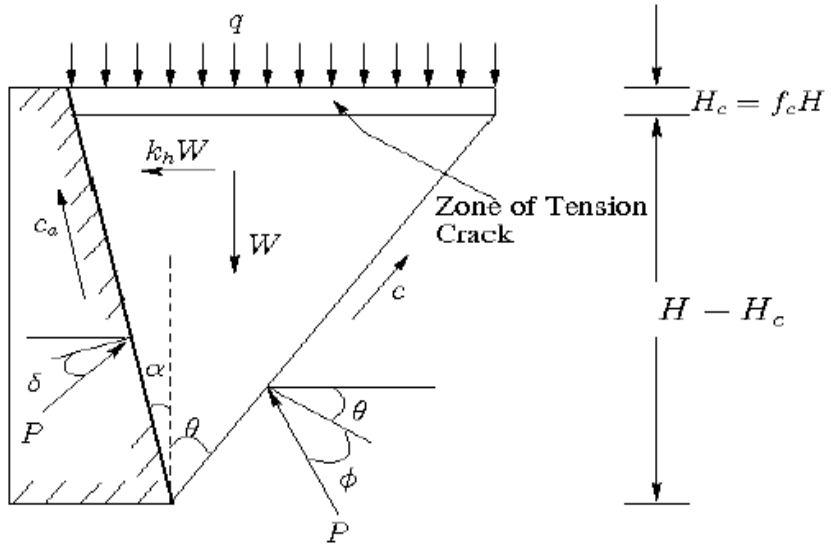

Figure 2.8 Planar Failure Wedge and Forces Acting on the Wedge [26].

The horizontal inertia force in seismic condition is replaced by a pseudo static force k_h where k_h is the horizontal coefficient of acceleration. By resolving the forces in vertical and horizontal directions and simplifying, the earth pressure can be expressed as (Prakash and Saran, 1966; Saran and Prakash, 1968) [26].

a. Saran and Prakash (1968) equations [22]:

- Dynamic Passive earth pressure:

$$(P_A)_{dyn} = \gamma H^2 (N_{a\gamma m})_{dyn} + qH(N_{aqm})_{dyn} - cH(N_{acm})_{dyn} \quad (2.18)$$

where, $(N_{ac})_{dyn}$, $(N_{aq})_{dyn}$, $(N_{ay})_{dyn}$ are the Earth Pressure Factor (EPF)s and are given by

$$(N_{ac})_{dyn} = \frac{\cos\beta \sec\alpha + \cos\phi \sec\theta_1}{\sin(\beta + \delta)} \quad (2.19)$$

$$(N_{a\gamma})_{dyn} = \frac{[(n+1/2)(\tan\alpha + \tan\theta_1) + n^2 \tan\alpha][\cos(\theta_1 + \phi) + \alpha_h \sin(\theta_1 + \phi)]}{\sin(\beta+\delta)} \quad (2.21)$$

$$(N_{aq})_{dyn} = \frac{[(n+1)\tan\alpha + \tan\theta_1][\cos(\theta_1 + \phi) + \alpha_h \sin(\theta_1 + \phi)]}{\sin(\beta+\delta)} \quad (2.20)$$

Where:

$$\beta = \theta_1 + \phi + \alpha \quad (2.21)$$

- **The dynamic earth pressure coefficients:**

$$\lambda_2 = \frac{(N_{a\gamma m})_{dyn}}{(N_{a\gamma m})_{stat}} \quad (2.22)$$

b. Point of Application (Prakash and Saran, 1966 and Saran and Prakash, 1968):

According to Indian standard (IS: 1893-2016) specifications, the pressures are located as follows [22].

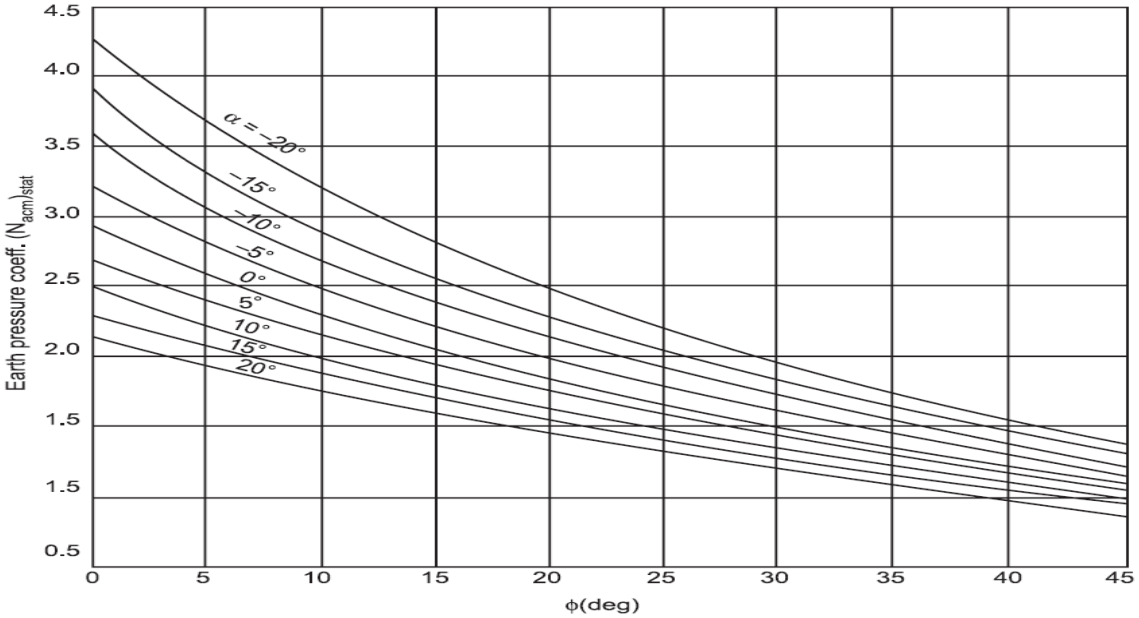

Figure 2.9 $(N_{acm})_{stat}$ versus f for all n (Prakash and Saran, 1966 and Saran and Prakash, 1968) [22].

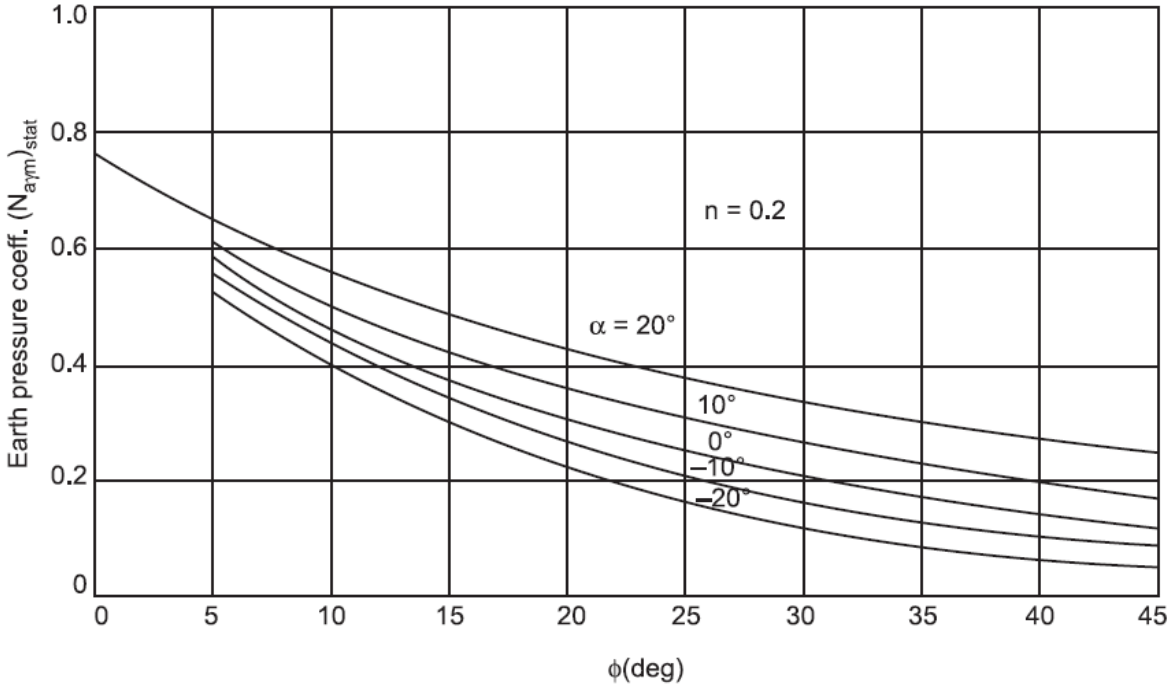

Figure 2.10 $(N_{a\Upsilon m})_{stat}$ versus f for n = 0.2 (Prakash and Saran, 1966; Saran and Prakash, 1968) [22].

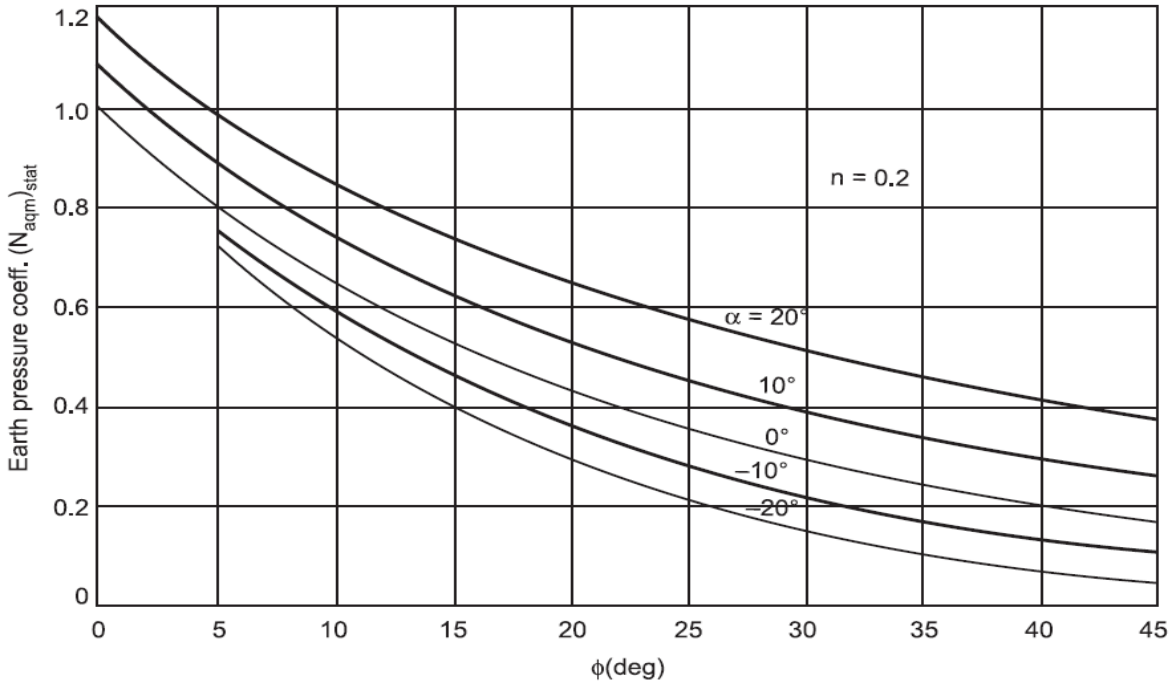

Figure 2.11 $(N_{aqm})_{stat}$ versus f for n = 0.2 (Prakash and Saran, 1966; Saran and Prakash, 1968) [22].

2.6 Conclusion:

Current theories, experimental findings and numerical studies for retaining walls subject to dynamic excitation have been briefly listed in a generally chronological order. Numerical analyses are an accurate way to solve relevant problems, while experiments are good but incur big cost to conduct an accurate one. In spite of these, the MO method is still a current main approach for practical use due to its simplicity. But the MO method becomes impractically complex when more factors like the influence of pseudo–dynamic, logarithmic failure plane is being considered, not to mention the widely known assumptions that are inherent with the MO method [8].

CHAPTER 03

Overview of PLAXIS 2D

3.1 Introduction:

The dynamic response of the retaining structures is a complex issue, and a major challenge in their design, especially under seismic loading conditions [27]. Due to their multiple uses and structural challenges they outline during normal circumstances and seismic events, retaining walls constitute an important concern for civil engineers. Design of these structures requires accurate determination of lateral earth pressure under various conditions [28].

Over the last decades, numerical methods have gained increasing importance in practical geotechnical engineering and numerical methods have become a standard tool in geotechnical design, widely accepted by the geotechnical profession. The advantages of numerical analyses for solving practical problems have been recognized, and developments in software and hardware allow their application in practice with reasonable effort [29]. For dynamic finite element analysis, the variations of acceleration in the soil is of great importance because these variations lead to equivalent thrusts through application of Newton's laws. Therefore, methodologies are developed to implement the effect of inertia into finite element modeling [15]. This chapter aims to present PLAXIS 2D, a widely used finite element software in geotechnical engineering, and to explore its application in the design of cantilever retaining walls and its analysis.

3.2 What is finite element:

The limitations of the human mind are such that it cannot grasp the behavior of its complex surroundings and creations in one operation. Thus the process of subdividing all systems into their individual components or 'elements', whose behavior is readily understood, and then rebuilding the original system from such components to study its behavior is a natural way in which the engineer, the scientist, or even the economist proceeds [30]. Finite element method (FEM) is one of the most commonly used approaches for designing of geotechnical structures. Process of modeling geometry of the problem with finite element method includes simplifications and approximations. Defined geometry is divided into a number of "finite elements" (which could be triangular or quadrilateral in shape), each consisting of a number of nodes. Each node has a number of degrees of freedom that implies to the unknowns in the boundary value problem [31]. Any type of soil condition could be simulated by using the finite element method. For given geometry;

applied loads, displacement boundary conditions, and material stress-strain law (i.e. constitutive model) [31].

3.3 Development of plaxis:

Development of PLAXIS began in 1987 at the Technical University of Delft as an initiative of the Dutch Department of Public Works and Water Management. The initial goal was to develop an easy-to-use 2D finite element code for the analysis of river embankments on the soft soils of the lowlands of Holland. In subsequent years, PLAXIS was extended to cover most other areas of geotechnical engineering. Because of continuously growing activities, a company named PLAXIS b.v. was formed in 1993. In 1998, the first PLAXIS version for Windows was released. In the meantime, a calculation kernel for 3D calculations was being developed. After several years of development, the PLAXIS 3D Tunnel program was released in 2001[32].

3.4 What is plaxis 2d:

Plaxis 2D is a two-dimensional finite element software used for analysis of any geotechnical problem. Identifying the problem is the key point at the beginning of analysis [31]. Plaxis program is a series of program designed to solve various geotechnical problems, it can analyze the stability in geotechnical issues so it needed to design many constructions such as foundation, retaining wall, etc. [33]. PLAXIS 2D is a package of 04 modules that are INPUT, CALCULATION, OUTPUT, CURVES [34].

1. Plaxis Input module :

The analysis of a new project with the software must starts by the creation of a geometry model. This geometry model is a 2D representation of the real three-dimensional and consist of three components which are points, lines and clusters. A geometry model should include a representative division of subsoil into distinct soil layers, structural objects, construction stage and loadings [34].

2. Calculation mode:

In the *Calculation mode*, a number of calculation phases can be defined. Different load cases and geometries are set to simulate a realistic building sequence. For every step, different groundwater conditions can be set, and construction elements could be activated. Excavation is simulated by deactivation of cluster [35].

3. Output mode :

In the third main part of PLAXIS is the output mode and is used for post processing of the calculation result. Deformations, strains and pore-pressures are visualized for every phase of the calculation and for construction elements bending moments and shear forces can be studied. Curves for e.g. safety factor analysis could be plotted [35].

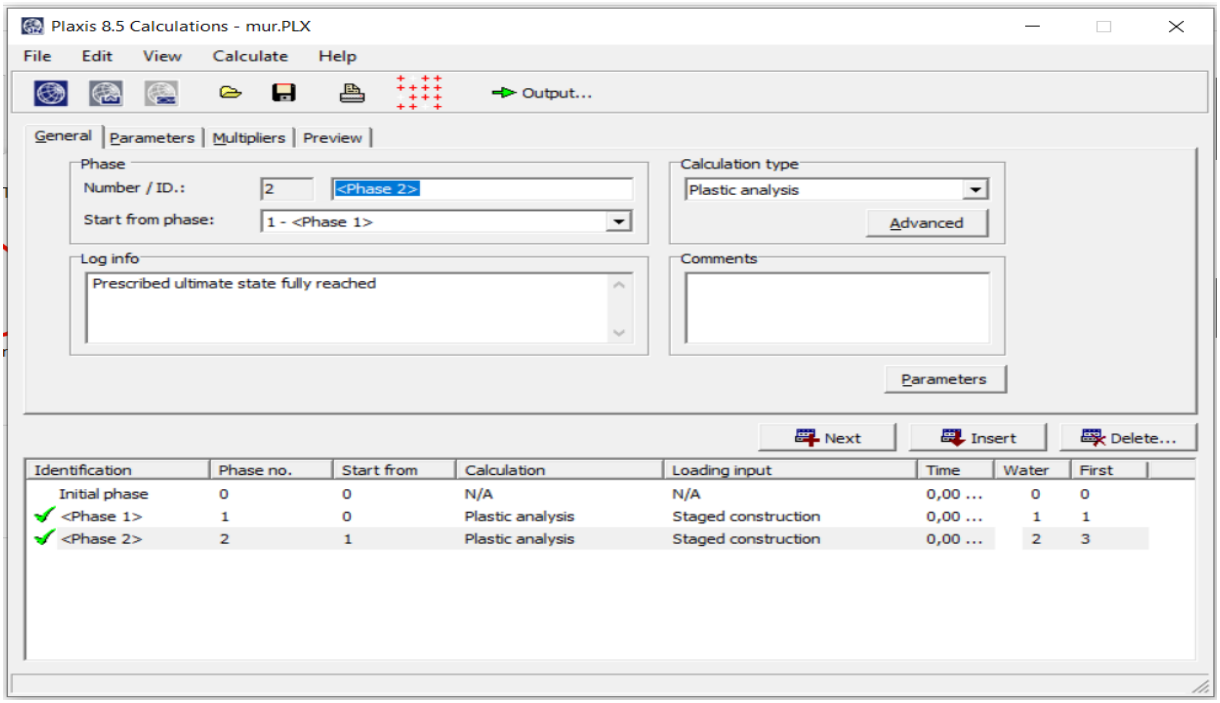

Figure 3.1 Main window of the calculations program.

4. Plaxis curves program :

The curve program is used to generate the stress paths, stress-strain diagrams and load displacement curves of pre-selected point in the geometry. These curves allow to visualize the variation of some quantities for various calculation and by this observed the local and global behavior of the soil [34].

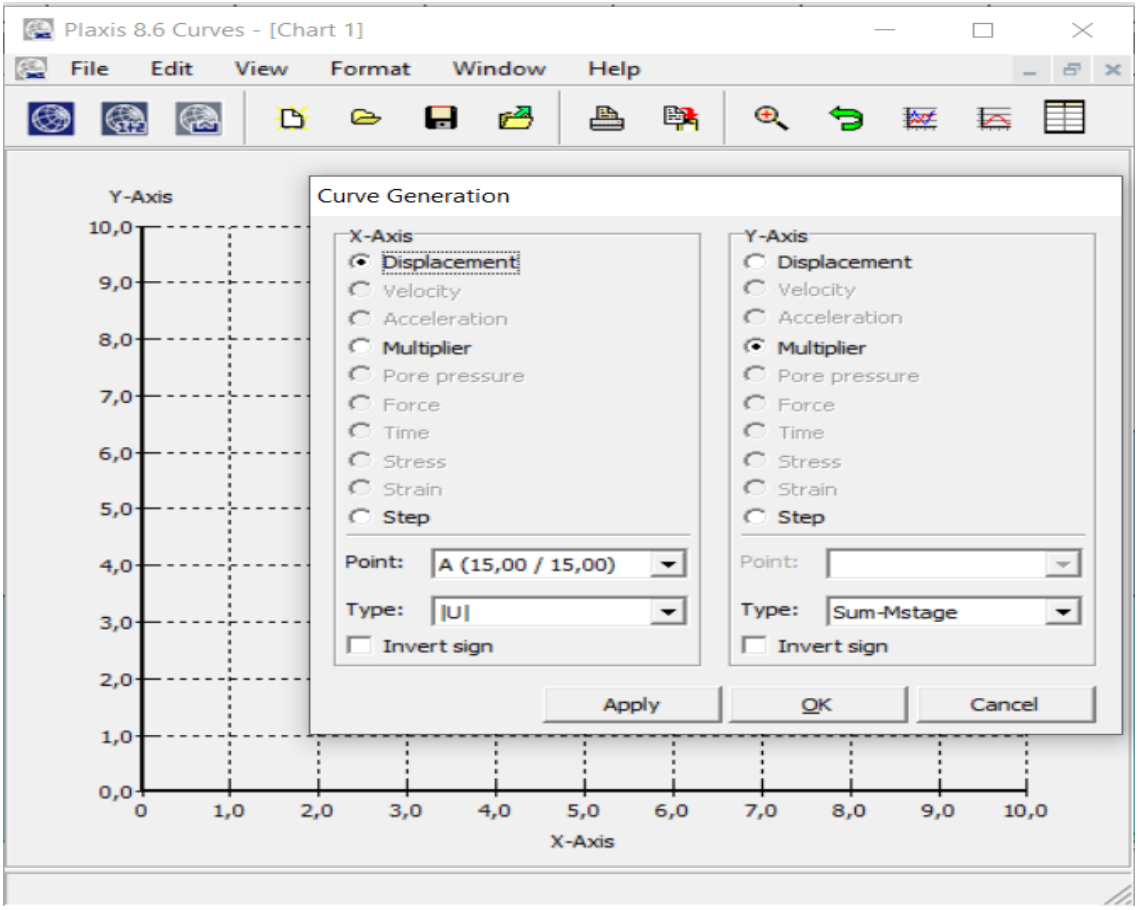

Figure 3.2 Main window of the curves program.

3.5 Overview of the Plaxis 2d code:

3.5.1 General setting:

If a new project is to be defined, the General settings window as shown in **Figure 3.3** appears. This window consists of two tab sheets. In the first tab sheet miscellaneous settings for the current project have to be given. A filename has not been specified

here;this can be done when saving the project.

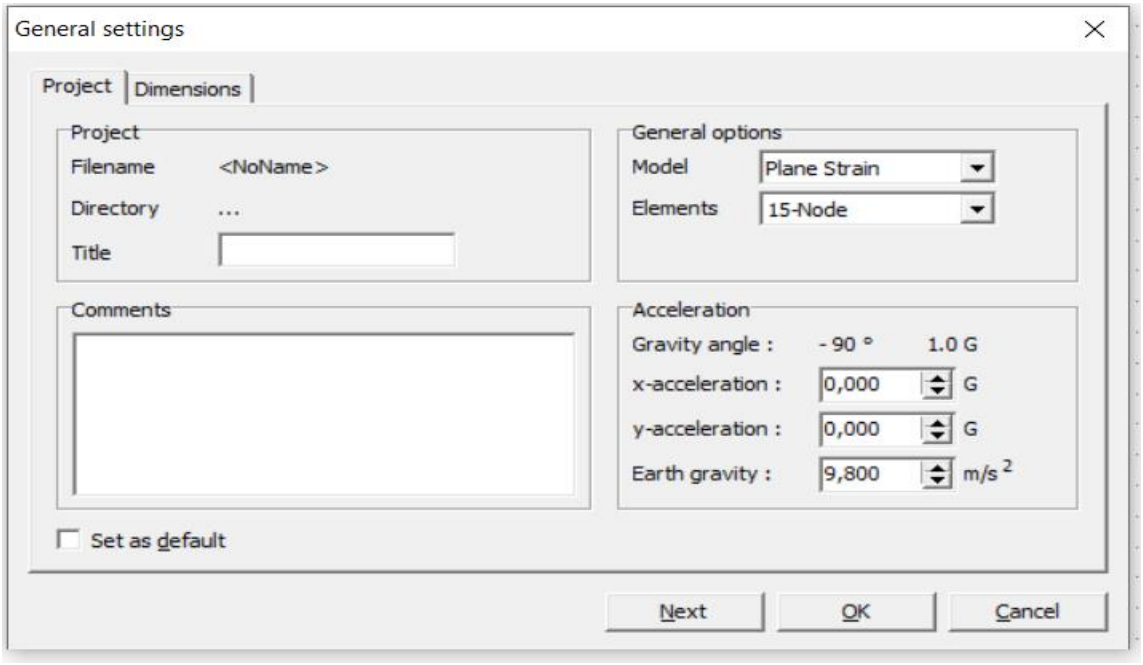

Figure 3.3 General settings window (Project tab sheet).

a) Elements:

During the generation of the mesh, clusters are divided into triangular elements. A choice can be made between 15-node elements and 6-node elements. The powerful 15-node element provides an accurate calculation of stresses and failure loads. In addition, 6-node triangles are available for a quick calculation of serviceability states. Considering the same element distribution (for example a default coarse mesh generation) the user should be aware that meshes composed of 15-node elements are actually much finer and much more flexible than meshes composed of 6-node elements, but calculations are also more time consuming. In addition to the triangular elements, which are generally used to model the soil, compatible plate elements, geogrid elements and interface elements may be generated to model structural behavior and soil-structure interaction.

b) Stress points :

In contrast to displacements, stresses and strains are calculated at individual Gaussian integration points (or stress points) rather than at the nodes. A 15- node triangular element contains 12 stress points as indicated in Figure 3.4a and a 6-node triangular element contains 3 stress points as indicated in Figure 3.4b. Stress points may be pre-selected for the generation of stress paths or stress-strain diagrams[36].

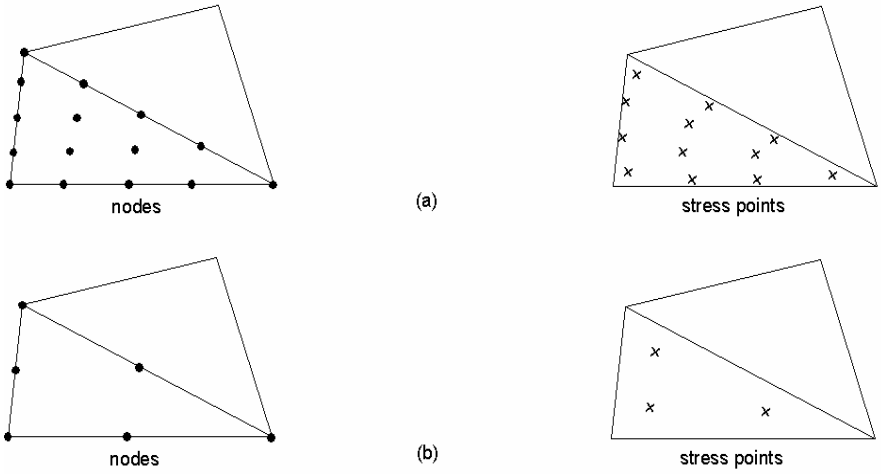

Figure 3.5 Nodes and stress points [36].

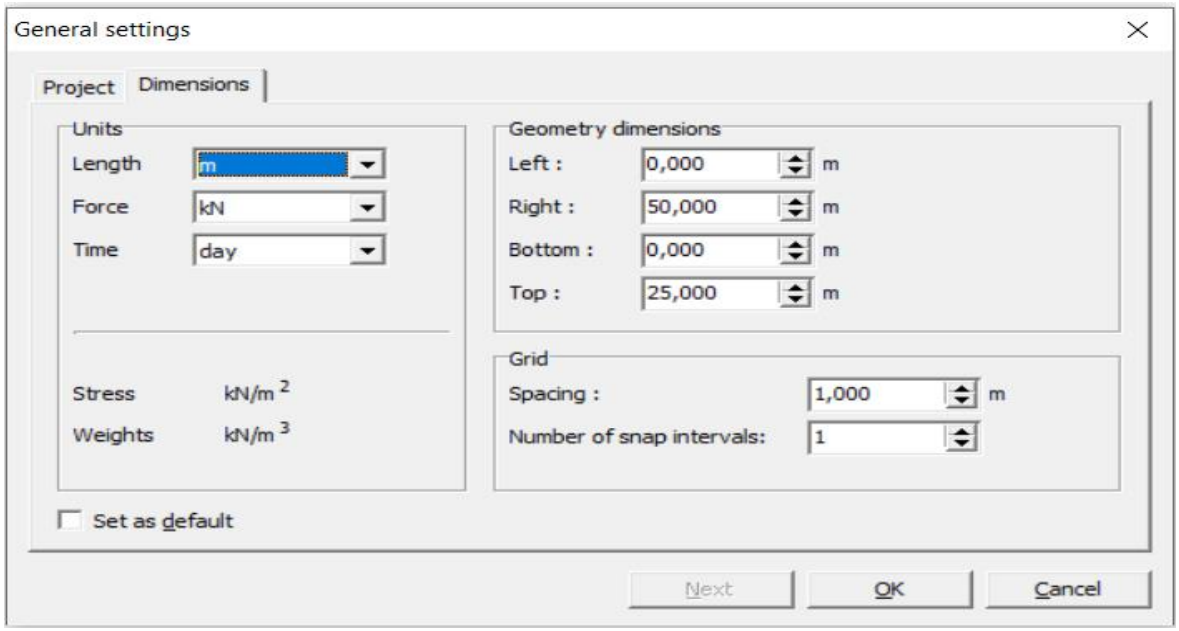

Figure 3.4 General settings window (dimensions tab sheet).

3.5.2 Materials models:

Selection of the material model and soil parameters will have a significant influence on the results of numerical analysis. In recent years, many constitutive soil models have been developed, so there are many options to be used in the simulation of soil behavior in finite element programs such as Plaxis, Midas GTS and Flac. However, each constitutive model has different capabilities and limitations [37].

a) Mohr-Coulomb Model (MC):

Mohr-Coulomb (MC) is the simplest model investigated in this study and it is a linear elastic-perfectly plastic model. Linear elasticity of the model is ensured by Hooke's law and the elastic region is assumed to be up to failure. Stress state at failure is predicted by Mohr-Coulomb failure criterion and a constant stress level is assumed in the plastic region for which the hardening of soil is ignored. In other words, the non-linear behavior of the soil is modelled with bilinear lines in MC model

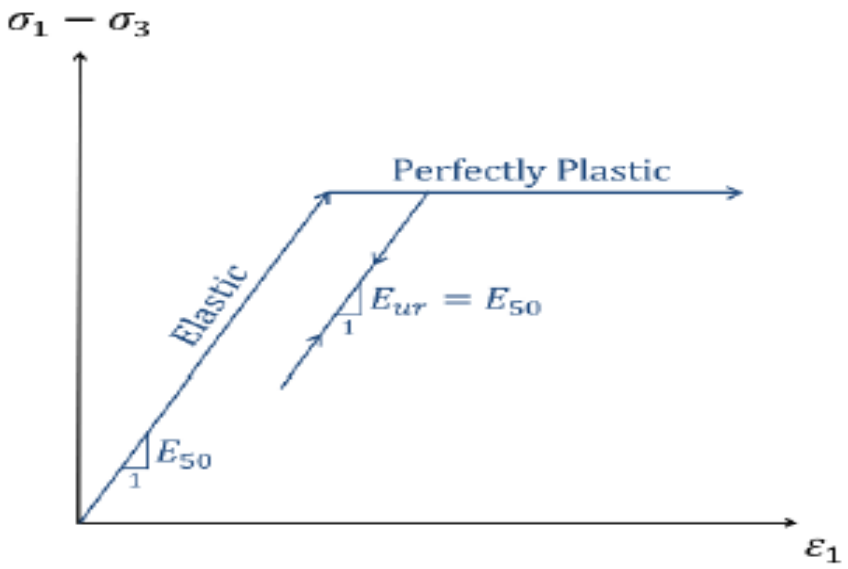

Figure 3.6 Mohr-Coulomb Model Soil Behavior [37].

b) The Hardening Soil Model:

Hardening soil (HS) is a more sophisticated model compared to Mohr-Coulomb in the way of simulating the soil behavior. Model is developed by Schanz (1998) and Shanz et al. (1999). The hyperbolic stress-strain relationship of the model is formulated by Kondner

(1963) which is also used in Duncan and Chang model (1970). However, the main difference of the hardening soil model is the use of plasticity rather than elasticity and the two types of hardening (isotropic), which are formulated by Vermeer (1978) [37].

3.5.3 Input of geometry objects:

The creation of a geometry model is based on the input of points and lines. This is done by means of a mouse pointer in the draw area. Several geometry objects are available from the menu or from the toolbar. The input of most of the geometry objects is based on a line drawing procedure. In any of the drawing modes, lines are drawn by clicking the left mouse button in the draw area. As a result, a first point is created. On moving the mouse and left clicking with the mouse again, a new point is created together with a line from the previous point to the new point. The line drawing is finished by clicking the right mouse button, or by pressing the <Esc> key on the keyboard.

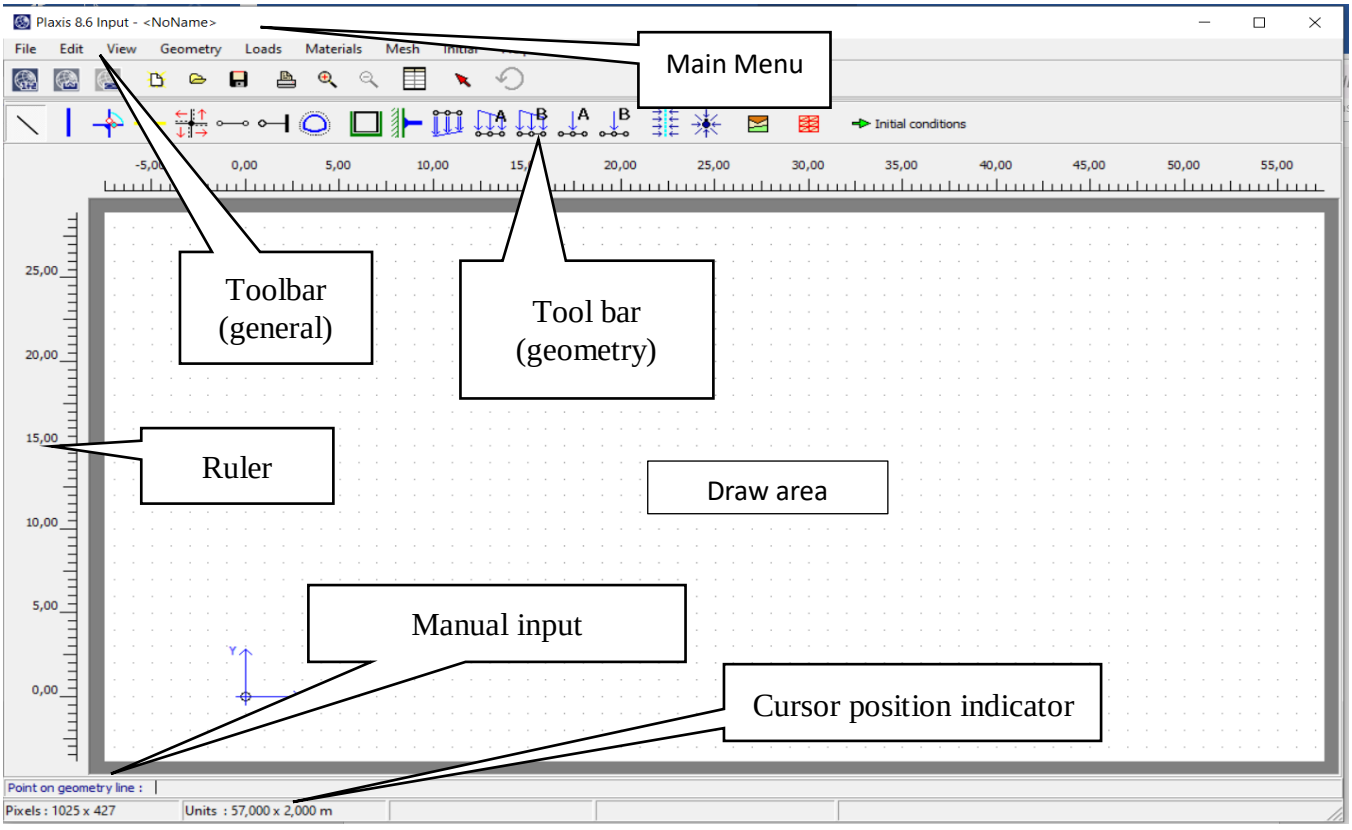

Figure 3.7 Main window of the Input program.

A. **Main menu :**

The main menu contains all the options that are available from the toolbars, and some additional options that are not frequently used.

B. **Tool bar (General) :**

This tool bar contains buttons for general actions like disk operations, printing, zooming or selecting objects. It also contains buttons to start the other programs of the PLAXIS package (Calculations, Output and Curves).

C. **Tool bar (Geometry) :**

This tool bar contains buttons for actions that are related to the creation of a geometry model. The buttons are ordered in such a way that, in general, following the buttons on the tool bar from the left to the right results in a completed geometry model.

D. Rulers :

At both the left and the top of the draw area, rulers indicate the physical coordinates, which enables a direct view of the geometry dimensions.

E. **Draw area :**

The draw area is the drawing sheet on which the geometry model is created. The draw area can be used in the same way as a conventional drawing program. The grid of small dots in the draw area can be used to snap to regular positions.

F. **Origin:**

If the physical origin is within the range of given dimensions, it is represented by a small circle, with an indication of the x- and y-axes.

G. **Manual input:**

If drawing with the mouse does not give the desired accuracy, then the Manual input line can be used. Values for x- and y-coordinates can be entered here by typing the corresponding values separated by a space. The manual input can also be used to assign new coordinates to a selected point or refer to an existing geometry point by entering its point number [36].

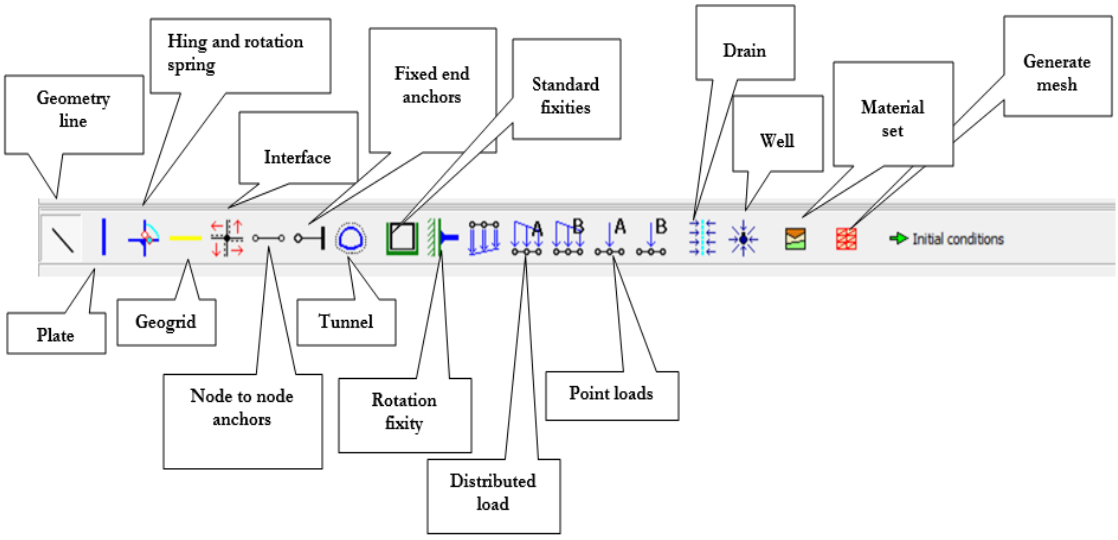

Figure 3.8 THE INPUT MENU.

3.6 Conclusion:

Overall, the development of the PLAXIS software and its associated soil models has been carried out with meticulous attention to detail. PLAXIS 2D allows engineers to accurately simulate soil behavior, structural components, and their interactions through the finite element method.

CHAPTER 4

Static and dynamic design of cantilever retaining Wall

4.1 Introduction:

The sizing and design of a cantilever retaining wall focus on determining the dimensions of the stem and base slab (heel and toe), These dimensions must be chosen to ensure the wall's structural stability, durability, and overall cost-efficiency. The wall must be verified to resist different loads, such as active earth pressure, the self-weight of the wall, and the weight of the backfill. The design process typically requires verification against sliding, overturning, and bearing capacity failure under both static and dynamic conditions.

4.1.1 Presentation of the cantilever retaining Wall:

The cantilever retaining wall shown below is backfilled with cohesionless soil having a unit weight of γ_s = 17 kN/m³ and an internal friction angle of ϕ = 35°. The concrete structure has a self-weight of 24.525 kN/m³, and the angle of interface friction between the backfill soil and the wall surface is δ = 20° with allowable soil bearing pressure of $\bar{\sigma}$ =2.2 bar, this retaining structure is located in the Wilaya of M'sila, a region of moderate seismicity (Zone III) according to the Algerian Seismic Regulations (RPA 2024). The structure belongs to Usage Group 2 and is situated on Site Class 3 (soft soil site).

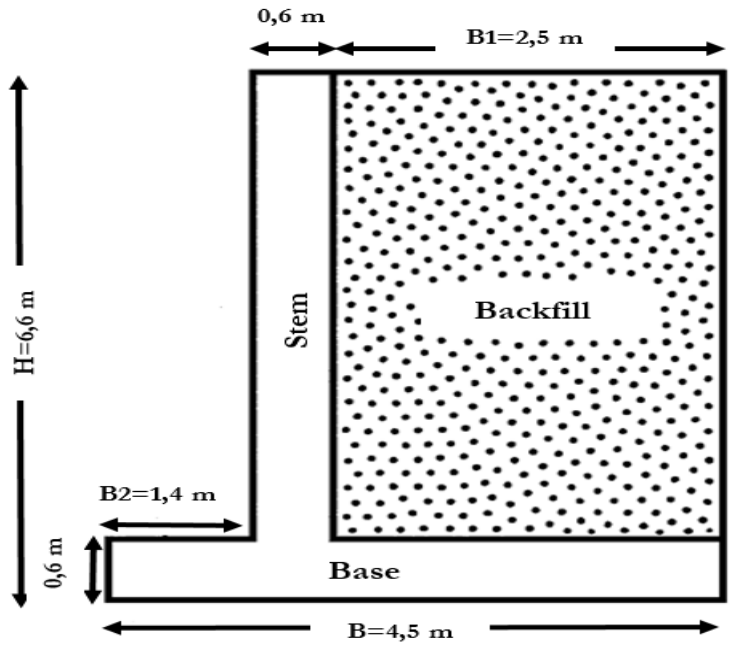

Figure 4.1 Details of the Cantilever Retaining Wall.

4.2 Determination of the weight and center of gravity of the cantilever retaining Wall:

Calculation of the total weight is essential for determining the resisting moment against sliding and overturning. The following figure shows the wall and backfill divided into subsections for the calculation of the weight and the centroids of the structural wedge for (backfill, stem, and base).

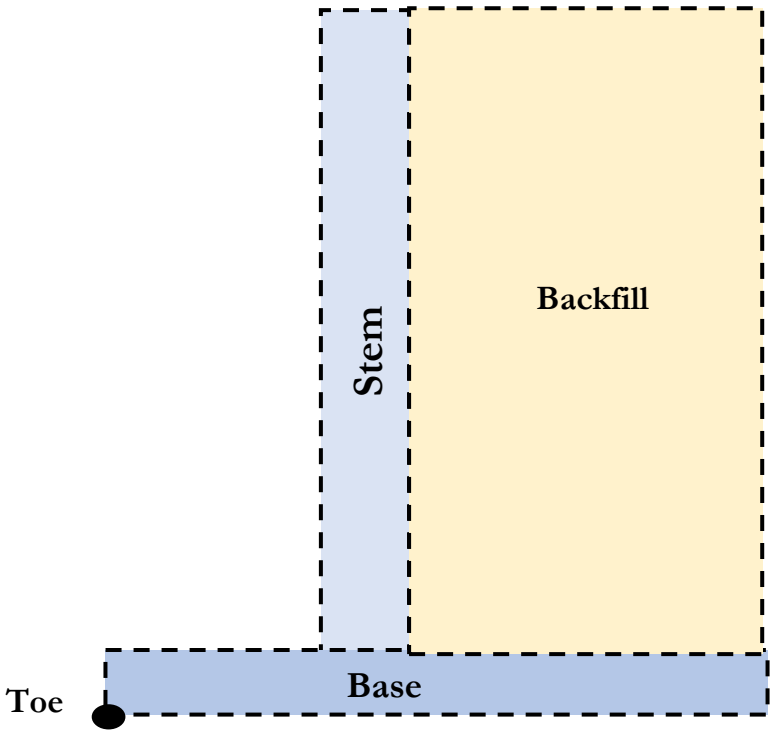

Figure 4.2 Division of the retaining wall into subsections for the calculation of internal forces and the center of gravity.

1) Determination of the weight for (backfill, stem and base) :

Calculation of the total weight is carried out using the equation below:

$$W = \Upsilon * V \qquad [\text{kN}]$$

V: Volume of (backfill, stem and base)

Figures (4.3,4.4 and 4.5) show the weights and centers of gravity of each subsection (backfill, stem, and base)

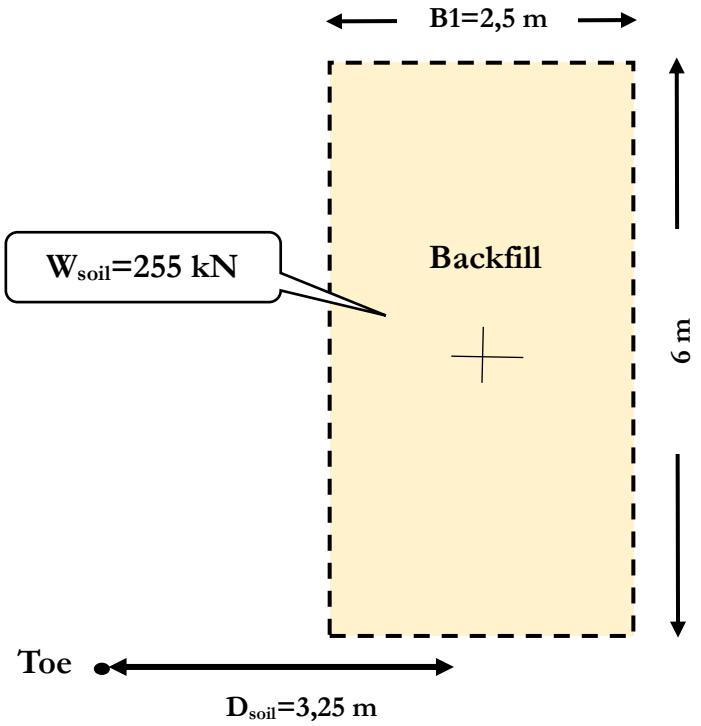

Figure 4.3 Backfill weight for the Cantilever Retaining Wall.

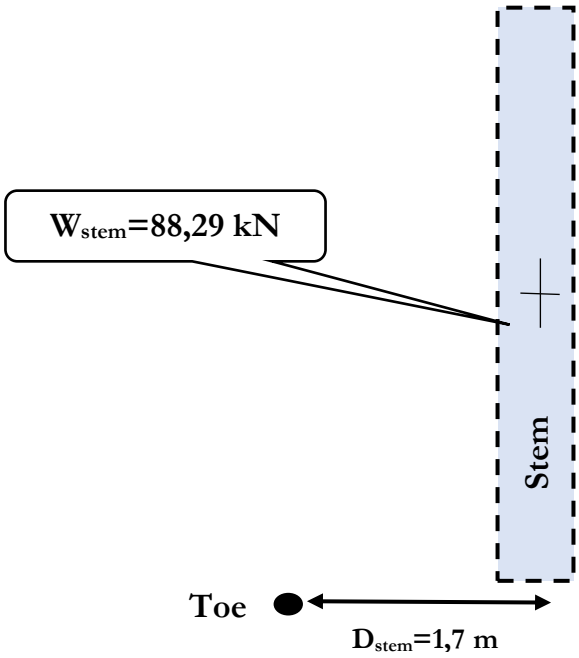

Figure 4.4 The stem weight for the Cantilever Retaining Wall.

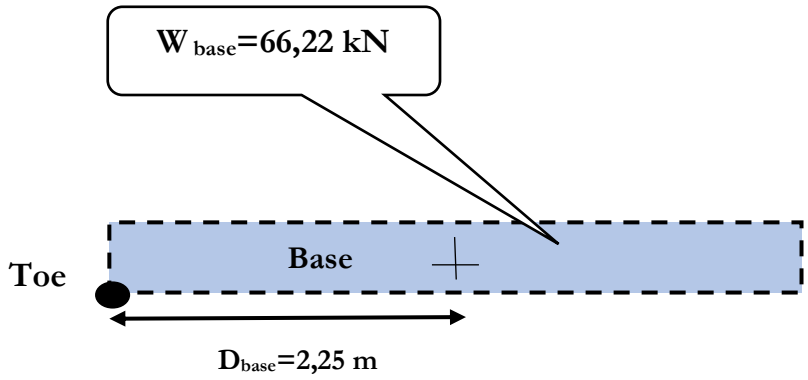

Figure 4.5 The base weight for the Cantilever Retaining Wall.

The results shown in the figures above are summarized in Table 4.1.

Table 4.1 The weight and center of gravity of the cantilever retaining Wall:

Description	Fv =Weight(kN)	D(m)	Moment(kN.m)
Backfill	255	3,25	828,75
Stem	88,29	1,7	150,093
Base	66,22	2,25	148,989375
∑stem, base	154,5075		299,082375
Totale	409,51		1127,83
Centroid of entire wall(D_{RW})	**1,94 m**		

4.3 Static Earth Pressure Analysis and cantilever Retaining Wall Stability Verification:

a. The active earth pressure coefficient

$$K_{a\ (static)}=\tan^2(45^\circ-\frac{\phi}{2})$$

b. The active earth pressure Pa acting on a wall is giving by

$$Pa_{\ (static)}=\frac{1}{2}\times \square s\times ka\times H^2$$

Table 4.2 shows the results of the active earth pressure and its coefficient.

Table 4.2 Static Lateral Earth Pressure Results:

ka	γ_s(kN/m³)	$Pa_{(static)}$(kN)	$D_{(static)}$(m)	Moment (kN.m)
0,271	17	82,92	2,6	215,60

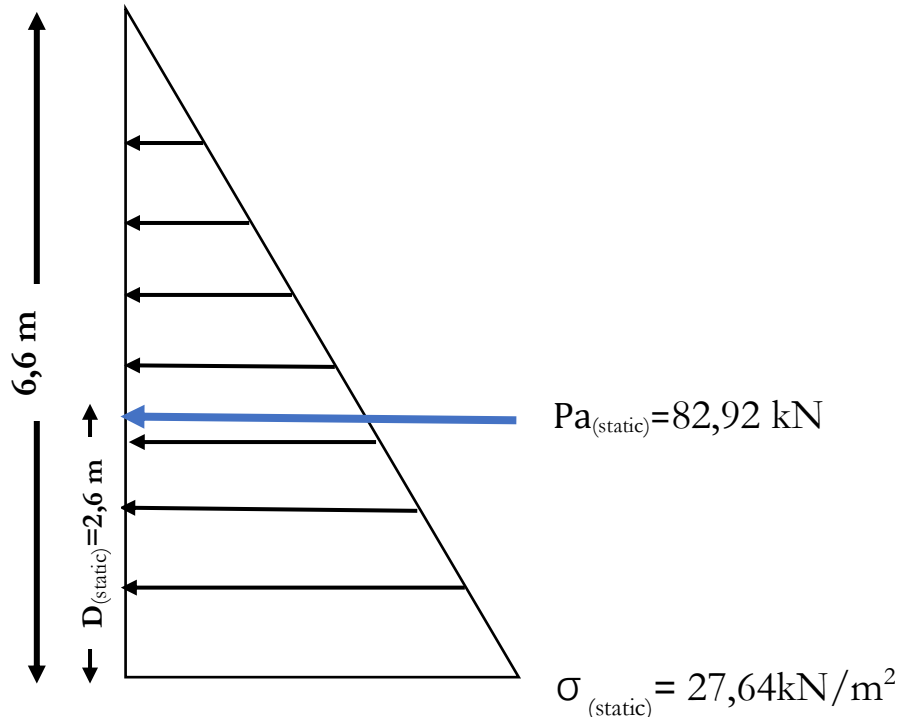

Figure 4.6 Static Lateral earth pressure for the Cantilever Retaining Wall.

There are still forces acting on the structural wedge that have yet to be determined specifically, the shear force (T) and the normal force (N) at the base of the wall. As shown, the following equations illustrate how the magnitudes of T and N are obtained through equilibrium analysis in the horizontal and vertical directions, respectively. The location of the normal force X is then determined by summing moments about the toe of the wall.

4.3.1 Calculation of the shear force (T) and the normal force (N):

a) The normal force (N)

+ ↑ $\sum F_v=0$

$N=W_s+W_b=255+154,51$

$N=409,51$ kN

b) The shear force (T)

+ → $\sum F_h=0$

$T=Pa=82,92$ kN

c) Calculation of X

$\sum M_{Toe}=0$

$X=\frac{-Pa*D5+Wb*D4+Ws*D1}{N}$ = 2,23m From the toe.

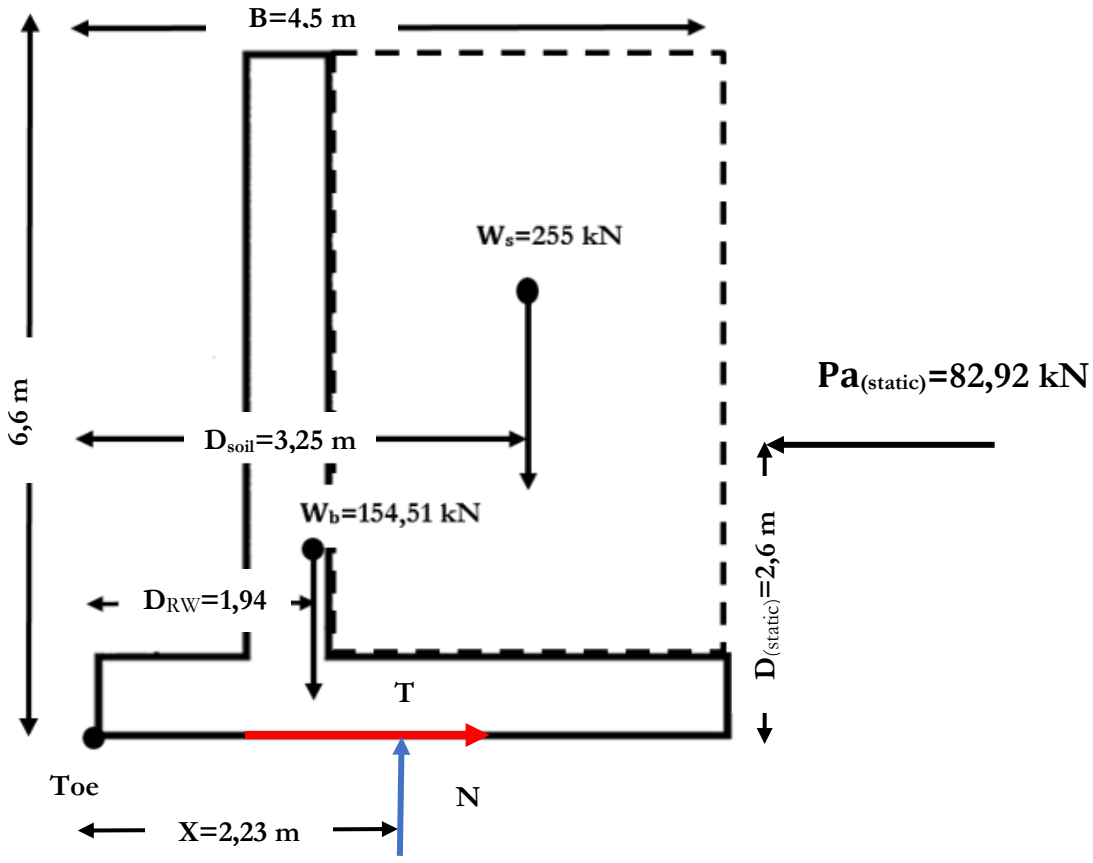

Figure 4.7 Free body diagram of the structural wedge.

4.3.2 Verification of a cantilever retaining wall against sliding:

The wall will remain in equilibrium in overturning, if the forces about the moment center resisting overturning are greater than or equal to the forces about the moment center causing overturning. The forces resisting overturning are the frictional resistance at the wall base, and the soil in front of the wall base [6]. The results of the safety factor against sliding are summarized in table 4.3.

Stability against sliding is verified using the equations below:

$$\mathbf{Fs}=\frac{Nu\times tan(\delta)}{pa} \quad , \quad \mathbf{T_{ult}}=\mathrm{Nu}\times\tan(\boldsymbol{\delta}) \quad , \quad \mathbf{Nu}=1{,}35\mathrm{N}$$

$$\mathbf{N}= W_{base}+ W_{stem}+ W_{soil}$$

$$\mathbf{T}=Pa_{(static)}$$

Table 4.3 Verification of a cantilever retaining wall against sliding:

δ(°)	Nu(kN)	T(kN)	T_{ult}(kN)	Fs
20	552,84	82,92	201,22	2,43

The factor of safety is

Fs=2,43 > 1,5 , Sliding stability is verified

4.3.3 Verification of a cantilever retaining wall against overturning:

failures occur when moment equilibrium is not satisfied; bearing failures at the base of the wall are often involved [5]. The results of the safety factor against sliding are summarized in table 4.3.

Table 4.4 Verification of a cantilever retaining wall against overturning:

Description	Fv =Weight(kN)	D(m)	Moment(kN.m)
T_{ult}(kN)	201,22	2,23	448,23
Pa(kN)	82,92	2,6	215,60
Fs	2,08		

Fs=2,08 >2 Overturning stability is verified

4.3.4 Verification of a cantilever retaining wall against Bearing capacity:

The footing should be sized to ensure that the maximum contact pressure does not exceed the bearing capacity of the soil. [3]. Stability against Bearing capacity is verified using the equations below

$$e=\frac{B}{2}-X \text{ and } \sigma_{max}=\frac{Nu}{B}*(1+\frac{6e}{B})<\bar{\sigma}$$

with $$\sigma_{min}=\frac{Nu}{B}*(1-\frac{6e}{B})>0$$

The results of the safety factor for bearing capacity are summarized in table 4.5.

Table 4.5 Verification of a cantilever retaining wall against Bearing capacity:

e(m)	σ_{max}(kN/m²)	σ_{min}(kN/m²)	$\bar{\sigma}$ (kN/m²)
0,022	122,88	119,19	220

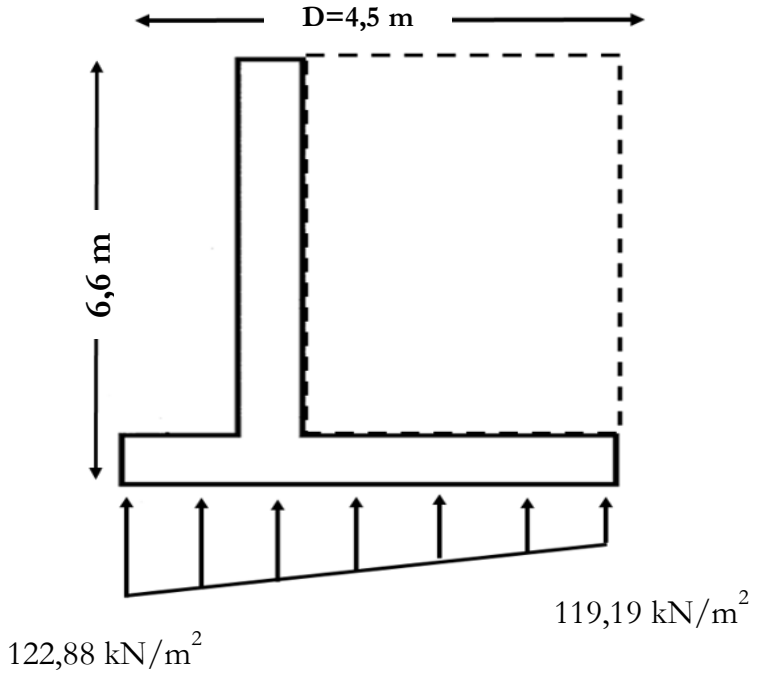

Figure 4.8 Bearing capacity Verification (static conditions).

4.4 Dynamic Earth Pressure Analysis and Cantilever Retaining Wall Stability Verification:

The dynamic response of earth-retaining structures is a complex issue. The design of these structures under seismic loading conditions is, therefore, quite challenging. Because there are not many case histories on field performance of earth-retaining structures, the theory of dynamic response has been based on the results from both model tests and numerical analyses. The most common approach to the seismic design of retaining walls, especially where the expected ground acceleration is less than or equal to 0.29g, involves estimating the loads imposed on the wall during earthquake shaking and then ensuring that the wall can resist those loads. Because the actual loading on retaining walls during earthquakes is extremely complicated, seismic pressures are usually estimated using the Mononobe-Okabe pseudo-static method [25].

4.4.1 Dynamic Active Earth Pressure (Pae) Calculation According to RPA 2024 Using the Mononobe-Okabe Theory for Cohesionless Soil:

According to RPA 2024, the stability verification is carried out using two seismic coefficients k_h and k_v. These coefficients are used to determine the horizontal and vertical forces acting on the retaining structure.

$$\mathbf{k_h}= \begin{cases} \frac{1}{2}\text{A.I.S: Flexible structures} \\ \frac{2}{3}\text{A. I.S: Semi-flexible structures} \\ \text{A.I.S: Rigid structures} \end{cases} \quad (10.24)$$

$$\mathbf{K_v}= \begin{cases} \pm \frac{1}{2} K_h \text{ Seismic situation of type 1} \\ \pm \frac{1}{3} K_h \text{ Seismic situation of type 2} \end{cases} \quad (10.25)$$

a) Determination of the Natural Period of Cantilever Retaining Walls:

The period of a retaining structure representing the he duration required for the structure to complete one full cycle of vibration, it is calculated using the following equations:

$$T_n=2\pi/\omega_n \quad , \quad K=3EI/L^3 \quad , \quad \omega_n=\sqrt{K/m}$$

The results of the Period of a Retaining Structure are summarized in table 4.6.

Table 4.6 Results for the natural period of the retaining structure:

Weight (kN)	Mass(kg)	EI	K(N/m)	ω_n (rad/s)	T_n(s)
88290	9000	578952000	8041000	29,89	0,021

With a period $T_n = 0.21 \leq 0.2$ s, the cantilever retaining wall is classified as a rigid structure.

b) Dynamic Earth Pressure calculation:

The results are obtained using the Mononobe–Okabe method for cohesionless soil, and the coefficients (A, I, S) are taken from RPA 2024, based on the characteristics of the cantilever retaining wall described above, results are shown in table 4.7.

Table 4.7 Earth pressure result based on RPA 2024:

A	I	S	K_h	K_v	P_{AE} (kN)
0,15	1	1,55	0,233	0,078	134,36

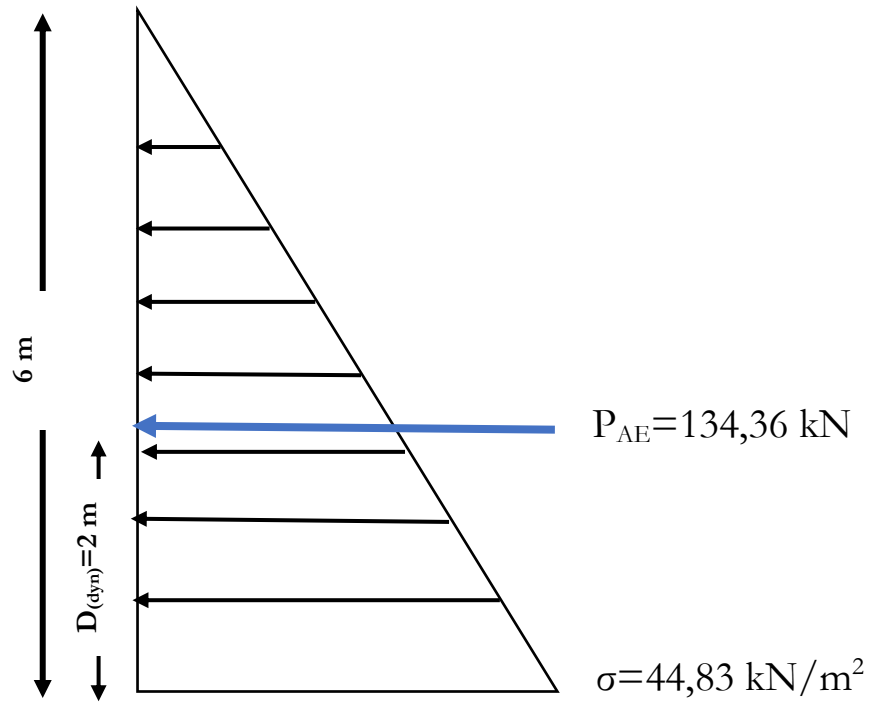

Figure 4.9 Dynamic Lateral earth pressure for the Cantilever Retaining Wall.

4.4.2 cantilever Retaining Wall Stability Verification according RPA 2024:

a) Verification of a cantilever retaining wall against sliding:

According to RPA 2024, the safety factor for verifying the stability against sliding of the retaining structure is 1,25.

Table 4.8 Verification of a cantilever retaining wall against sliding:

δ(°)	Nu(kN)	T(kN)	T_{ult}(kN)	Fs
20	552,84	134,36	201,22	1,50

Fs=1,5 >1,25 Sliding stability is verified

b) Verification of a cantilever retaining wall against overturning:

According to RPA 2024, the safety factor for verifying the stability against sliding of the retaining structure is 1,3.

Table 4.9 Verification of a cantilever retaining wall against overturning:

X(m)	T_{ult}(kN)	P_{AE}(kN)	$D_{(dyn)}$(m)	Fs
2,10	201,22	134,36	2	1,57

Fs=1,57 >1,3 Overturning stability is verified

c) Verification of a cantilever retaining wall against Bearing capacity:

The results of the safety factor for bearing capacity are in table 4.10.

Table 4.10 Verification of a cantilever retaining wall against Bearing capacity:

e(m)	σ_{max} (kN/m²)	σ_{min} (kN/m²)	$\bar{\sigma}$ (kN/m²)
0,152	123,06	97,94	220

With

$\sigma_{max} < \bar{\sigma}$ and $\sigma_{min} > 0$ **Stability is confirmed.**

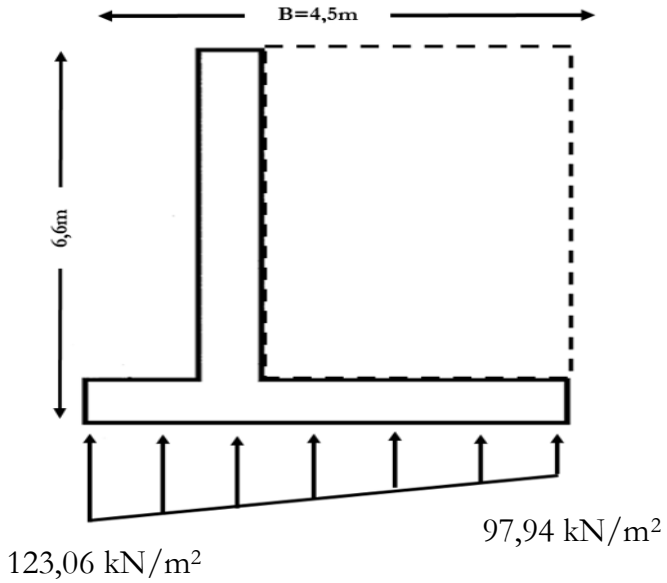

Figure 4.10 Bearing capacity Verification (dynamic conditions).

4.5 Reinforcement of a concrete Cantilever Retaining Wall:

cantilever retaining wall is a widely used structural system for retaining earth in civil engineering projects. Its effectiveness depends mostly on reinforcement to resist the lateral pressures exerted by soil, surcharge loads…...

4.5.1 Stem reinforcement:

Is a vertical cantilever beam fixed at the base, subjected to lateral earth pressure that varies linearly with depth, with the maximum pressure occurring at the bottom. The results of the stem reinforcement design are presented in table 4.11.

Table 4.11 Stem Reinforcement Results for Cantilever Retaining Wall:

Mu(kN.m)	σs(MPa)	fe(MPa)	fc_{28}(MPa)	As(cm^2)
362,78	347,8	400	25	19,5
Harmful cracking				

According to the table of equivalent sections, the choice of reinforcement is **7HA20=21,994 cm^2**

4.5.2 Base reinforcement:

Proper base reinforcement is critical to ensuring the structural stability and durability of a cantilever retaining wall. The base slab, which comprises the heel and the toe, is subjected to various loads, including soil pressure, self-weight, and surcharge loads. steel reinforcement is strategically placed within the base to resist shear forces and bending moments. This reinforcement helps ensure the wall remains stable and safe against sliding, overturning, and structural failure. Calculation of the ultimate bending moment at point B ($\mathbf{Mu_{(B)}}$) is as follows:

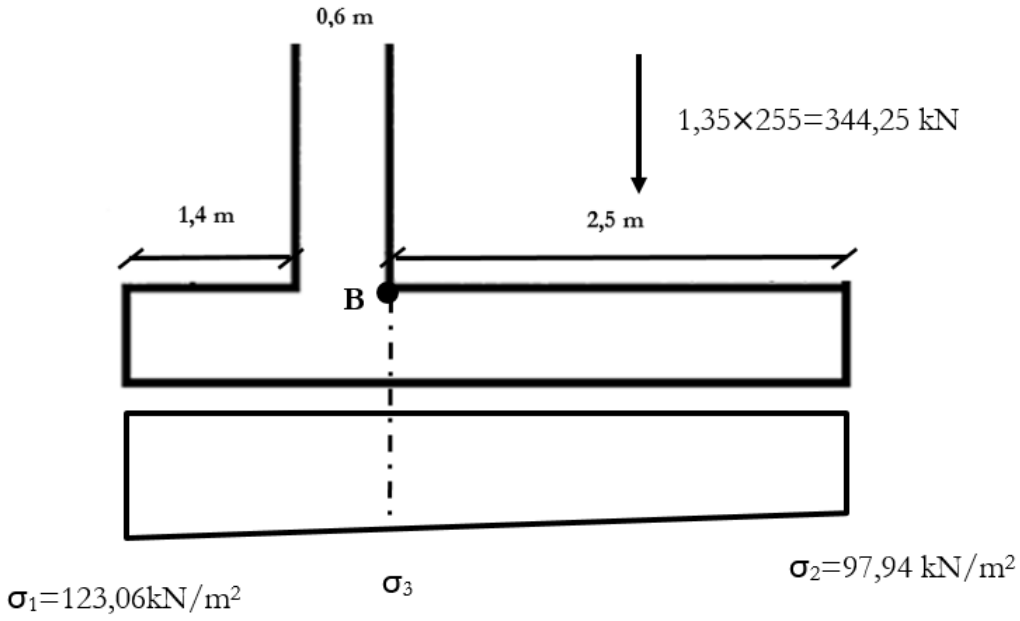

Figure 4.11 The design bending moment at the base of the wall at point B.

a) Ground bearing pressure:

$$\sigma_3=\sigma_2+x=97,94+(123,06-97,94)\times 2,5/4,5$$

$$\mathbf{\sigma_3= 111,89\ kN/m^2}$$

b) Design moment at point B, Mu:

$$Mu=(344,25\times 2,5)/2 + (89,39\times 2,5\times 1,25)/4 - (97,94\times 2,52)/2 - (13,95\times 2,5\times 2,5)/2\times 3$$

$$Mu= 430,31 + 69,84 - 306,06 - 130,81$$

$$\mathbf{Mu= 63,28\ kN.m}$$

The following table presents the results of the base reinforcement.

Table 4.12 Base Reinforcement Results for Cantilever Retaining Wall:

$Mu_{(B)}$(kN.m)	σs(MPa)	Fe(MPa)	fc_{28}(MPa)	As(cm²)
63,28	347,8	400	25	6,4
Harmful cracking				

According to the table of equivalent sections, the choice of reinforcement is **6HA12=6,786 cm²**

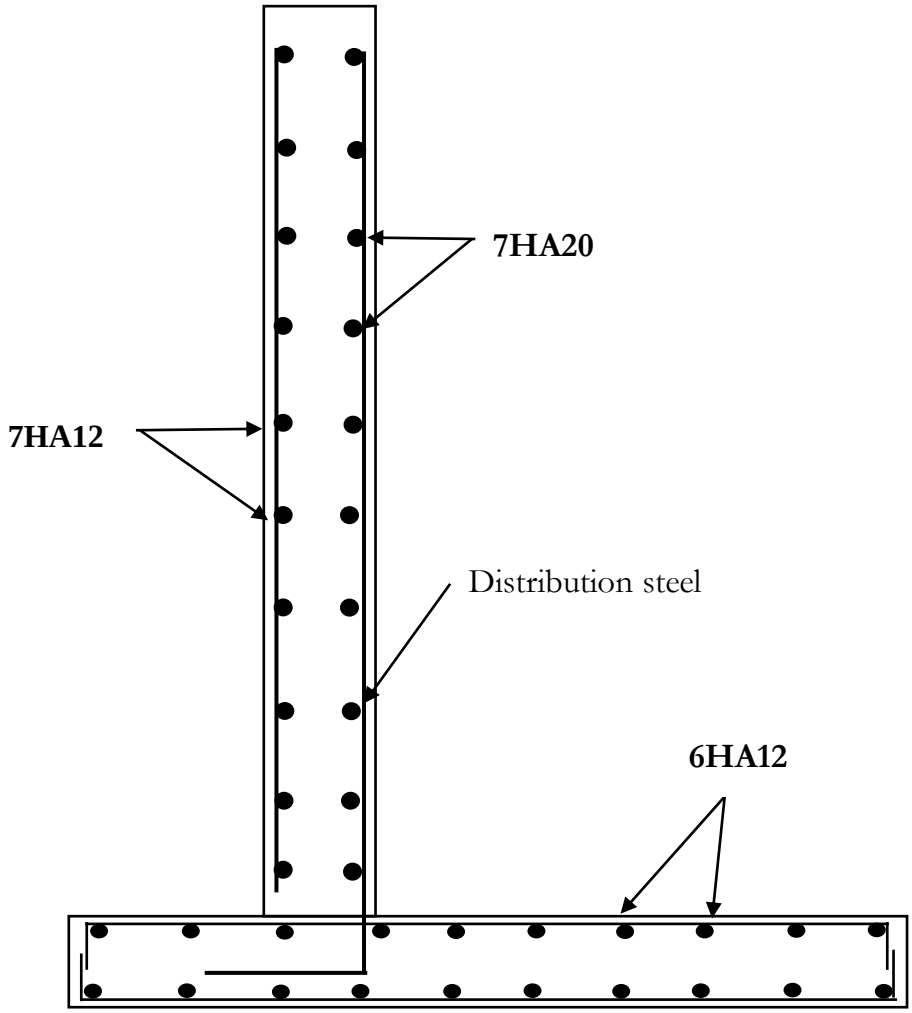

Figure 4.12 Cantilever retaining wall reinforcement.

4.6 Conclusion:

In this chapter, we designed and reinforced a cantilever retaining wall with cohesionless soil (as commonly used in the field), after verifying the wall's stability against sliding, overturning, and bearing capacity. The results obtained in this chapter will be used in the analysis presented in Chapter 5.

CHAPTER 5

Analytical & Numerical Modeling of a cantilever retaining wall

5.1 Introduction:

This chapter focuses on the numerical modeling and analysis of a reinforced concrete cantilever retaining wall using the finite element software PLAXIS 2D. The aim is to simulate the wall's performance under different geotechnical and structural conditions, through this numerical modeling approach, the study seeks to overcome the simplifications of analytical methods and deliver a more accurate and realistic understanding of the wall's deformation behavior and overall stability. Modeling plays a fundamental role in geotechnical studies, as it directly influences the accuracy of diagnostic and predictive analyses regarding the behavior of both soil and structural elements. Our work begins by describing the **geometrical configuration** of the wall and the **mechanical properties** of the soil model. It then details the **modeling steps**, including mesh generation, boundary conditions, and calculation phases. Finally, the results of the simulation are presented and discussed, including comparisons with theoretical (analytical) results where applicable. in this chapter, numerical analyses are conducted using Plaxis software (**version 8.6**), and the corresponding results are systematically presented and discussed.

5.2 Presentation of case study:

The present case study focuses on the geotechnical and structural analysis of a T-shaped reinforced concrete cantilever retaining wall. The wall has a height of 6 meters, a base width of 4.5 meters, and a base thickness of 0.6 meters. The wall is founded on a soil layer 9 meters thick and retains an embankment with a thickness of 6 meters. The overall model width considered for the analysis is 50 meters, the wall is assumed to be fully rigid. Figure 5.1 and Figure 5.2 shows a representation of the different elements of the retaining wall model: the wall, the foundation soil and the backfill. The geotechnical and mechanical characteristics of the backfill material, the foundation soil and the natural ground are summarized in Tables 5.1 and 5.2 respectively.

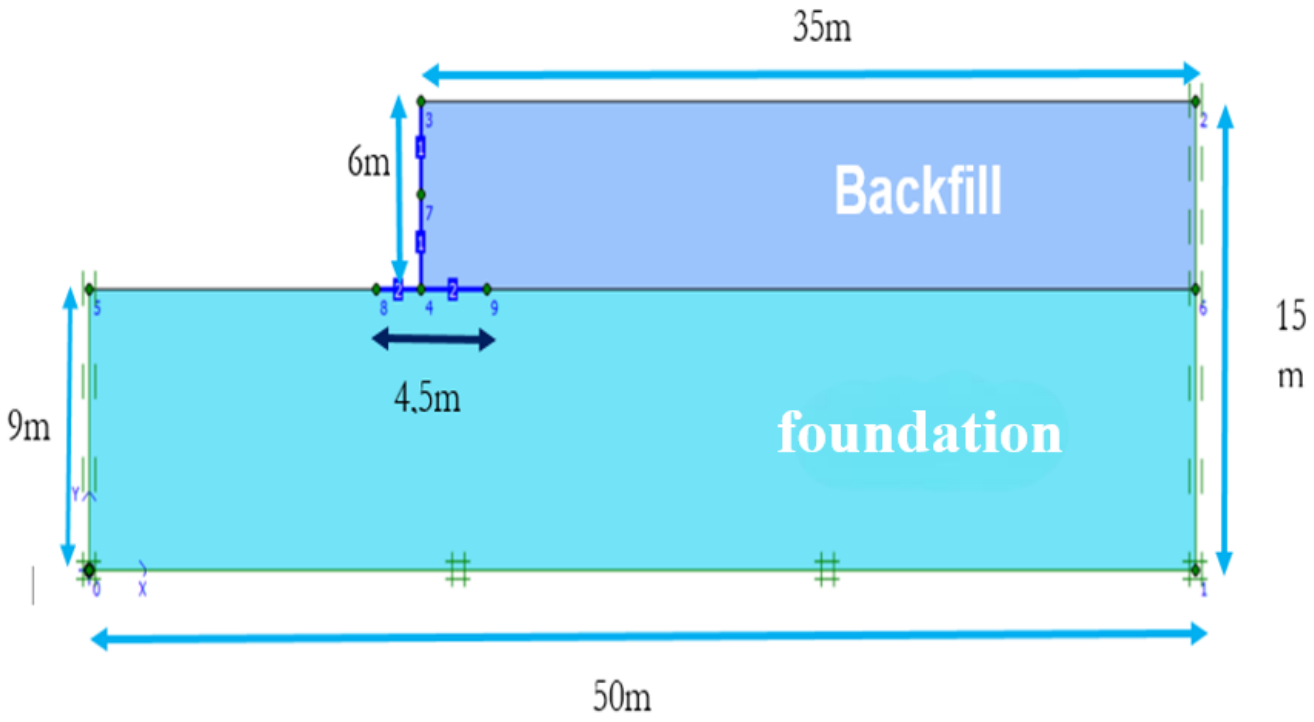

Figure 5.1 Model of a reinforced concrete cantilever retaining wall.

Table 5.1 Soil properties used for the numerical analyses:

Parameters	Symbols(units)	Backfill			Foundation soil
Unsaturated unit weight	Υ_{unsat} (kN/m³)	17			18
Effective Young modulus	E_{ref} (kN/m²)	30000			40000
Poisson's ratio	υ	0,2			0,2
Cohesion	C_{ref} (KPa)	0	5	10	25
Friction angle	ϕ (°)	35			20
Angle of dilatancy	Ψ(°)	2			2
Interface	Rinter	0.66			0.66

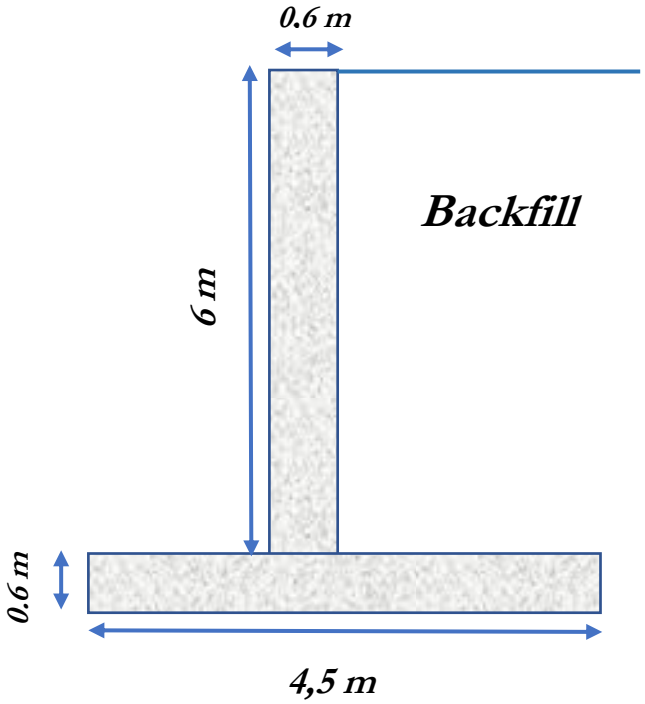

Figure 5.2 cantilever retaining wall Model.

Table 5.2 Properties used for the numerical analyses of the retaining wall:

Parameters	Name	RW	Unit
Normal stiffness	EA	1.930E 07	kN/m
Bending rigidity	EI	5.970E 07	kN.m²
Poisson's ratio	υ	0,2	-

5.3 Dynamics Analytical results:

5.3.1 Mononobe-Okabe Method (cohesionless soil):

The analytical results obtained using the Mononobe-Okabe approach show the values of dynamic active earth pressure ($\mathbf{P_{AE}}$) in cohesionless soil conditions, the coefficient of dynamic active earth pressure ($\mathbf{K_{AE}}$), and the total displacement of the cantilever retaining wall under different peak ground acceleration (**PGA**) levels. The relevant equations are presented in Chapter 2, Section (2.11). All the results are presented in the table 5.3.

Table 5.3 Results of Mononobe-Okabe (MO) method for cohesionless soil (c =0):

PGA(g%)	P_{AE} (kN/m)	K_{AE}	U(cm)
0	82,92	0,271	3,09
0,1	104,36	0,341	3,89
0,15	116,15	0,421	4,33
0,2	128,68	0,421	4,8
0,25	142	0,464	5,3
0,3	156,15	0,51	5,83
0,35	171,18	0,559	6,39
0,4	187,16	0,612	6,98
0,45	204,16	0,667	7,62
0,5	222,27	0,726	8,29
0,55	241,59	0,79	9,01
0,6	262,27	0,857	9,78
0,65	284,48	0,93	10,61
0,7	308,45	1,008	11,51
0,75	334,47	1,093	12,48
0,8	362,98	1,186	13,54
0,85	394,6	1,29	14,72
0,9	430,32	1,406	16,05
0,95	471,9	1,542	17,61
1	523,08	1,709	19,52

The diagrams on the (**Figure 5.3**) illustrates the development of dynamic active earth pressure with varying peak ground acceleration (PGA).The result at (0%g) represents the static (non-seismic) active earth pressure (Pa), while the values corresponding to PGAs ranging from (0.1%g to 1%g) indicate the dynamic active earth pressure(P_{AE}). From the diagram. The total dynamic active earth pressure (P_{AE}) can be summarized using the following relationship: $\mathbf{P_{AE} = Pa + \Delta P_{AE}}$

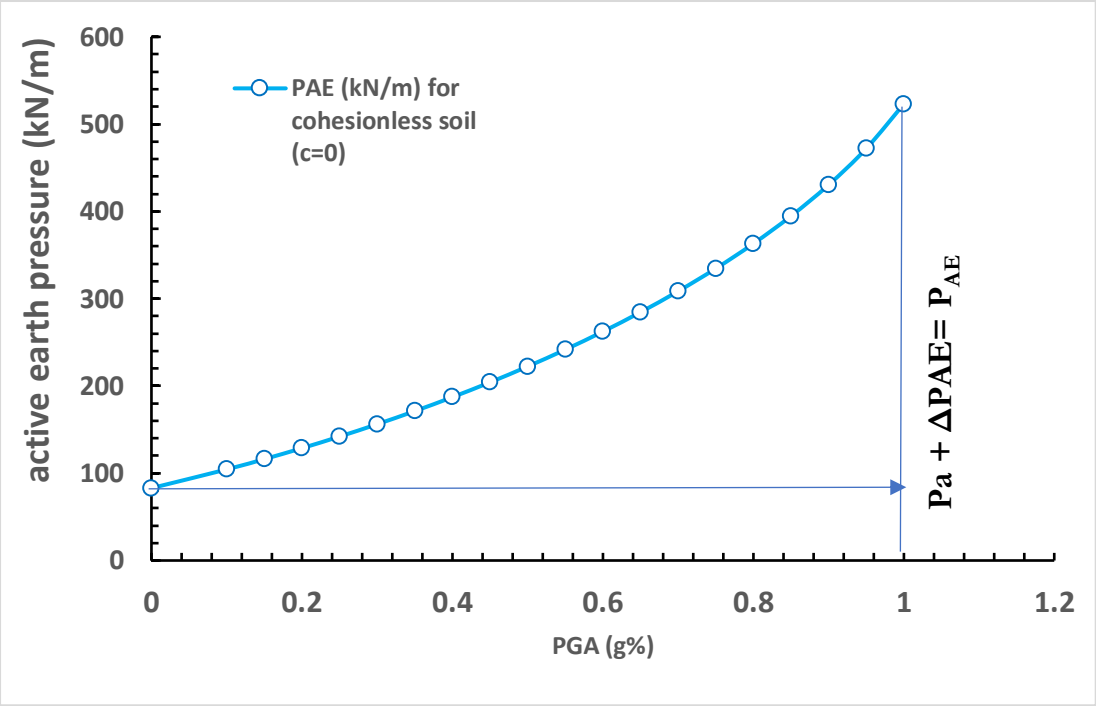

Figure 5.3 Dynamic active earth pressure P_{AE} (kN/m) for cohesionless soil by MO (c=0).

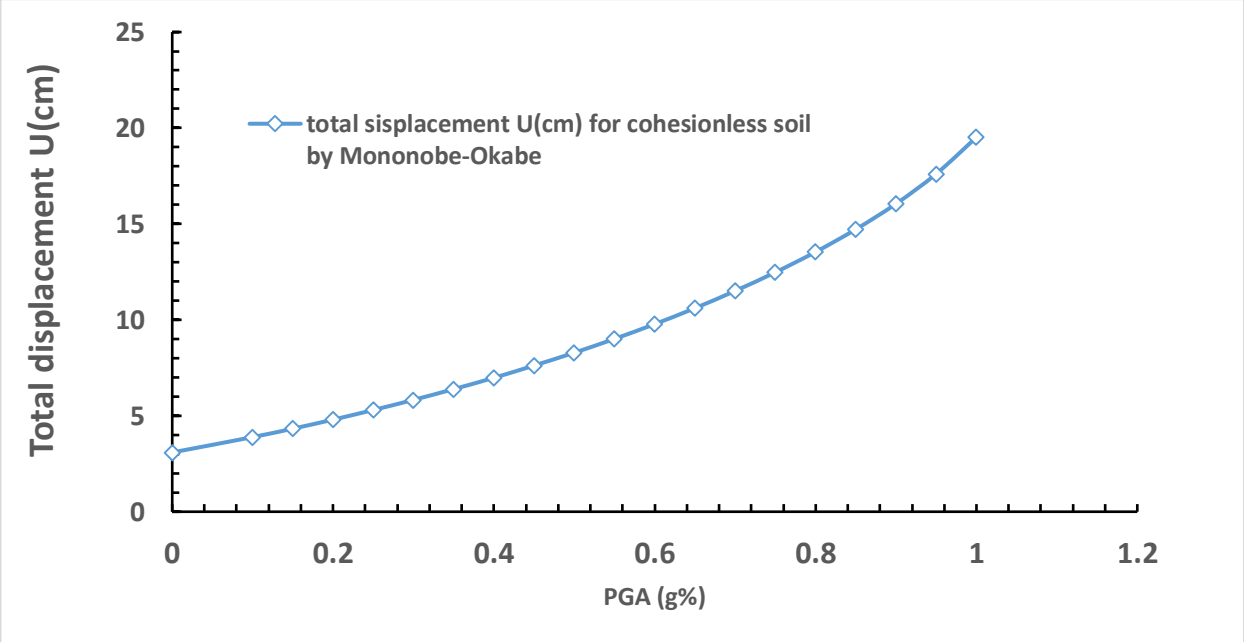

Figure 5.4 Total displacement U(cm) for cohesionless soil by MO (c=0).

a) Analysis of the Analytical results for cohesionless soil by MO:

Both curves show how the dynamic active earth pressure (P_{AE}) and total displacement (U) reacted using the MO method with cohesionless soil. As the peak ground acceleration (PGA) begins to increase, both P_{AE} and U start to increase. When the PGA

reaches around (0.3g%), both P_{AE} and displacement (U) begin to increase rapidly and become significantly larger, this reveal that the soil becomes more sensitive to seismic activity as ground acceleration step up.

5.3.2 Dynamic Earth Pressure (Saran and Prakash 1986) for cohesive Soils (c-ϕ):

The analytical results obtained using the Saran and Prakash 1986 approach show the values of dynamic active earth pressure ($\mathbf{P_{AE}}$) in cohesive soil conditions in both c=5 kPa and c=10 kPa, the earth pressure coefficients ($\mathbf{N_{aqm}}$,$\mathbf{N_{\gamma m}}$) depend on the parameters (α, n, and ϕ) The corresponding equations are provided in Chapter 2.Similarly, the dynamic earth pressure coefficient (λ) is also determined using an equation found in Chapter 2.and the total displacement of the cantilever retaining wall under different peak ground acceleration (**PGA**) levels. The static earth pressure coefficients are

($\mathbf{N_{acm}}$)stat=1,4 obtained from (Figure 2.9)

($\mathbf{N_{aqm}}$)stat=0,28 obtained from (Figure 2.11). All the results are presented in table 5.4 and table 5.5.

Table 5.4 Analytical results by (Saran and Prakash 1986) for (c-ϕ) soil C=5kPa:

PGA(g%)	$N_{(aqm)dyn}$	$N_{(a\gamma m)dyn}$	λ	P_{AE} (kN/m)	U (cm)
0	0,255	0,157	0,83	29,3	1,09
0,1	0,355	0,257	1,35	61,67	2,59
0,15	0,405	0,307	1,62	89,69	2,7
0,2	0,455	0,357	1,88	109,85	4,1
0,25	0,505	0,407	2,14	130,01	4,85
0,3	0,555	0,457	2,41	150,17	5,6
0,35	0,605	0,507	2,67	170,32	6,35
0,4	0,655	0,557	2,93	190,48	7,11
0,45	0,705	0,607	3,19	210,64	7,86
0,5	0,755	0,657	3,46	230,8	8,61
0,55	0,805	0,707	3,72	250,96	9,36
0,6	0,855	0,757	3,98	271,12	10,12
0,65	0,905	0,807	4,25	291,28	10,87
0,7	0,955	0,857	4,51	311,44	11,62
0,75	1,005	0,907	4,77	331,6	12,37
0,8	1,055	0,957	5,04	351,76	13,12
0,85	1,105	1,007	5,30	371,92	13,88
0,9	1,155	1,057	5,56	392,08	14,63
0,95	1,205	1,107	5,83	417,11	15,38
1	1,255	1,157	6,09	432,4	16,13

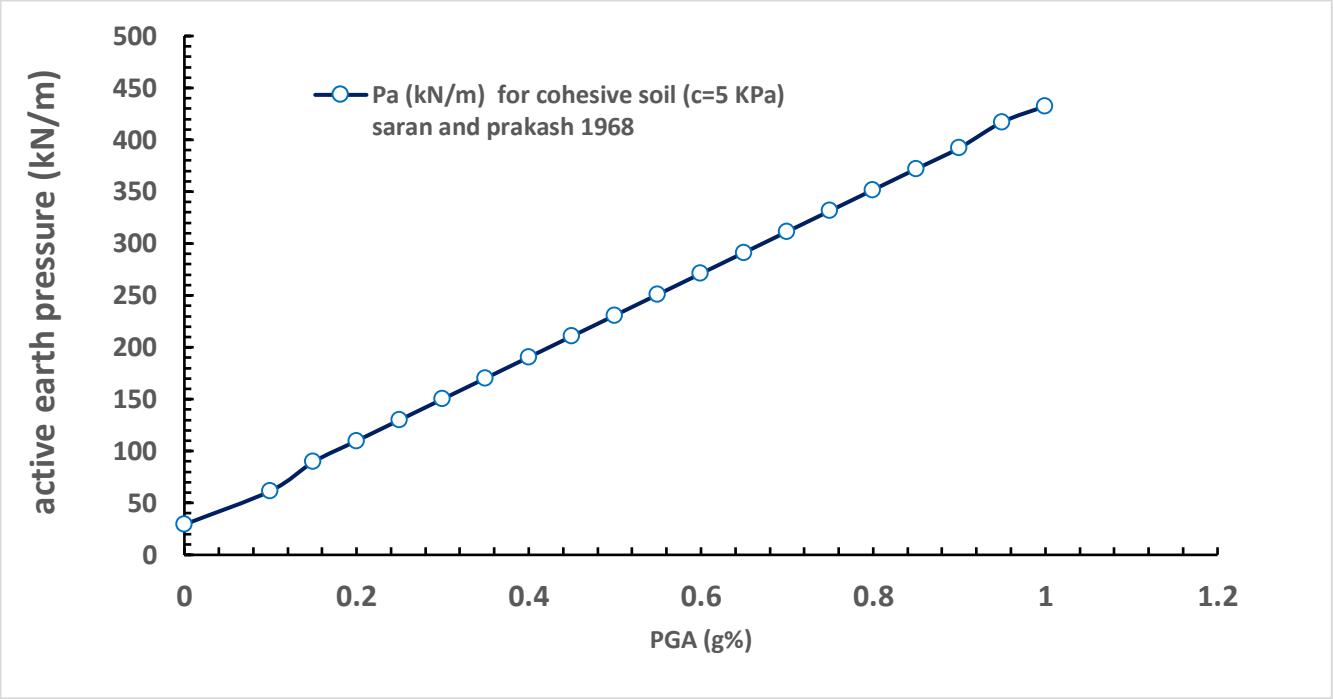

Figure 5.5 Dynamic active earth pressure P_{AE}(kN/m) for (C=5) by saran and Prakash 1968.

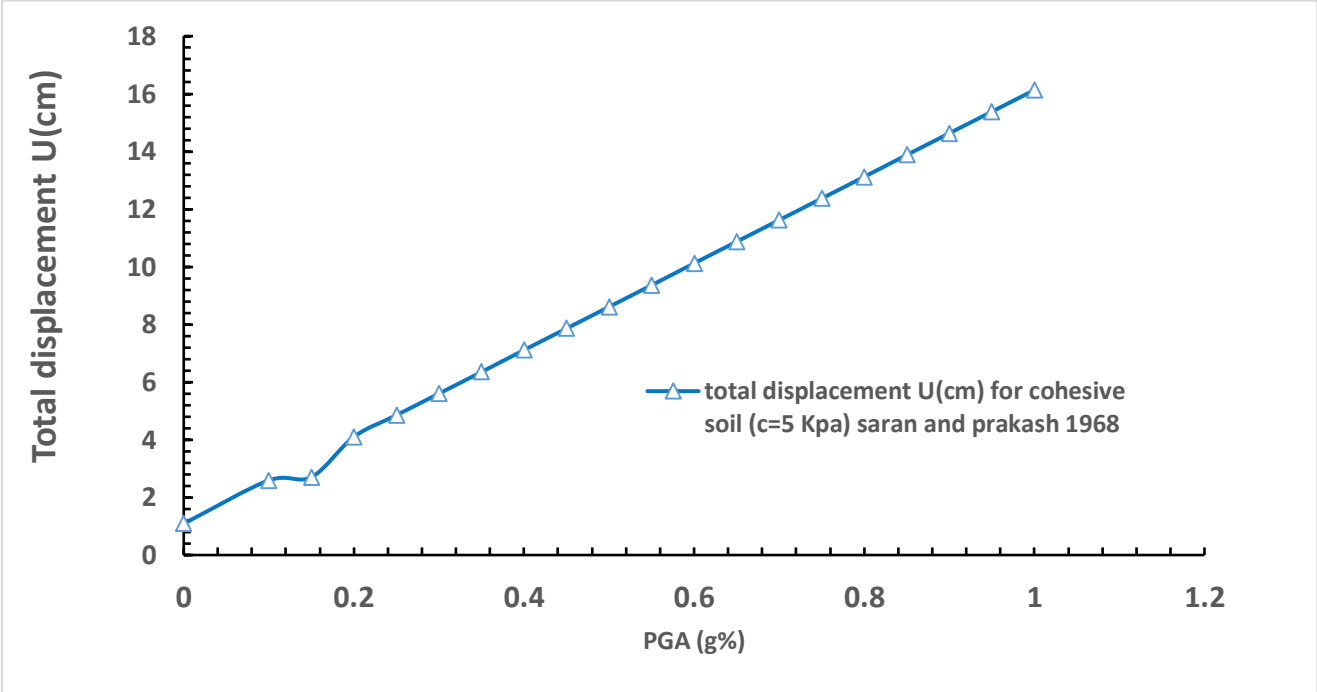

Figure 5.6 Total displacement U(cm) for C=5 by saran and Prakash 1968.

a) Analysis of the Analytical results for cohesive soil C=5KPa, by Saran and Prakash 1968:

For cohesive soil c=5 kPa the curves of P_{AE} and displacement (U) shows active earth pressure increases almost linearly with PGA increasing. This reveal the relationship between dynamic earth pressure and PGA is nearly linear. Displacement also increases with PGA, but it shows some fluctuations at lower PGA values (0.1g to 0.2g). when the PGA is (0.2g% to 1%g), displacement increases almost linearly.it is clear, higher ground acceleration (PGA) leads to larger displacements.

Table 5. 5 Analytical results by (Saran and Prakash 1986) for (c-ϕ) soil C=10kPa:

PGA(g%)	$N_{(aqm)dyn}$	$N_{(aYm)dyn}$	λ	P_{AE} (KN/m)	U (cm)
0	0,255	0,204	1,08	-3,75	-0,130
0,1	0,355	0,304	1,60	20,03	0,747
0,15	0,405	0,354	1,87	31,92	1,191
0,2	0,455	0,404	2,13	43,81	1,634
0,25	0,505	0,454	2,39	55,70	2,078
0,3	0,555	0,504	2,65	67,59	2,522
0,35	0,605	0,554	2,92	79,48	2,965
0,4	0,655	0,604	3,18	91,37	3,409
0,45	0,705	0,654	3,44	103,26	3,852
0,5	0,755	0,704	3,71	115,15	4,296
0,55	0,805	0,754	3,97	127,04	4,740
0,6	0,855	0,804	4,23	138,93	5,183
0,65	0,905	0,854	4,50	150,82	5,627
0,7	0,955	0,904	4,76	162,71	6,070
0,75	1,005	0,954	5,02	174,59	6,514
0,8	1,055	1,004	5,29	186,48	6,958
0,85	1,105	1,054	5,55	198,37	7,401
0,9	1,155	1,104	5,81	210,26	7,845
0,95	1,205	1,154	6,08	222,15	8,288
1	1,255	1,204	6,34	234,04	8,732

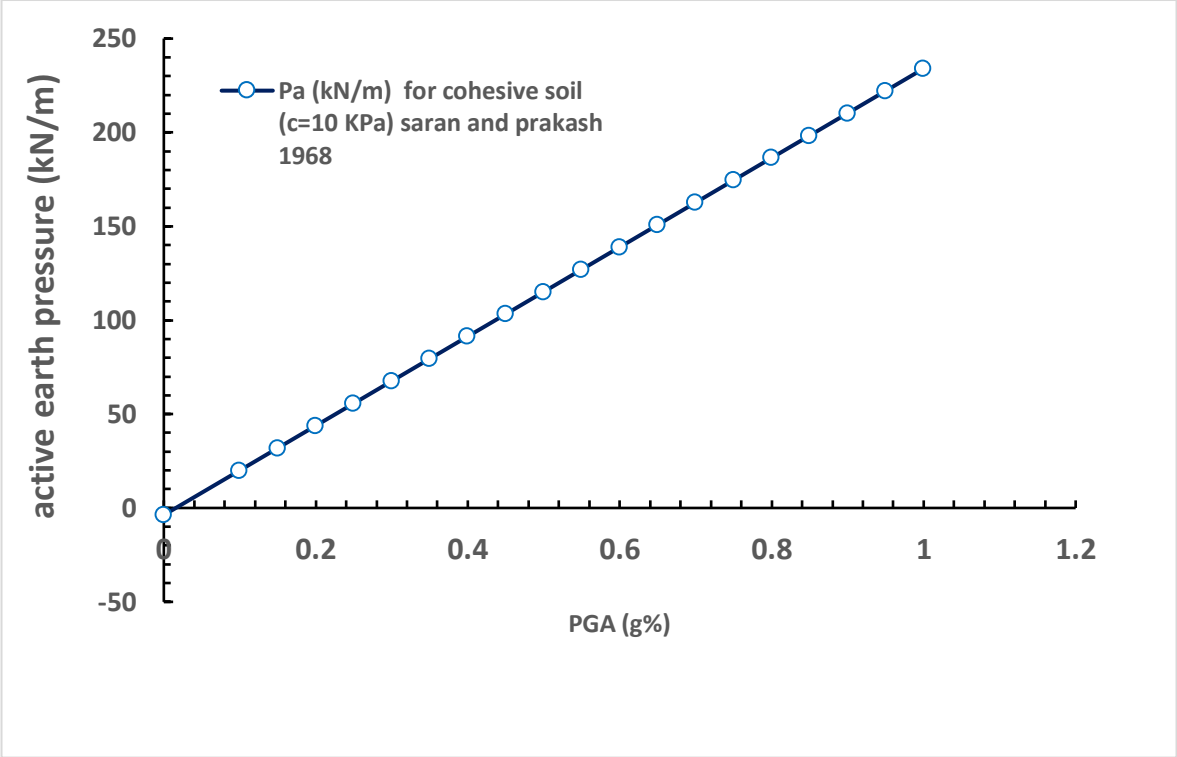

Figure 5.7 Dynamic active earth pressure P_{AE}(kN/m) for (c=10) by saran and Prakash 1968.

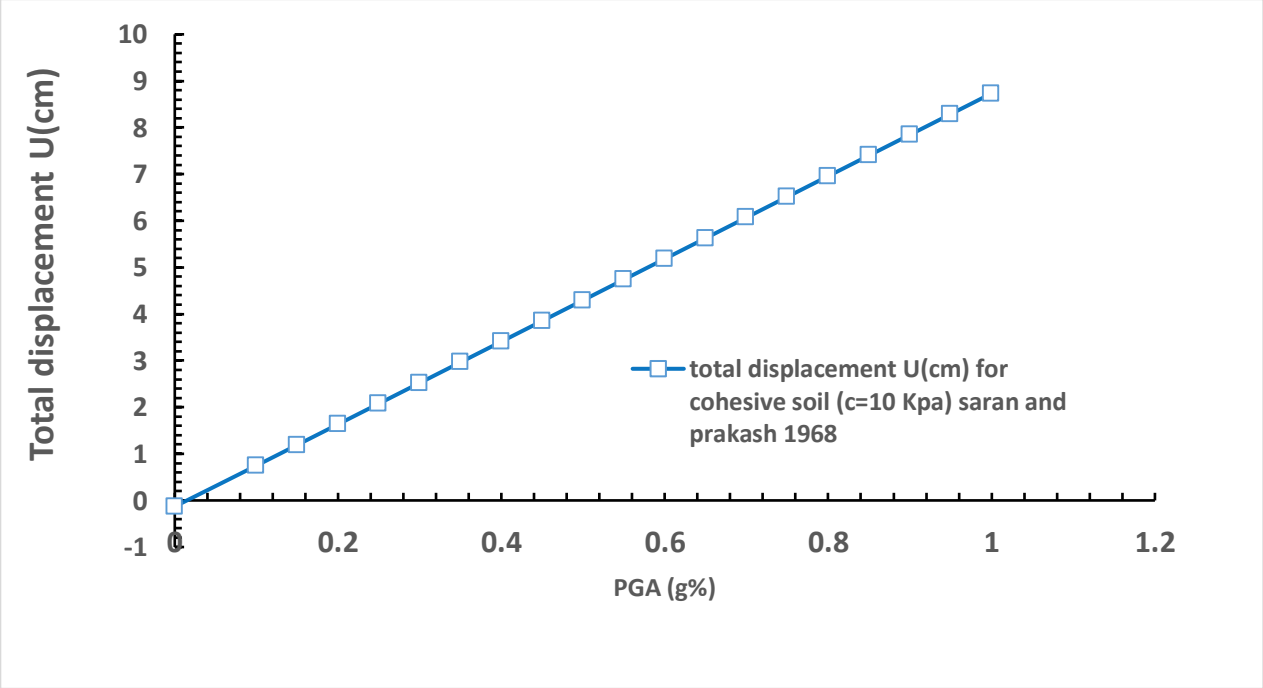

Figure 5.8 Total displacement U(cm) for c=10 by saran and Prakash 1968.

b) Analysis of the Analytical results for cohesive soil C=10KPa, by Saran and Prakash 1968:

The results are almost similar to the previous graphs for C=5 kPa, the increase of PGA causes a direct increase in both (**P_{AE} and displacement**), this retaining structure experience notable changes under seismic loading.

c) Comparison of analytical results for cohesionless soil by (MO) and for (c-ϕ) soil based on Saran and Prakash 1986:

Figures 5.9 and 5.10 present the analytical results of dynamic active earth pressure and displacement for two types of soils using different methods. For cohesionless soil, the analysis is based on the Mononobe-Okabe method, while for c-ϕ soil, the results are derived from the approach proposed by Saran and Prakash (1986). These figures allow for a direct comparison between the two analytical methods, highlighting the differences in earth pressures and displacements.

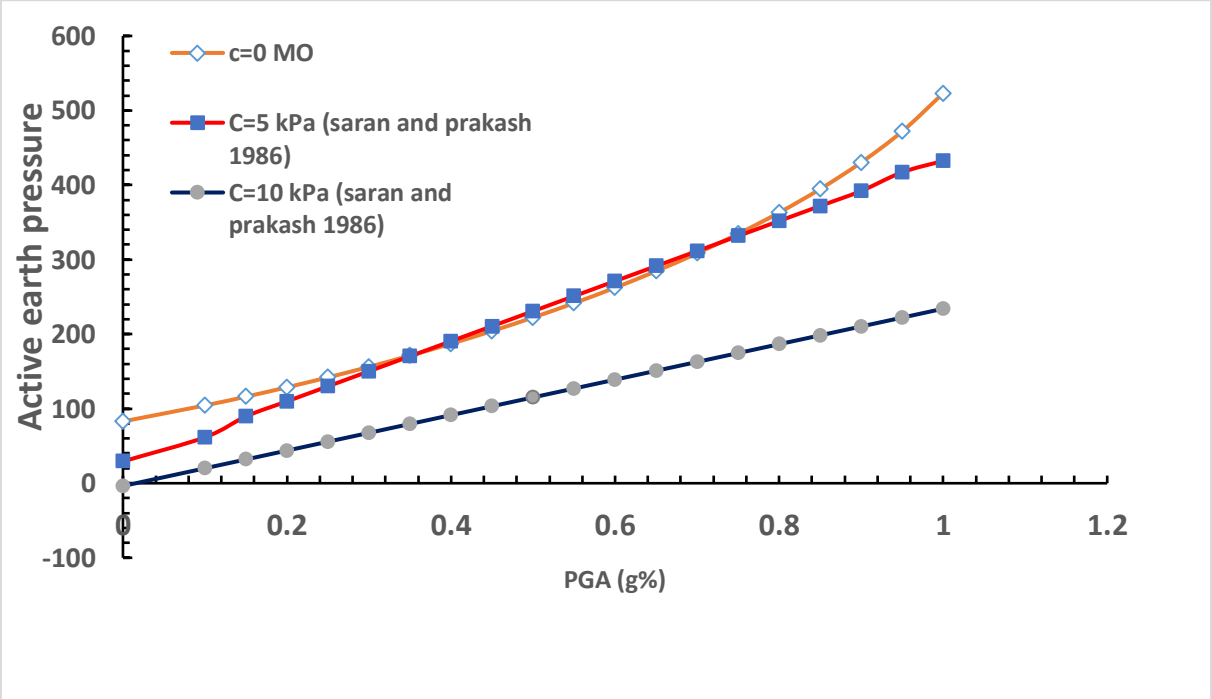

Figure 5.9 Comparison of Dynamic Analytical Methods for Active Earth Pressure P_{AE}(kN/m).

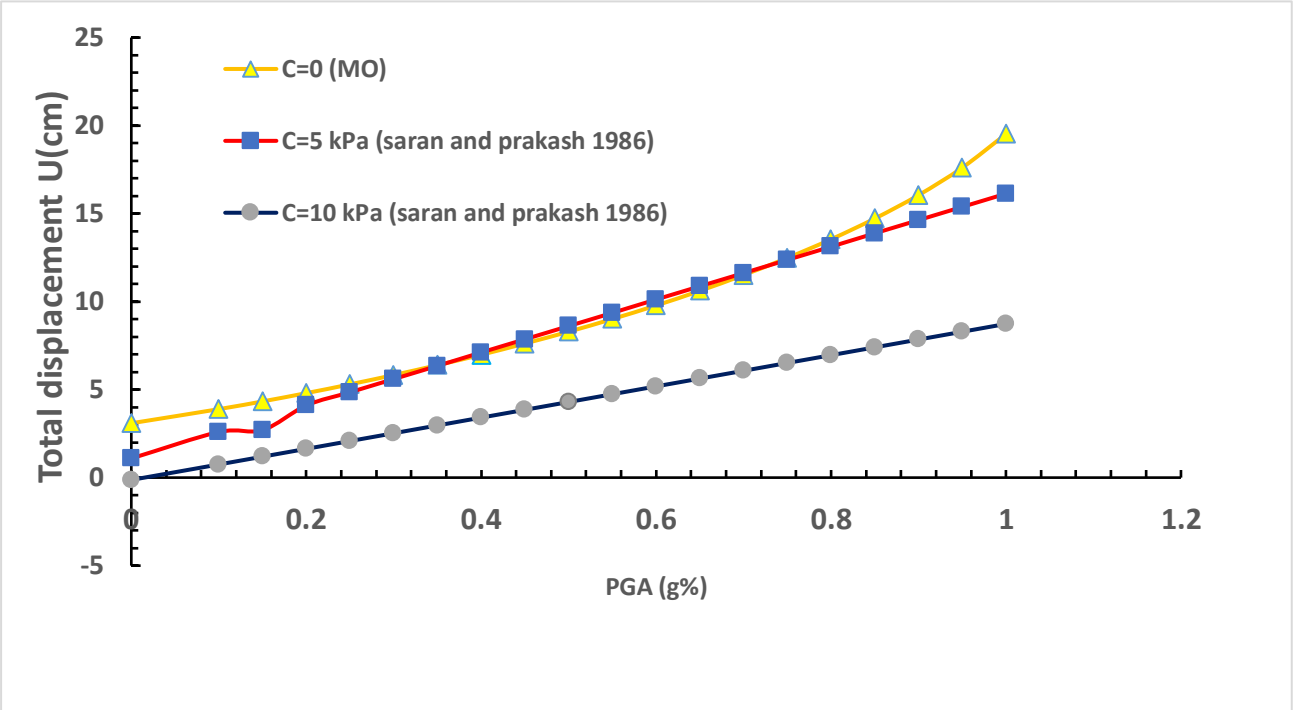

Figure 5.10 Comparison of Dynamic Analytical Methods for Total Displacement U(cm)

A comparative analysis of displacement behavior under dynamic loading reveals distinct differences between cohesionless and cohesive soils. The cohesionless soil, analyzed using the Mononobe-Okabe method (c = 0 kPa), exhibits the highest displacement across all levels of Peak Ground Acceleration (PGA), the absence of cohesion reveals high displacement. with a sharp and nonlinear increase as PGA rises. In contrast, cohesive soils, analyzed using the Saran and Prakash method, show progressively lower displacement with increasing cohesion. For example, the soil with c = 5 kPa shows moderate displacement, with a more gradual increase relative to PGA. The soil with c = 10 kPa demonstrates the lowest displacement and a near-linear response, indicating greater resistance to dynamic loading. Overall, the comparison clearly shows that the presence of cohesion substantially improves the soil's ability to withstand seismic-induced displacement.

5.4 Numerical analysis of the stability of the retaining wall:

In order to design the retaining wall, arbitrary dimensions are chosen and analyses performed on Plaxis 2d v8.6 to verify if the wall remains stable under the loads applied to it. The main checks are the serviceability checks which include vertical and horizontal displacements of the wall subjected to lateral pressures, this is done by trial and error of the wall's dimensions [3]. The numerical study was performed for fifteen-node elements and plane strain model conditions.

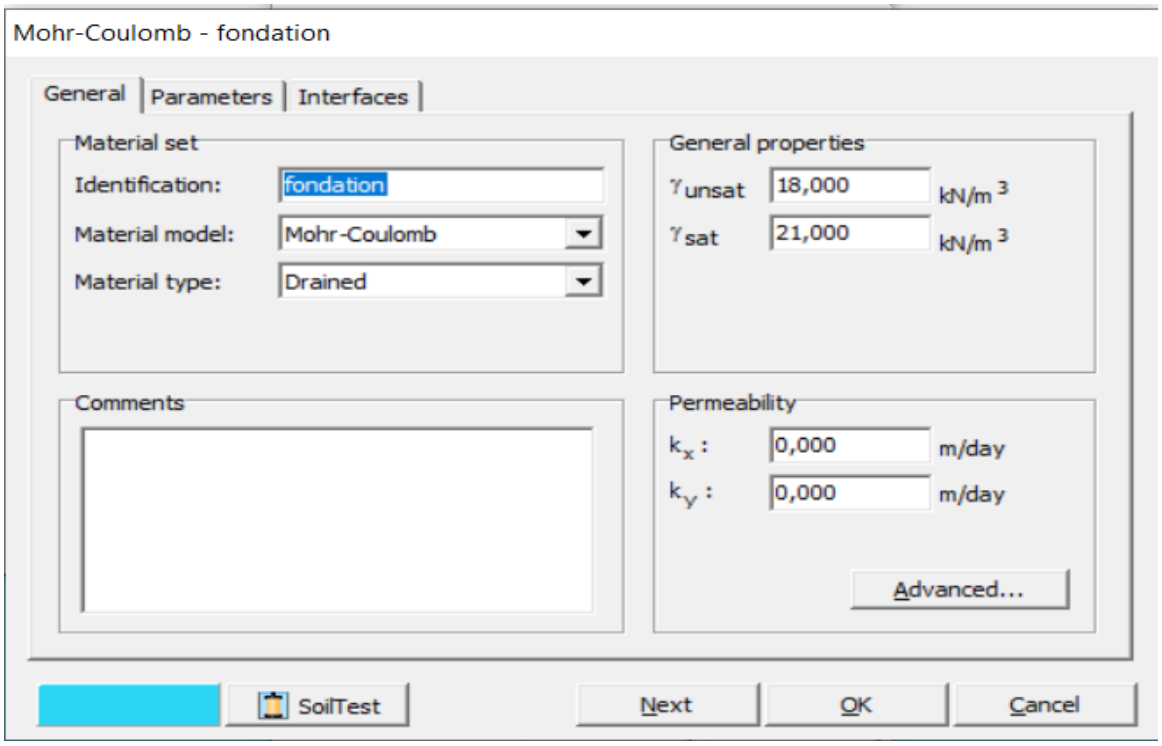

Figure 5.11 Parameters of Mohr-coulomb soil model (foundation).

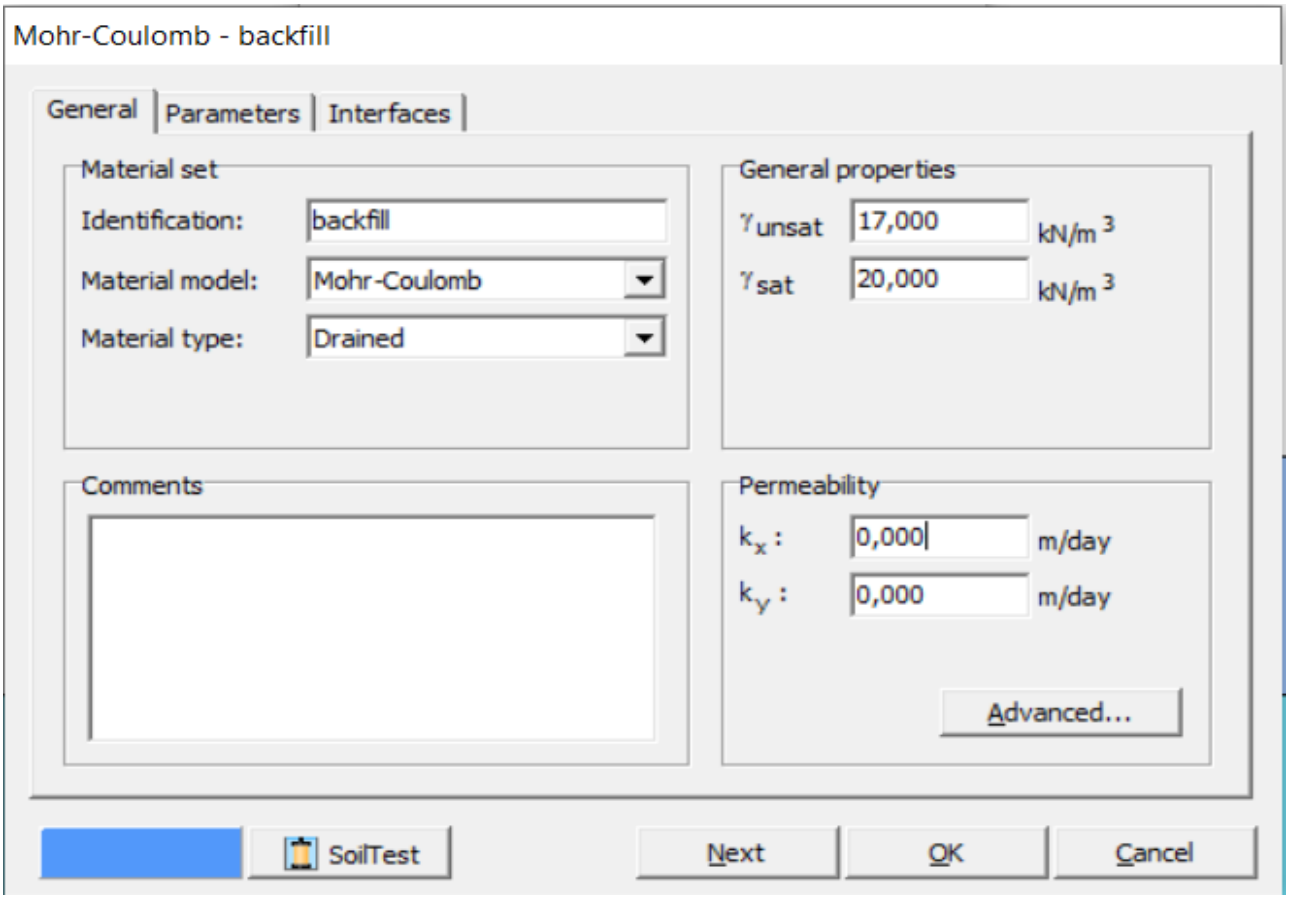

Figure 5.12 Parameters of Mohr-coulomb soil model (Backfill).

5.4.1 Mesh generation:

When the geometry model is complete, the finite element model (or mesh) can be generated. PLAXIS allows for a fully automatic mesh generation procedure, in which the geometry is divided into elements of the basic element type and compatible structural elements, if applicable. The mesh generation takes full account of the position of points and lines in the geometry model, so that the exact position of layers, loads and structures is accounted for in the finite element mesh. [36].

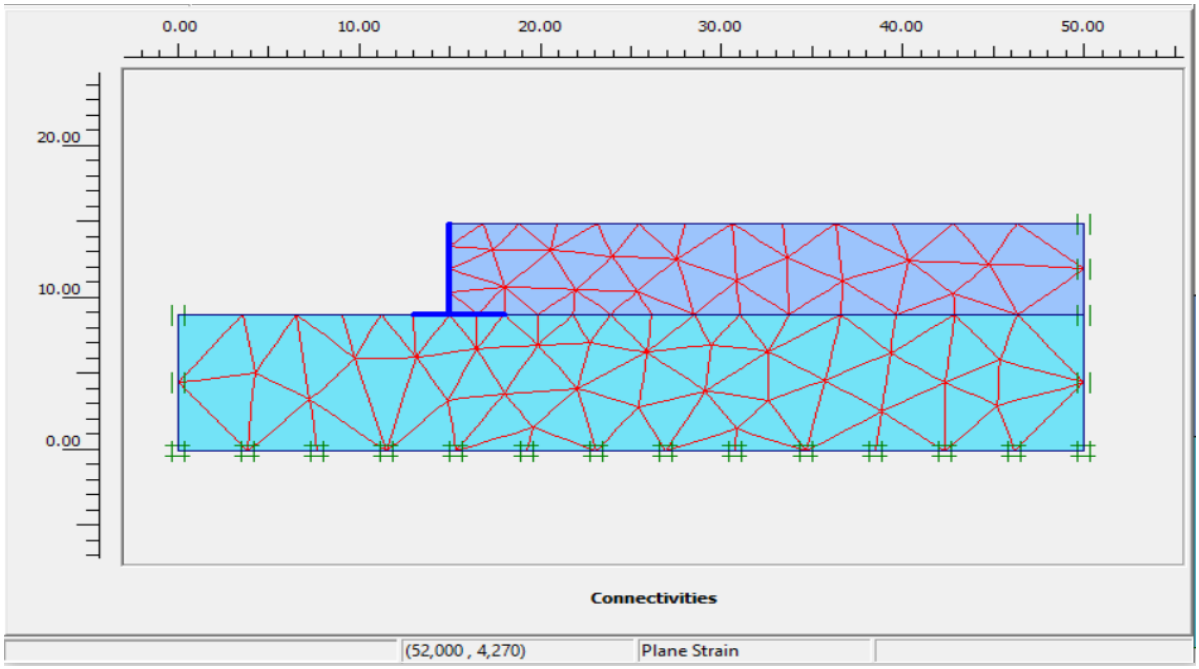

Figure 5.13 cantilever retaining wall generated mesh results.

5.4.2 Calculation phase:

The analysis performed is the plastic analysis with 2 stages of construction. The different stages of construction are defined starting from the initial phase which is the geometry of the project followed by the addition of the backfill [3].

Identification	Phase no.	Start from	Calculation	Loading input	Time	Water	First
Initial phase	0	0	N/A	N/A	0,00 ...	0	0
<Phase 1>	1	0	Plastic analysis	Staged construction	0,00 ...	1	1
<Phase 2>	2	1	Plastic analysis	Total multipliers	0,00 ...	1	26

Figure 5.14 calculation phases.

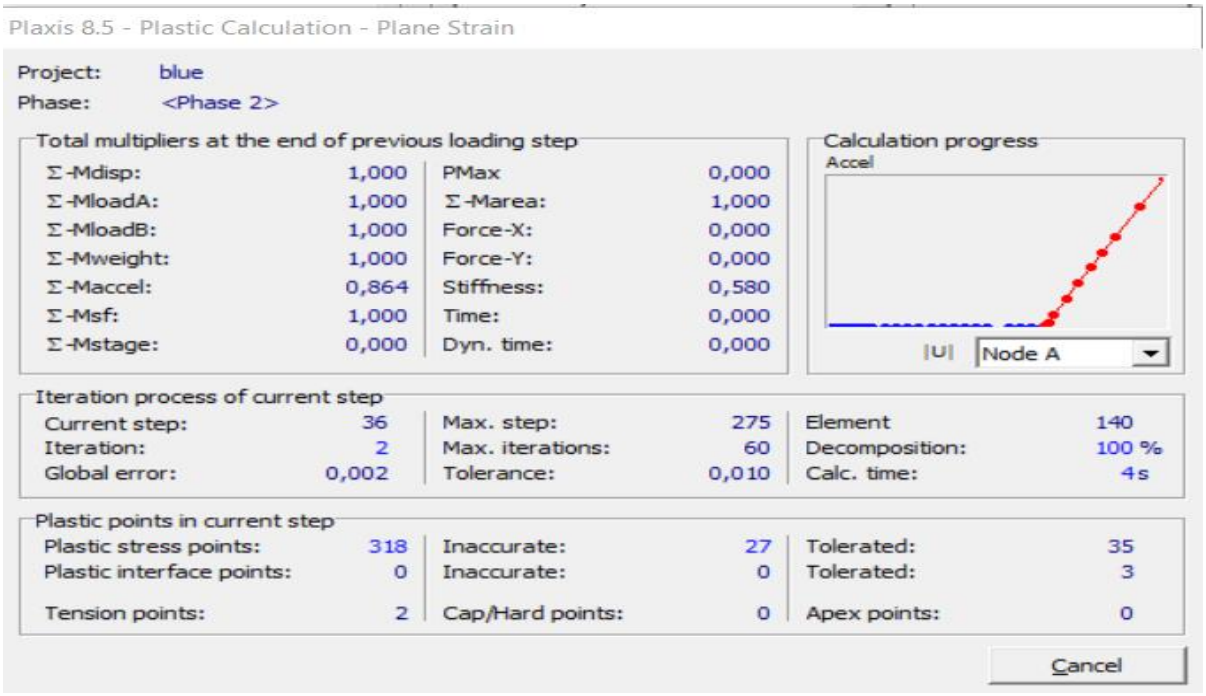

Figure 5.15 calculation window.

5.4.3 Presentation of output results from analysis on Plaxis 2d:

The FEM conception by PLAXIS was able to estimate the following results: deformations, horizontal and vertical displacements, global stability, axial forces, shear forces and bending moments on the retaining wall [3].

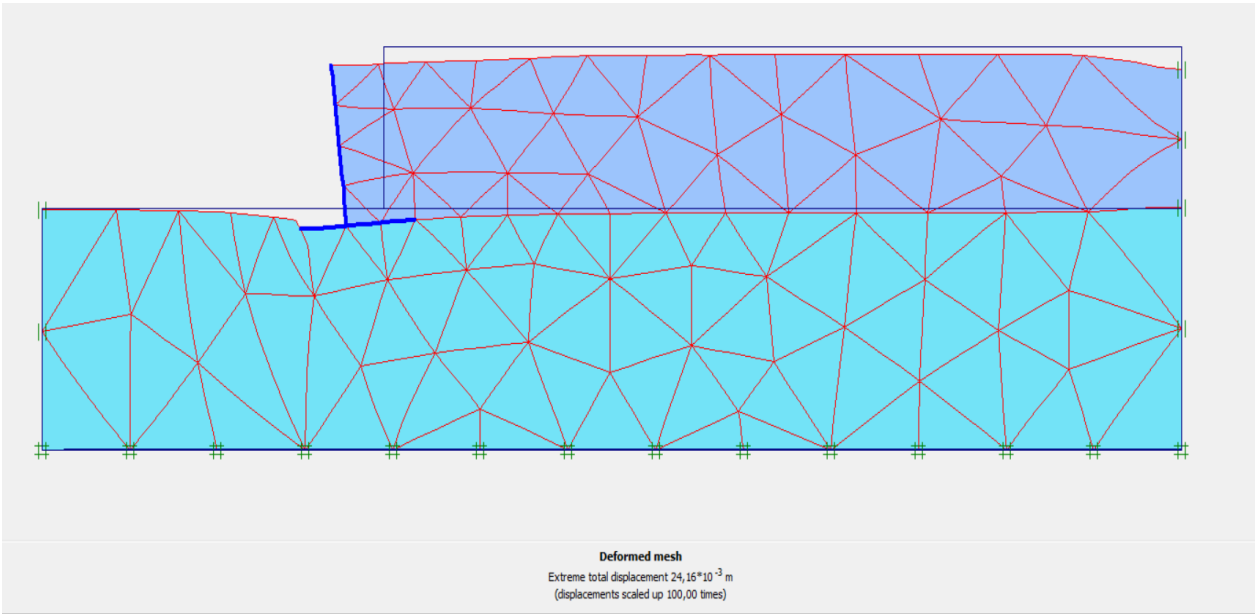

Figure 5.16 deformed mesh of total displacement.

5.4.4 Plaxis 2d results example:

The results presented below pertain to Point A, with an acceleration coefficient of α_h =0.1g and a cohesion value of c=5 kPa, indicating cohesive soil conditions (c ϕ).

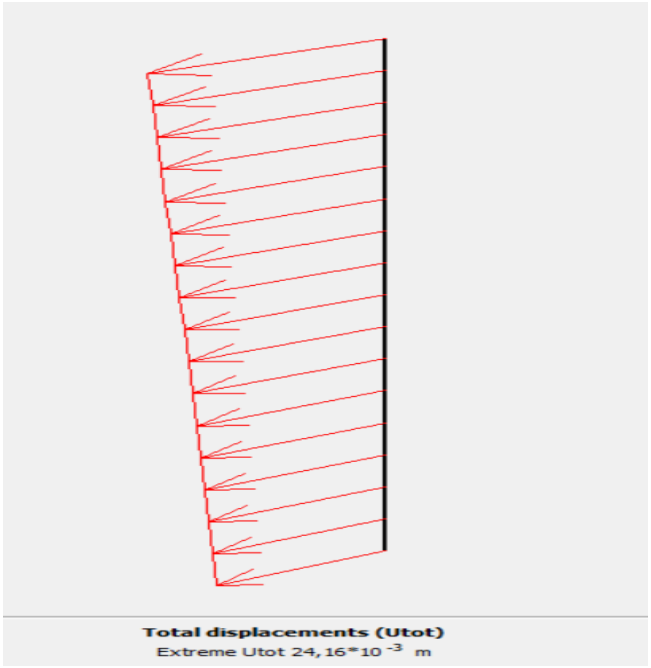

Figure 5.17 total displacement.

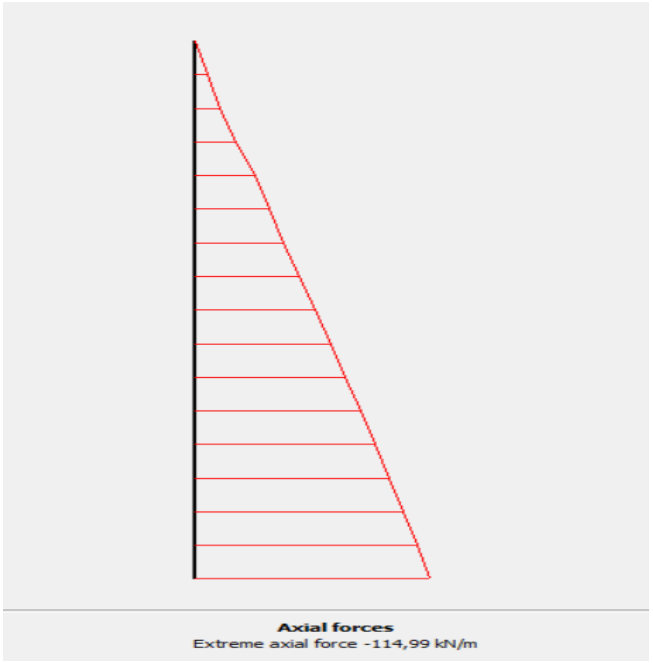

Figure 5.18 axial forces.

a) Shear forces and bending moments results for α_h=0.1g and c=5 kPa:

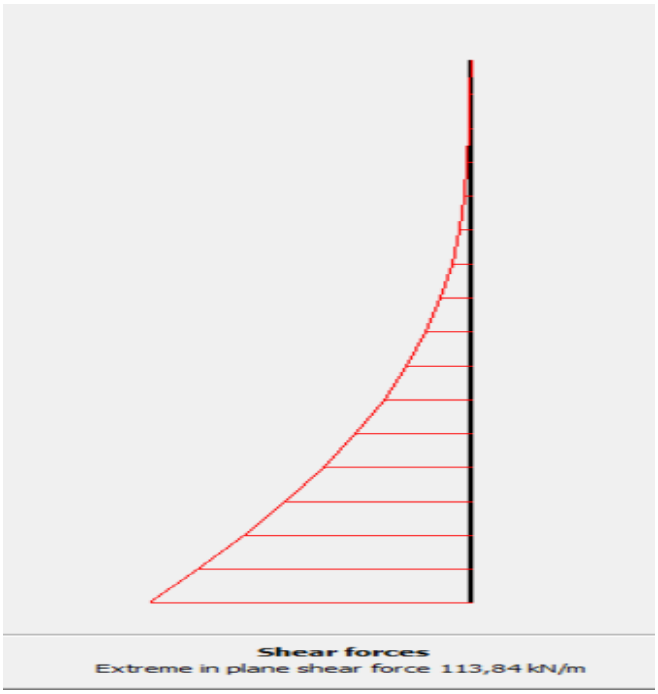

Figure 5.19 shear forces.

Figure 5.20 bending moments.

b) Horizontal and vertical displacement:

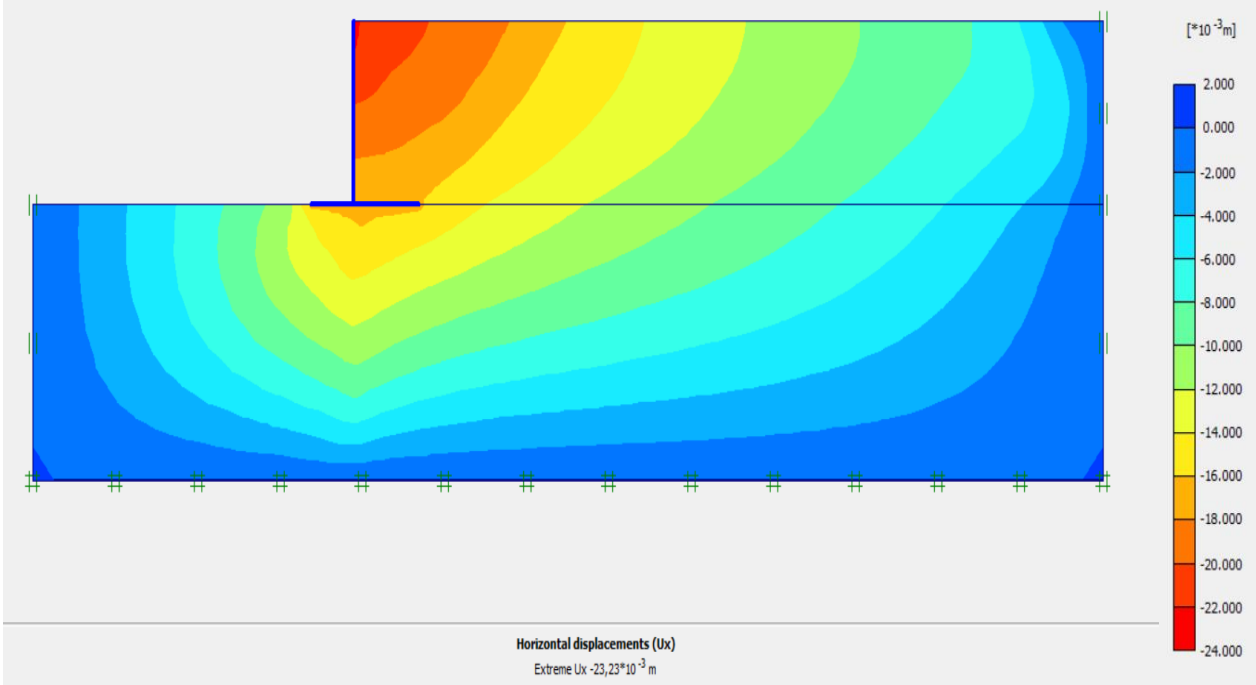

Figure 5.21 horizontal displacement (Ux).

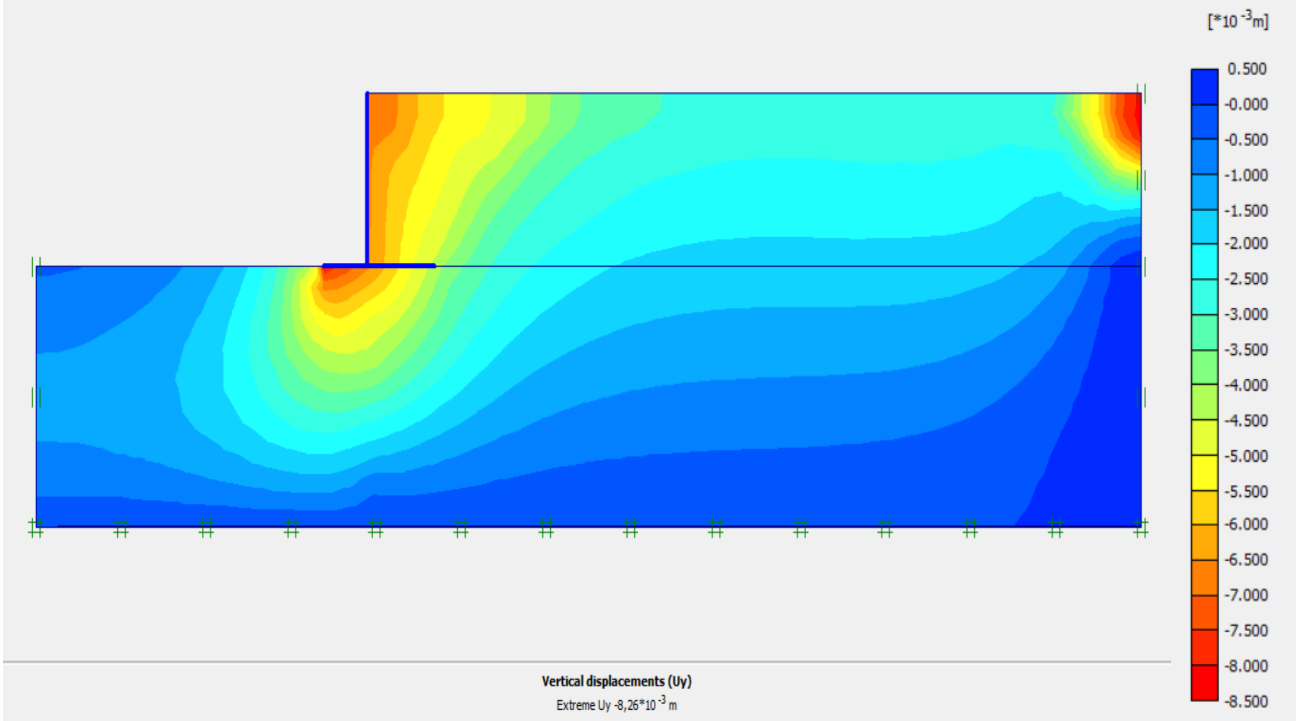

Figure 5.22 vertical displacement (Uy).

The figures above show the numerical results for α_h=0.1g and c=5 kPa which are presented in the table 5.6.

Table 5.6 Results of αh=0.1g and c=5 kPa obtained from Plaxis 2d:

Name	valeur	Unit
Axial forces	114,99	kN/m
Shear forces	113,84	kN/m
Bending moments	182,77	kN.m
Horizontal displacement (Ux)	2,323	cm
Vertical displacement (Uy)	0,826	cm
Total displacement	2,416	cm

5.5 Dynamic numerical results by (plaxis 2d):

The numerical results obtained using the finite element software plaxis 2d shows the values of dynamic active earth pressure (P_{AE}) and the total displacement of the cantilever retaining wall under different peak ground acceleration (PGA) levels for different backfill Cohesion values c=0, c=5kPa, c=10kPa. All the results obtained using the finite element software PLAXIS 2D, as shown in figures (Figure 5.24 and Figure 5.25), were recorded at the top of the cantilever retaining wall, specifically at Point A.

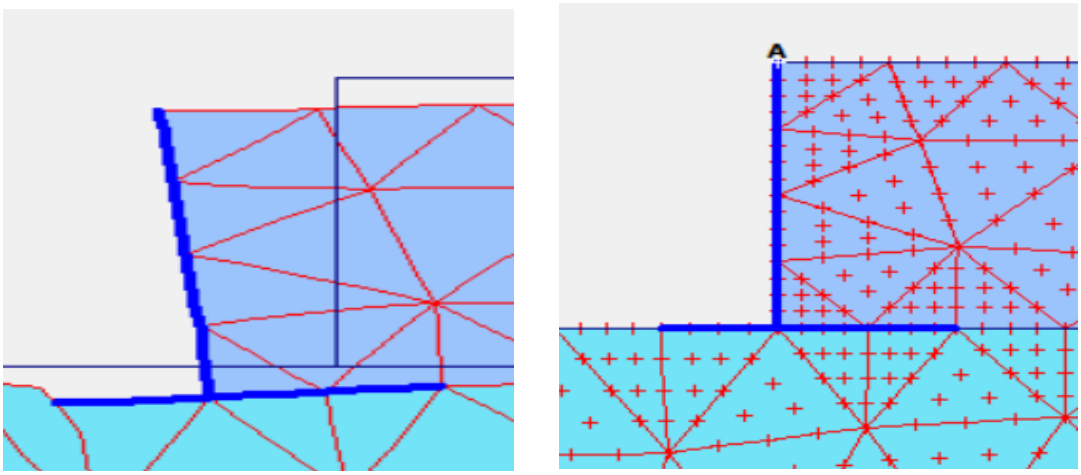

Figure 5.23 point of application of the total displacement and active earth pressure by plaxis 2d.

All the results are presented in table 5.7.

Table 5.7 Numerical results of (plaxis 2d) for c=0, c=5kPa, c=10kPa:

	c=0		c=5 (kPa)		c=10 (kPa)	
PGA(g%)	Pa (KN/m)	U(cm)	Pa (KN/m)	U (cm)	Pa (KN/m)	U (cm)
0	93,75	1,85	78,7	1,32	75,96	1,2
0,1	129,33	2,967	113,84	2,42	110,58	2,31
0,15	146,9	3,567	131,37	3,35	127,64	2,89
0,2	164,61	4,244	149,01	3,61	144,7	3,48
0,25	184,39	5,014	167,42	4,29	161,61	4,11
0,3	207,3	5,979	186,53	5,08	178,67	4,79
0,35	232,73	7,279	207,1	5,98	196,53	5,60
0,4	256,53	10,791	229,39	8,98	214,75	6,81
0,45	260,73	10,888	259,34	13,01	233,42	9,52
0,5	256,43	10,832	259,97	12,94	254,14	11,77
0,55	255,9	10,731	216,13	12,99	250,17	11,59
0,6	257,82	10,942	259,83	12,84	255,86	11,72
0,65	256,08	10,937	259,94	13,04	256,05	11,79
0,7	257,2	11,077	258,77	13,08	259,08	11,95
0,75	255,78	10,683	255,77	12,61	254,72	11,78
0,8	256,22	10,901	261,83	12,86	254,87	11,91
0,85	257,56	10,626	260,02	12,96	252,47	11,53
0,9	257,77	11,344	259,67	12,91	257,05	11,57
0,95	257,44	10,808	262,61	12,76	257,73	11,68
1	256,92	10,776	259,57	12,86	253,76	11,74

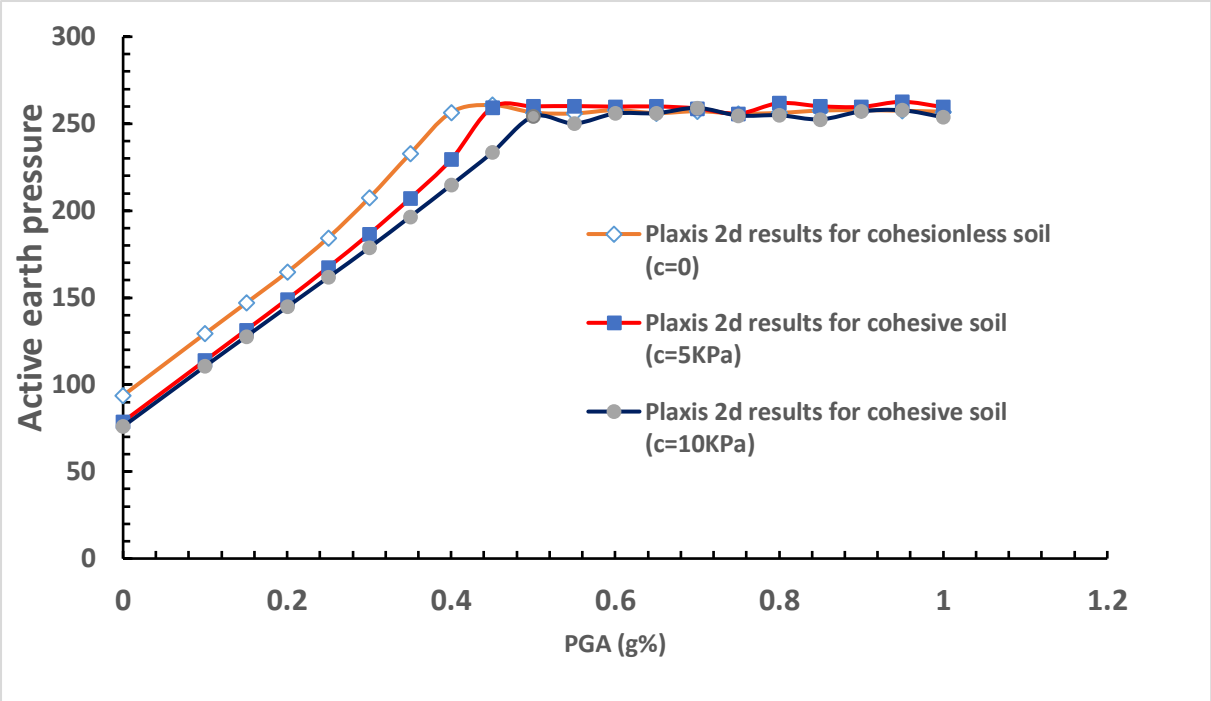

Figure 5.24 Numerical results of active earth pressure P_{AE}(kN/m) for cohesionless and cohesive soil by Plaxis 2d.

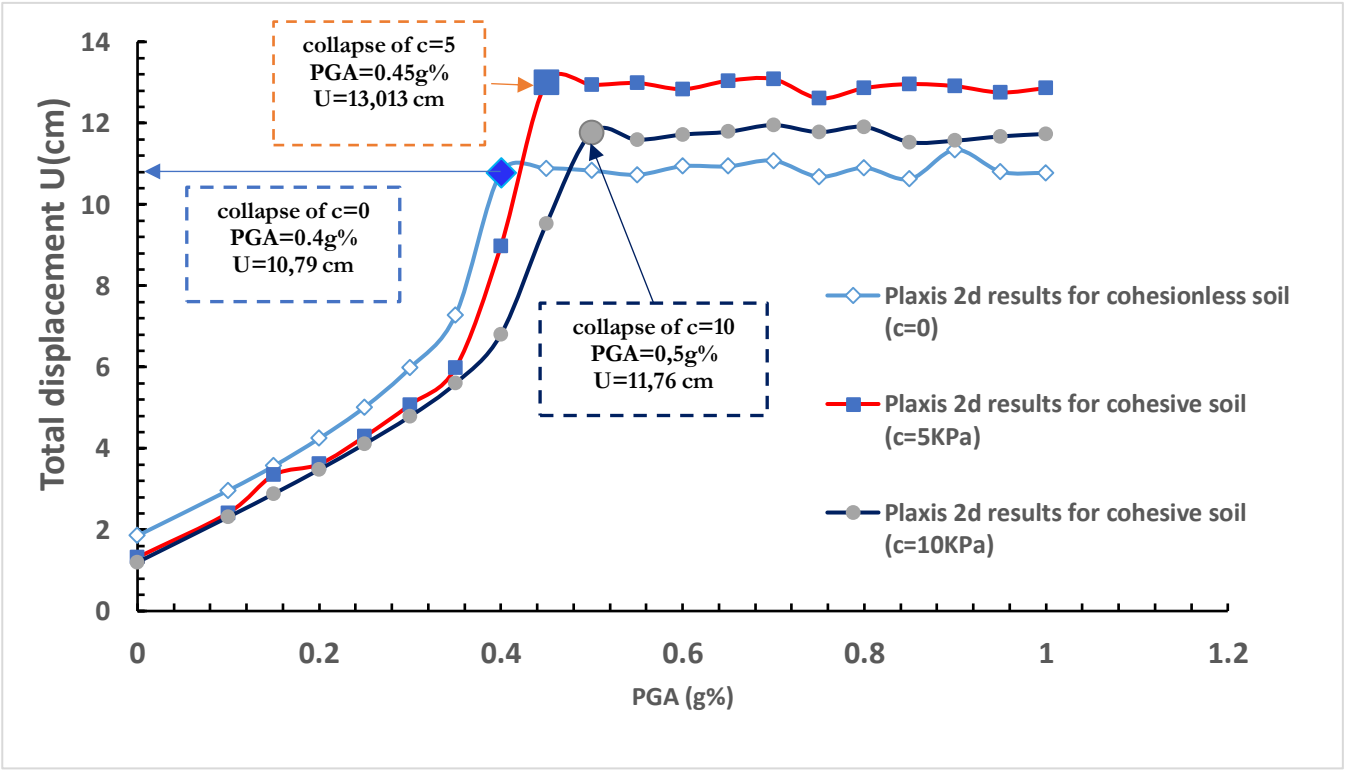

Figure 5.25 Numerical results of total displacement U(cm) for cohesionless and cohesive soil by Plaxis 2d.

The comparison of the numerical results for C = 0, C = 5 kPa, and C = 10 kPa is presented in table5.8.

Table 5.8 comparison of the numerical results for c = 0, c = 5 kPa, and c = 10 kPa:

Soil Type	Initial Displacement For PGA(0 – 0.4g%)	Collapse PGA(g%)	Seismic Resistance	Post-Collapse Behavior
Cohesionless Soil C=0 kPa	High	0.4	Low	Displacement and pressure stabilize after collapse
Cohesive soil C= 5 kPa	Medium	0.45	Medium	Displacement and pressure stabilize after collapse
Cohesive soil C=10 kPa	Low	0.5	High	Displacement and pressure stabilize after collapse

5.5.1 Analysis of the Numerical results for cohesionless and cohesive soils by plaxis 2d:

All three soil types show a linear increase in both active earth pressure P_{AE} and displacement U(cm) for PGA values below (0.4g%). The cohesionless soil shows comparatively higher displacement between (0 and 0,4g%) until it collapses at PGA = 0.4g%. contrary, the soil with high cohesion (c = 10 kPa) express lower initial displacement and collapse at PGA = 0.5g, having more resistance to seismic excitation. The medium-cohesion soil (c = 5 kPa) displays higher displacement than c=10kpa case and collapses at PGA = 0.45g%. Following the collapse in each case, the displacement and active earth pressure curves became more stable.

5.5.2 Results discussions:

The analysis investigates the Evaluation of the seismic performance of the soil, considering two different soil conditions. At low **PGA** levels, all soils show similar elastic behavior. However, as **PGA** increases, the dynamic earth pressure and displacement

responses begin to show different results Due to the varying characteristics and properties of the different soil types.

a) **For the first soil type (cohesionless, c = 0),** early collapse is observed due to its reliance on internal friction for shear strength, which is primarily derived from the friction angle between sand particles. Under seismic loading, these particles can easily move past one another, leading to premature failure. However, this soil type is characterized by excellent drainage properties, which remains one of its key advantages.

b) **For the second soil type (cohesive soil with c = 5 kPa and c = 10 kPa),** the particles are more tightly bonded due to cohesive forces, resulting in greater compaction. This interparticle bonding provides additional shear strength, enabling the soil to better resist deformation and absorb more seismic energy before failure occurs.

5.6 Comparative Study of the Numerical results and Analytical Results for cohesive backfill (c=5 kPa):

Figure 5.26 and Figure 5.27 present a comparative analysis between the analytical methods proposed by **Saran** and **Prakash 1968**, and the numerical simulation results obtained using **PLAXIS 2D**, with a cohesive backfill (c=5 kPa).

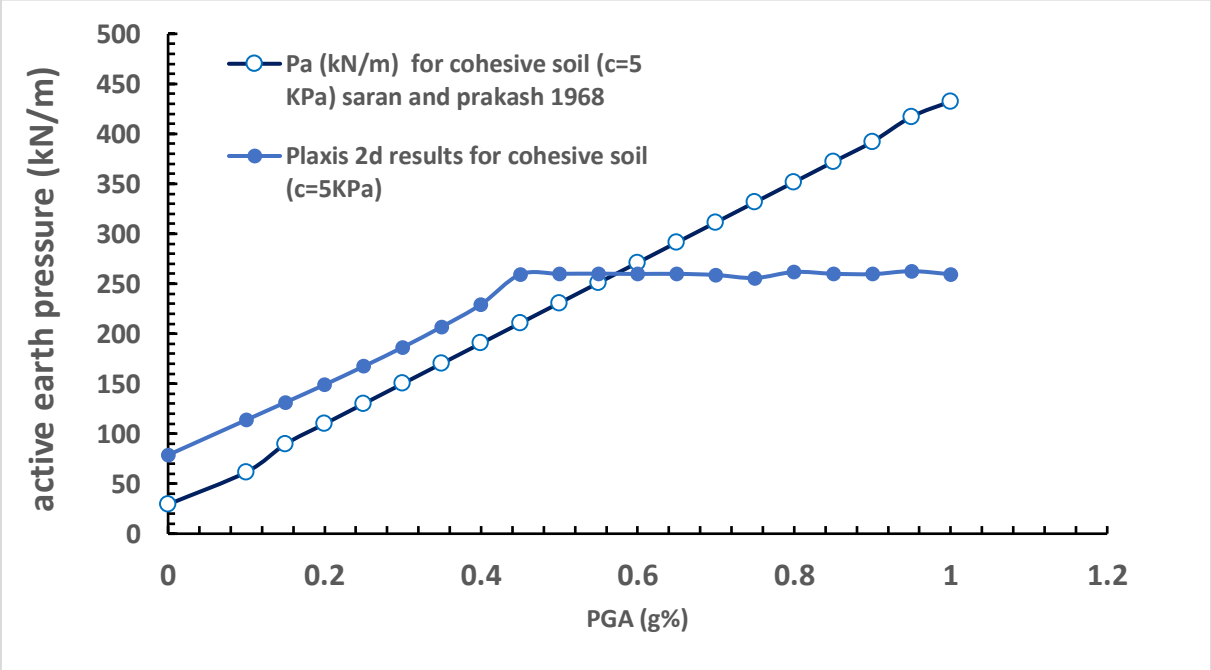

Figure 5.26 analytical and Numerical results of active earth pressure P_{AE}(kN/m) for cohesive soil (c=5KPa) by saran and Prakash and Plaxis 2d.

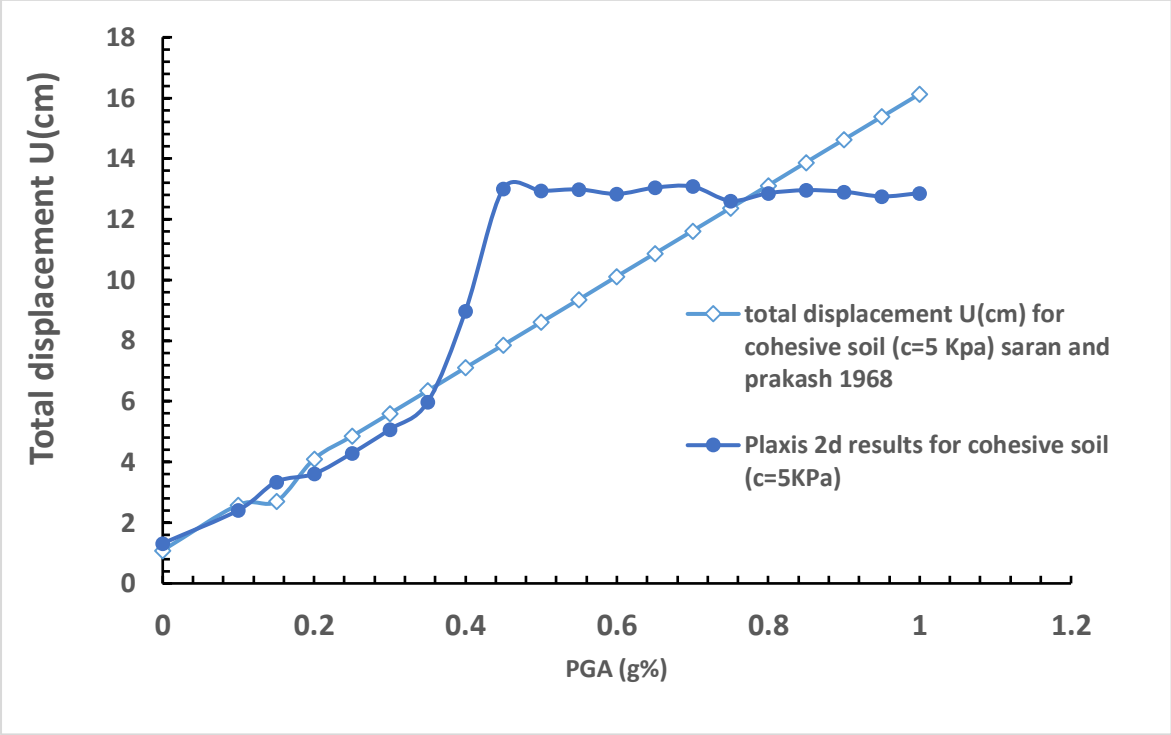

Figure 5.27 analytical and Numerical results of total displacement (cm) for cohesive soil (c=5KPa) by saran and Prakash and Plaxis 2d.

The analytical curves proposed by Saran and Prakash 1968 demonstrate continuous displacement and dynamic active earth pressure without indicating any failure, making them suitable for approximate estimations. In contrast, the numerical results obtained using PLAXIS 2D provide a more realistic and precise representation, capturing the full range of deformations experienced by the cantilever retaining wall under varying PGA values and the exact point of collapse.

5.7 Conclusion:

In this chapter, both analytical and numerical approaches were employed to evaluate the seismic performance of a retaining wall with cohesive backfill (c–ϕ soil). The results obtained were subsequently compared with those corresponding to a cohesionless backfill, in order to analyze the influence of backfill type on the wall's response under seismic loading. Through our study, we found that using backfill soil with both cohesion and internal friction (c-ϕ soil), whether analyzed using the analytical approach proposed by Saran and Prakash or the numerical method implemented in PLAXIS 2D, is more effective and economically viable compared to using cohesionless backfill soil.

GENERAL CONCLUSION

Cantilever retaining walls play an essential role in ensuring the stability and safety of slopes and in preventing soil collapse, particularly where roads are built on slopes or in areas with significant elevation changes. These walls are used to resist lateral earth pressure and stabilize the surrounding soil, reducing the risk of structural failure. Cantilever retaining walls serve as a vital defense against ground movement, helping to ensure the reliability and safety of transportation infrastructure.

The objective of this thesis is to evaluate the seismic performance of a reinforced concrete T-shaped cantilever retaining wall with cohesive backfill (c-ϕ), both analytically—using Mononobe-Okabe theory for cohesionless soil and Saran and Prakash methods for cohesive soil—and numerically, using the finite element program PLAXIS 2D, which provides clear and interpretable results.

This thesis is divided into two main parts. The first part presents a comprehensive literature review on cantilever retaining walls, focusing on their structural behavior, typical failure modes, and the influence of various soil properties. It explores the fundamental principles behind retaining wall design and provides insights into the factors that contribute to their stability or failure under different loading conditions. The second part of the thesis is dedicated to the practical analysis of cantilever retaining walls, utilizing both analytical and numerical methods. Analytical approaches include the application of the Mononobe-Okabe theory and the method proposed by Saran and Prakash (1968) for evaluating seismic earth pressures. In parallel, numerical modeling is conducted using PLAXIS 2D to simulate the wall behavior under seismic loading, offering a more detailed and realistic understanding of its performance. Numerical modeling focuses on a T-shaped reinforced concrete cantilever retaining wall with a height of 6 meters, a base width of 4.5 meters, and a base thickness of 0.6 meters. The analysis includes an evaluation of the wall's stability, the combination of these methods provides a robust framework for assessing the seismic response of cantilever retaining walls in various soil conditions. This study has highlighted the distinct mechanical

behaviors of cohesionless and cohesive soils under seismic loading. Cohesionless soils, governed solely by internal friction, tend to exhibit lower shear resistance during seismic events due to the absence of cohesive bonds, which can result in early deformation or structural failure. However, their excellent drainage properties make them advantageous in specific engineering applications. In contrast, cohesive soils—characterized by both internal friction and cohesion—demonstrate superior compaction and interparticle bonding. These properties contribute to enhanced resistance to deformation and allow the soil to absorb greater amounts of seismic energy, effectively delaying failure compared to cohesionless soils.

The practical findings of this research confirm that cantilever retaining walls constructed with cohesive backfill (c–ϕ soil) can perform reliably under seismic conditions. This research constitutes a scientific contribution aimed at supporting the integration of the Saran and Prakash method into the RPA 2024 seismic design code, by demonstrating its effectiveness in evaluating the performance of cantilever retaining walls under seismic loading.

.

Bibliographic references

[1] BROOKS H., NIELSEN J.P., **Basics of Retaining Wall Design, 10th Edition**, HBA Publications, Newport Beach, California, www.hbap.com, 1992.

[2] DHAMDHERE D.R., RATHI V.R., KOLASE P.K., **Design and Analysis of Retaining Wall**, 2nd International Conference on Emerging Trends in Science, Engineering & Technology, Mahratta Chamber of Commerce, Industries and Agriculture, Pune (India), 29th–30th September 2018, www.conferenceworld.in, Conference World, ISBN: 978-93-87793-46-0.

[3] MASSO NKONLA L.E., **Design of an Earth Retaining Wall Working Also as a Floor Slab for a Building: Case Study of a Retaining Wall in Bastos Yaoundé**, Master's in Civil Engineering, Option: Geotechnics, NASPW Yaoundé, 2020–2021, Supervised by Pr. Simonetta COLA.

[4] RADKE S., KAWALE V., DONGRE P., KORE K., RAKHADE V., LANDEKAR K., A **Review on Designing of Loft Retaining Wall & Comparison with Other Types of Retaining Walls**, International Journal of Research Publication and Reviews, Vol. 5, Issue 5, May 2024, pp. 8707–8711, Smt. Radhikatai Pandav College of Engineering, Nagpur, India, www.ijrpr.com, ISSN: 2582-7421

[5] GROUP SIX MEMBERS, **Retaining Walls Notes**, Construction Technology Two (QUS 2101), Department of Construction Economics and Management, School of Built Environment, College of Engineering, Design, Art and Technology, Makerere University, Kampala, Compiled under the supervision of Mr. Semanda Julius, September 21, 2018.

[6] PARNELL D.W., **Earth Retaining Walls and Structures**, Course No. ERS101, 5 PDH Credits, Original Courseware, Online-PDH, Merritt Island, FL, 1265 San Juan Dr., Release Date: April 2018, Copyright © 2009 Online-PDH – All Rights Reserved.

[7] BALAJI V., SHAMEEM BANU S., **Comparative Study on Cantilever and Counterfort Retaining Walls Designed Using STAAD Pro**, International Research Journal of Modernization in Engineering Technology and Science, Vol. 4, Issue 3,

March 2022, Jawaharlal Nehru Technological University Kakinada, Andhra Pradesh, India, www.irjmets.com, e-ISSN: 2582-5208, Impact Factor: 6.752

[8] YANG S., CHEGNIZADEH A., NIKRAZ H., **Review of Studies on Retaining Wall's Behavior on Dynamic / Seismic Condition**, International Journal of Engineering Research and Applications, Vol. 3, Issue 6, Nov–Dec 2013, pp. 1012–1021, Curtin University of Technology, Perth, Australia, www.ijera.com, ISSN: 2248-9622.

[9] YAZDANI M., AZAD A., FARSHI A., TALATAHARI S., **Extended "Mononobe-Okabe" Method for Seismic Design of Retaining Walls**, Journal of Applied Mathematics, Vol. 2013, Article ID 136132, 10 pages, Department of Civil and Environmental Engineering, Tarbiat Modares University, Tehran, Iran, Civil Engineering Faculty, Islamic Azad University, Tehran, Iran, Department of Civil Engineering, University of Tabriz, Tabriz, Iran, http://dx.doi.org/10.1155/2013/136132, Received: 7 May 2013, Revised: 11 July 2013, Accepted: 21 August 2013, Academic Editor: Ga Zhang, Copyright © 2013 Mahmoud Yazdani et al.

[10] YADAV P.A., PADADE A.H., DAHALE P.P., MESHRAM V.M., **Analytical and Experimental Analysis of Retaining Wall in Static and Seismic Conditions: A Review,** International Journal of Civil Engineering and Technology, Vol. 9, Issue 2, February 2018, pp. 522–530, Article ID: IJCIET_09_02_051, Department of Civil Engineering, Shri Ramdeobaba College of Engineering and Management, Katol Road Nagpur, India, http://www.iaeme.com/ijciet/issues.asp?JType=IJCIET&VType=9&IType=2, ISSN Print: 0976-6308, ISSN Online: 0976-6316, IAEME Publication, Scopus Indexed.

[11] PATIL S.S., BAGBAN A.A.R., **Analysis and Design of Reinforced Concrete Stepped Cantilever Retaining Wall**, International Journal of Research in Engineering and Technology (IJRET), Vol. 4, Issue 2, February 2015, Walchand Institute of Technology, Solapur, Maharashtra, India, Available at: http://www.ijret.org, eISSN: 2319-1163, pISSN: 2321-7308.

[12] CHAUGULE V.S., BHADKUMBE A.C., PATIL S.M., KANNAMWAR P.V**., A Review on Behaviour of Retaining Wall**, Proceedings of Conference on Advances

on Trends in Engineering Projects (NCTEP-2019), in association with Novateur Publications, IJIERT, ISSN: 2394-3696, ISBN: 978-93-87901-03-2, Dr. D. Y. Patil College of Engineering and Innovation, Varale, Pune, India, February 15–16, 2019, Paper ID: CE 113.

[13] KARAJEH D.K., **Analysis and Design of Different Types of Earth Retaining Structures for Different Soil Properties and Load Conditions in Hebron**, Graduation Project, Civil & Architectural Engineering Department, College of Engineering, Palestine Polytechnic University, Hebron – Palestine, Supervised by Dr. Mohamed Taha Alsayyed Ahmad, January 2021.

[14] SAYEED S.M., REDDY S., MYTHILI K., **Seismic Analysis and Design of Cantilever Retaining Walls**, International Journal of Science Engineering and Advance Technology (IJSEAT), Vol. 2, Issue 10, October 2014, Aurora's Scientific Technological & Research Academy, Bandlaguda, Hyderabad, ISSN: 2321-6905.

[15] ERTUĞRUL Ö.L., **A Finite Element Modeling Study on the Seismic Response of Cantilever Retaining Walls**, Master's Thesis, Graduate School of Natural and Applied Sciences, Middle East Technical University, Department of Civil Engineering, September 2006.

[16] ALI A.F., MOHAMMED M.A., **Soil-Structure Interaction of Retaining Walls under Earthquake Loads**, Journal of Engineering, Vol. 19, No. 7, July 2013, University of Baghdad, pp. 795.

[17] THAPA MAGAR A., **Earthquake Response of Different Types of Retaining Walls**, Department of Civil and Transport Engineering, Geotechnics and Geohazards, Norwegian University of Science and Technology, Supervised by Gudmund Reidar Eiksund (BAT), Co-supervised by Amir M. Kaynia (NGI), Submission Date: June 2016.

18] YAVAN O., LEBLEBİCİ T., TUNCAN A., **Behavior of Retaining Walls Constructed in the Saturated Clay and Water-Saturated Sand Soils Under the Dynamic Loads**, Kırklareli University Journal of Engineering and Science, Vol. 8, No. 2, 2022, pp. 253–272, University of Kırklareli, Eskisehir Technical University, DOI: 10.34186/klujes.1183631, Geliş Tarihi: 03.10.2022, Kabul Tarihi: 22.11.2022.

[19] WAGNER N.B., **Seismic Earth Pressure on Basement Walls with Cohesionless Backfill**, PhD Dissertation, Department of Civil and Environmental Engineering, Graduate Division, University of California, Berkeley, Spring 2016, Supervised by Prof. Nicholas Sitar (Chair), Prof. Jonathan Bray, and Prof. Panayiotis Papadopoulos, Copyright © Nathaniel Bryce Wagner, 2016.

[20] PURI V.K., PRAKASH S., WIDANARTI R., **Retaining Walls Under Seismic Loading**, Proceedings of the Fifth International Conference on Case Histories in Geotechnical Engineering, Missouri University of Science and Technology, 16 April 2004, Southern Illinois University, Carbondale, Illinois.

[21] FANG Y.S., YANG Y.C., CHEN T.J., **Retaining Walls Damaged in the Chi-Chi Earthquake**, Canadian Geotechnical Journal, Vol. 40, pp. 1142–1153, 2003, doi: 10.1139/T03-055, © 2003 NRC Canada.

[22] SARAN S., **Dynamics of Soils and Their Engineering Applications**, Taylor & Francis Group, CRC Press, Boca Raton, FL, 2021, ISBN-13: 978-0-367-52987-1 (Hardback), Printed on acid-free paper, Version Date: 20190704, © 2021 by Taylor & Francis Group, LLC.

[23] CHAKRABARTI M.A., MESTRI P.T., **Seismic Analysis of Cantilever RCC Retaining Wall**, Proceedings of the 9th U.S. National and 10th Canadian Conference on Earthquake Engineering, Toronto, Ontario, Canada, July 25-29, 2010, Paper No. 127.

[24] TING N.H., **Earthquake-Induced Tilt of Retaining Wall with Saturated Backfill**, M.S. Civil Engineering (1991), Massachusetts Institute of Technology, B.S. Civil Engineering (1986), National Taiwan University, Taipei, Republic of China, Submitted to the Department of Civil and Environmental Engineering in Partial Fulfillment of the Requirements for the Degree of Doctor of Philosophy at the Massachusetts Institute of Technology, May 1993, © Nai-Hsin Ting, 1993. All rights reserved.

[25] HAZIRBABA K., **A Critical Review on Seismic Design of Earth-Retaining Structures**, Jordan Journal of Civil Engineering, Volume 13, No. 1, 2019, pp. 61, © 2019 JUST. All Rights Reserved, Associate Professor, Department of Civil and Infrastructure Engineering, American University of Ras Al Khaimah, P.O. Box 10021, Ras Al Khaimah, UAE, E-Mail: kenan.hazirbaba@aurak.ac.ae, Co-authors: Omer

Mughieda, Associate Professor, Abu Dhabi University, Abu Dhabi, UAE, and Ghassan Abu-Lebdeh, Professor, American University of Sharjah, Sharjah, UAE.

[26] BAISHYA S., **Evaluation of Seismic Active Earth Pressure Using Horizontal Slice Method and Log-Spiral Failure Surface**, Conference Paper, September 2012, North Eastern Regional Institute of Science and Technology (NERIST), Arunachal Pradesh, India, Co-authors: A. Sarkar & A. K. Dey, Former Under-Graduate Students, NERIST, Arunachal Pradesh, India.

[27] ALSAIDI A. M**., Stability Analysis of Gravity Wall Using PLAXIS 2D v-8.6 (Study Case in Piyungan Road-Batas Gunung Kidul, Yogyakarta)**, Prepared as a Condition of Completing Study Program of Bachelor Degree at the Department of Civil Engineering, Universitas Muhammadiyah Surakarta, Faculty of Engineering, 2018

[28] BADR M. M., SHAFIQU Q. S. M., **Predicting the performance of retaining structure under seismic loads by PLAXIS software**, Journal of the Mechanical Behavior of Materials, Volume 32, Article ID 20220251, 2023.

[29] SCHWEIGER H. F., FABRIS C., AUSWEGER G., HAUSER L., **Examples of successful numerical modelling of complex geotechnical problems**, Innovative Infrastructure Solutions, Volume 4, Issue 2, 2019, https://doi.org/10.1007/s41062-018-0189-5.

[30] ZIENKIEWICZ O.C., TAYLOR R.L., ZHU J.Z., **The Finite Element Method: Its Basis and Fundamentals**, Sixth Edition, Elsevier Butterworth-Heinemann, 2005.

[31] ÖZYÜREK Y.E., **Two Dimensional Finite Element Modeling for the Multi Tier Pile Wall with Anchor Shoring System**, A Thesis Submitted to the Graduate School of Natural and Applied Sciences of Middle East Technical University, in Partial Fulfillment of the Requirements for the Degree of Master of Science in Civil Engineering, September 2019.

[32] BRINKGREVE R.B.J., BROERE W., Waterman D., **Plaxis 2D - Version 8**, Edited by R.B.J. Brinkgreve & W. Broere, Delft University of Technology & PLAXIS b.v., The Netherlands, with co-operation of R. Al-Khoury, K.J. Bakker, P.G. Bonnier, H.J. Burd, G. Soltys, P.A. Vermeer, PLAXIS bv, P.O. Box 572, 2600 AN DELFT, Netherlands, ISBN 90-808079-6-6, © 2004 PLAXIS bv.

[33] EL YAMOUNI B., EL KHANNOUSSI F., KHAMLICHI A., **Numerical modelling of reinforced concrete gravity retaining walls under seismic loads**, Department of Industrial and Civil Sciences and Technologies, National School of Applied Sciences at Tetouan, Abdelmalek Essaadi University, Tetouan, Morocco, The 8th International Conference of Euro Asia Civil Engineering Forum 2022, IOP Conf. Series: Earth and Environmental Science 1195 (2023) 012060, IOP Publishing, doi:10.1088/1755-1315/1195/1/012060.

[34] MANGUELLE T. C., **Modelling the ground surface settlement induced by underground excavation, Case study: Extension of metro line 12 in France**, Thesis submitted in partial fulfillment of the requirements for the degree of Master in Civil Engineering, Option: Geotechnical Engineering, Presented by: MANGUELLE THIERRY CLAUDE, Supervisor: Pr.Eng. SIMONETTA COLA, NASPW Yaoundé, 2019-2020.

[35] PERSSON H., SIGSTRÖM D., **Staged excavation in soft clay supported by a cantilever sheet pile wall - Numerical analysis and field measurements of the effect of using a wailing beam**, Master of Science Thesis in the Master's programme Geo and Water Engineering, Department of Civil and Environmental Engineering, Division of GeoEngineering, Geotechnical Engineering, Chalmers University of Technology, Göteborg, Sweden, 2010. Master's Thesis 2010:41.

[36] PLAXIS bv, **PLAXIS V8 Introductory Version**, Tutorial Manual, PLAXIS bv, P.O. Box 572, 2600 AN Delft, Netherlands.

[37] AKTAŞ ENGIN T., **Finite Element Analysis of a Deep Excavation: A Case Study**, Middle East Technical University, Graduate School of Natural and Applied Sciences, Master of Science Thesis in Civil Engineering, July 2019